# AN AGE-, SEX- AND SPATIALLY-STRUCTURED STOCK ASSESSMENT OF THE INDIAN OCEAN SWORDFISH FISHERY 1950-2015, USING STOCK SYNTHESIS

PREPARED BY: IOTC SECRETARIAT[1], 25 AUGUST 2015

---

[1] dan.fu@fao.org, fabio.fiorellato@fao.org, lucia.pierre@fao.org, kevin.sullivan@fao.org

# Contents

**SUMMARY**

This report presents a stock assessment for Indian Ocean swordfish (*Xiphias gladius*) using *Stock Synthesis 3* (SS3). The assessment uses a spatially disaggregated, sex explicit, and age structured model that integrates several sources of fisheries and biological data into a unified framework. The assessment includes catch data grouped into 12 separate fisheries covering the period from1950 through to 2015, 11 CPUE series, and length composition data from 8 fisheries. Key elements and core assumptions in the assessment model are summarised below:

- The population is age-, sex-structured (dimorphic growth), and spatially partitioned into 4 areas (north-west, north-east, south-west, south-east). The model describes differential depletion and recruitment by area, but movement between areas was not estimated.
- There are 12 fisheries, defined by fleet and region. Standardised CPUE series (as relative abundance indices) are available from Japanese (4, by region), Taiwanese (4, by region), Portuguese (SW), Spanish (SW), and Indonesia (NE) longline fleets. Length composition data are available from 8 fisheries. The model assumes that the Japanese CPUE indices are proportional to the population density of swordfish in each region.
- The model assumes that there is a shared spawning stock and total recruitment follows a Beverton-Holt relationship, with annual deviates and temporal variability in the proportional distribution of recruits among regions.
- The model uses two length-based, double normal selectivities: longline and gillnet/other.
- Estimated parameters include virgin recruitment, selectivity functions, recruitment deviations, catchability coefficients, and the spatial pattern of recruitment.
- Fixed parameters include: stock recruit steepness, variances on recruitment and CPUE errors, life history parameters describing growth, M, maturity schedule.

The assessment attempted to quantify uncertainty with respect to  i) key assumptions that are difficult to justify, ii) parameters that are difficult to estimate, and iii) interactions among them in the permutations. Stock status was estimated for 162 models based on 3 reference cases (54 models each) running a permutation of the parameters, including combinations of the following options:

- Three CPUE options (3 reference cases):  Japanese + Portuguese CPUE, Taiwanese + Portuguese CPUE, and All CPUE series (all are equally weighted except for less weight for Taiwanese CPUE),
- Three growth/maturity/natural mortality options: CSIRO estimates from SE Indian Ocean fin rays samples, Taiwan estimates from the Indian Ocean equatorial region fin ray samples, new CSIRO estimates from SW pacific otolith samples,
- Three values of stock recruit steepness: h=0.55, 0.75, 0.95,
- Recruitment sigma: 0, 0.2, 0.4,
- Effective sample sizes for size composition data: 10% and 1% of observed, with maximum sample size capped at:  20, and 2, respectively.
-

Estimates from the majority of models under the three reference cases suggested the Indian Ocean Swordfish stock as a whole is currently not overfished, and not subject to overfishing.  Management quantities estimated for the assessment grid that combines all models from three references cases (IO-Grid, 162 models) are summarized below (mean and 90% quantiles from the weighted distribution of the MPD estimates)

- $SSB_{2015}$ / $SSB_{MSY}$ = 2.30 (1.32–4.52),
- $F_{2015}$ / $F_{MSY}$ to be 0.57 (0.22–1.09).
- $SSB_{2015}$ / $SSB_0$ = 0.47 (0.34–0.65)
- MSY = 39 610 t (24 170–67 660 )

- Current catch 34 144 t

The results of 10 years projections over a range of constant catch levels (60, 80, 100, 120, and 140% of current) are summarized in a management decision table (Kobe 2 Strategy Matrix), based on a weighted average of the model result. Projections from models under the grid-IO suggest the risk of the spawning biomass falling below the target (SSBMSY) is less than 10% by 2025 if the catch remains at the current level. A higher risk is estimated from models using Taiwanese + Portuguese indices (grid-TWN), which estimated a 24% probability that spawning biomass will be below SSBMSY in 2025 under the current catch level.

A sensitivity was conducted to the current assumption that the Japanese standardised CPUE is proportional to the population density in each area (where the CPUE provides additional prior information on abundance in a region relative to other regions). Alternative regional weighting factors were derived based on unfished biomass estimated from sub-regional models (one for each region and each model included catch and observational data from that region only). The sensitivity model is fitted to the Japanese indices rescaled by the alternative weighting factors (to approximate a model without the shared catchability constraint). The sensitivity was run over the same permutation of parameters (54 models) and produced more pessimistic results, suggesting that the stock is not overfished, but is probably subject to overfishing. Management quantities from the sensitivity trial were (mean and 90% quantiles from the weighted distribution of the MPD estimates):

- SSB2015 / SSBMSY = 1.17 (0.90–1.65)
- F2015 / FMSY = 1.07 (0.62– 1.51).
- SSB2015 / SSB0 = 0.30 (0.23–0.42 )
- MSY = 25 696 t (19 935 – 35 210)
- Current catch 34 144 t

There is also uncertainty in the catch data used in the assessment. The estimates by IOTC Secretariat show a two-fold increase of catch for the north-east longline fishery in 2014 (and 2015) (a result of applying the disaggregation procedure to the reported catch from Indonesian fresh tuna longline fleet using Taiwanese fresh tuna longline catches as a proxy). The assessment here instead used a much lower estimate (based on the average catch from 2011-2013 for the Indonesian fresh tuna longline fleet). The sensitivity run (over the same permutation of parameters) using the IOTC estimates did not change estimated stock status much, but suggested a slightly higher risk in projections.

# 1. INTRODUCTION

## 1.1 Fishery overview

Swordfish (*Xiphias gladius*) are a large pelagic species, broadly distributed throughout the Indian Ocean to a southern limit of 50° S. Indian Ocean swordfish have been taken by the Japanese longline fleet primarily as by-catch, since the early 1950s (Figure 1). The population was not heavily exploited before targeted fisheries began in the early 1990s. At this time the Taiwanese longliners began taking large numbers, initially in the SW region, followed by the other regions. As the Fresh Tuna longline fishery developed in the late 1980s, annual catches rapidly increased to reach a peak of about 35,000 in the late 1990s–early 2000s. The European longline fleet (predominantly from Spain) started a targeted fishery in the 1990s, while only small numbers are reported in the driftnet fisheries, and purse seine catches are very rare. Total catches have declined substantially over the past few years (generally attributed to large effort decreases in the longline fleets due to risk of piracy). Swordfish are a high value catch that represent an increasingly important source to many coastal nations in Indian Ocean. This report provides a stock assessment for swordfish in the Indian Ocean.
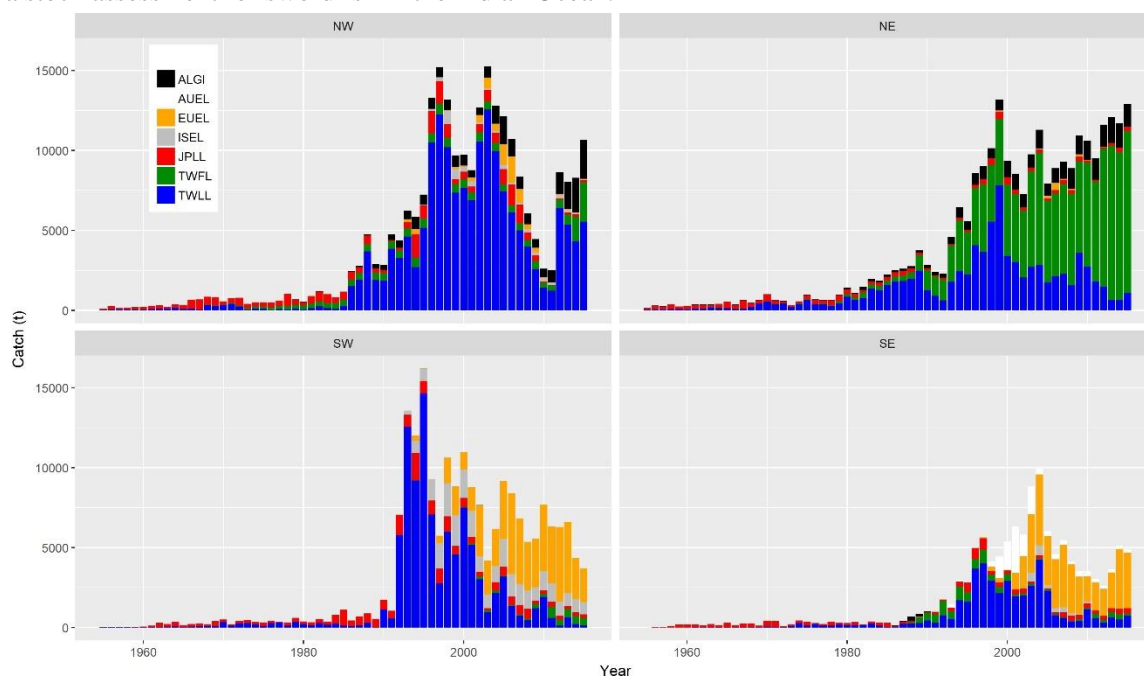


**Figure 1: Total swordfish catch in tonnes by fishery fleet over time for the North-west (NW), North-east (NE), South-west (SW), and South-east (SE) regions in the Indian Ocean. (The catch from Indonesian fresh tuna longline fleet in 2014 and 2015 was assumed to be equal to the average catch of 2011-2013).**

## 1.2 Biology and stock structure

Swordfish are highly fecund, migratory fish that grow quickly in the early years and reach their maximum size at about 15 years of age (Ward & Elscot 2000). Swordfish have a wider geographical distribution than other billfish and tuna. They routinely move between surface waters and great depths and do not form schools. Female swordfish grow faster and live longer than males, and they have different distributions depending on size (Ward & Elscot 2000).

Stock structure of Indian Ocean samples of swordfish were examined using genetic analyses. Lu et al. (2006) describe mitochondrial DNA evidence for three possible population delineations within the Indian Ocean (but recognised that increased sample sizes would be desirable), suggesting samples drawn from the waters off northern Madagascar and the Bay of Bengal were 2 distinct groups compared to the other populations from the Indian Ocean and West Pacific. In the Indian Ocean, a large continuous

larval distribution in the eastern Indian Ocean is described in Nishikawa et al (1985). Unfortunately, other regions of the Indian Ocean were not as heavily sampled. Some evidence suggests that there may be genetic distinction within the IO, and this is the subject of ongoing investigation of the IOSSS project led by IFREMER, Reunion (Bradman et al. 2010. Bourjea et al 2011). Results obtained in 2013 (WPB 2013, Muths 2013) did not identify any clear differences in genetic structure within this ocean, suggesting it is appropriate to consider swordfish as a single population in the Indian Ocean.

## 1.3  Previous assessments

A number of surplus production models were fitted to Indian Ocean broadbill swordfish catch and CPUE data as a first attempt at a formal model-based stock assessment at the 5th IOTC Working Party on Billfish (Anon. 2006).  These models yielded plausible inferences about the impact of the swordfish fishery on the whole of the Indian Ocean population.

Kolody (2009) conducted preliminary work toward an Indian Ocean swordfish stock assessment using Stock Synthesis 3. The prime motivation for developing the SS3 model in 2009 was to increase the resolution of spatial processes, so that the differential and possibly elevated depletion in the SW Indian Ocean could be more explicitly described. The model population was age-structured, sex disaggregated, and spatially disaggregated into 4 regions. Kolody (2010, 2011) updated the assessment, with a particular focus on the SW region where a separate model was run assuming the SW constituted a separate stock.

The CPUE in the SW region declined much faster than the other regions. The first attempt to explicitly quantify the south-west (SW) sub-population (under the assumption that it may represent a discrete population) indicated that it was probably highly depleted (Martell 2010). Kolody (2010, 2011) conducted a similar, but extended analysis to explore the implications of several key uncertainties in the SW region, and demonstrated that there are plausible interpretations of the data that are much more optimistic. The WPB has noted that there is evidence that the SW region may be subject to the highest exploitation rates in the Indian Ocean, and thus represents the highest priority from a conservation perspective (WPB 2009).

Sharma & Herrera (2014) updated the assessment for the Indian Ocean Model. Based on the most recent evidence (Muths 2013), there are no differences in genetic structure obtained from the SW Region and the entire IO Region (Muths et. al. 2013). As such, only one stock assessment was examined.

This report provides an updated stock assessment for swordfish in the Indian Ocean using fishery data up to 2015, and builds on the work by Sharma & Herrera (2014), and Kolody (2010, 2011), assuming a single Indian Ocean population stock (IO), but spatially  disaggregated into  four areas (Figure 2). The model incorporates the following updates:

- Three additional year of data (2013-2015),
- Improved information on nominal catches and catch and effort data from IOTC database
- Revised CPUE time series for the Japanese and Taiwanese fleets,
- Addition of the Indonesia CPUE in the North-east (NE) region,
- Addition of the new growth estimates from the 2016 CSIRO study

The assessment provides estimates of stock status and reference management quantities. Model uncertainties are characterised under combinations of model assumptions and parameter values using a grid approach. The assessment also explored the sensitivity to the current regional weighting assumption based on the Japanese CPUE.
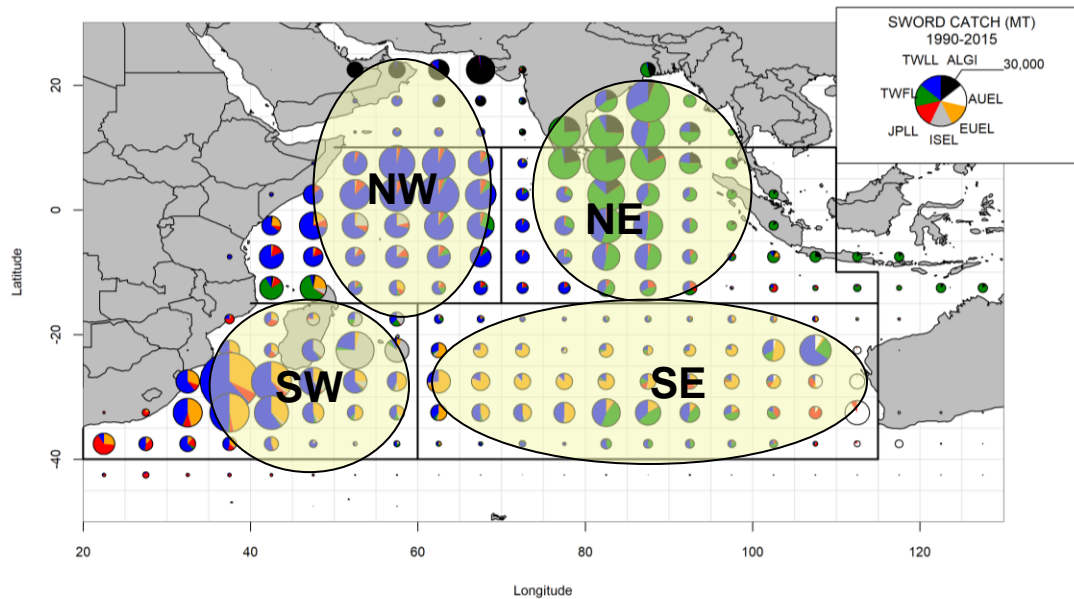
**Figure 2: Spatial structure showing the 4 areas used in the assessment model, and distribution of SWO catch in the Indian Ocean by fleet aggregated for 1990-2015.**

## 2. OBSERVATIONS AND MODEL INPUTS

There are many different fisheries catching swordfish in the Indian Ocean (Table 1), with vastly different gear types and levels of data quality (IOTC 2017). Since 2011, SS3 assessments identified 12 fleets (compared to 24 fleets in the 2010 assessment), based on spatial disaggregation of these fisheries (Table 2). The simplification was undertaken because the stock status inferences were not very sensitive to the selectivity assumptions. There is enough uncertainty about the stationary selectivity assumptions, and the poor size composition data, that we would not expect the size composition data to be very informative about year-class strength. Six fleets were maintained in the SW region to allow analysis of this component of the fishery at higher resolution.

**Table 1: Fishery definitions for the Indian Ocean Swordfish.**

| Name | Description |
|---|---|
| ALGI | Gillnet, trolling and other minor artisanal fisheries |
| AUEL | Longline fishery of Australia (target is SWO) |
| EUEL | EU longliners targetting SWO plus other longliners assimilated to EU longliners |
| ISEL | Semi-industrial longline fleets operating in Reunion(EU.France), Mayotte(EU.France), Madagascar, Mauritius and the Seychelles |
| JPLL | Longline fishery of Japan plus other fleets assimilated to the Japanese fleet |
| TWFL | Fresh-tuna longline fleets of Taiwan and Indonesia, plus other fresh-tuna longline fleets assimilated to those |
| TWLL | Large scale tuna longline fleet of Taiwan,China, plus other longline fleets assimilated to the Taiwanese fleet |

**Table 2: Fleet definitions (number 1–12) and CPUE series (13–22) for the SS3 Assessment. Suffixes denote regions within the Indian Ocean as indicated in Figure 1: NW – North-West; NE – North-East; SW – South-West; SE – South-East.**

| Name | number | Area | Description |
|---|---|---|---|
| GI_NE | 1 | NE | Northeast Gillnet and other non-longline/-handline gears |
| LL_NE | 2 | NE | Northeast all longline and handline gears |
| GI_NW | 3 | NW | Northwest Gillnet and other non-longline/-handline gears |
| LL_NW | 4 | NW | Northwest all longline and handline gears |
| GI_SE | 5 | SE | Southeast Gillnet and other non-longline/-handline gears |
| LL_SE | 6 | SE | Southeast all longline and handline gears |
| ALGI_SW | 7 | SW | Southwest Gillnet and other non-longline/-handline gears |
| EUEL_SW | 8 | SW | Southwest European and assimilated longliners (target SWO) |
| ISEL_SW | 9 | SW | Southwest semi-industrial longliners (target SWO) |
| JPLL_SW | 10 | SW | Southwest Japan and assimilated longliners (target tunas) |
| TWFL_SW | 11 | SW | Southwest fresh-tuna longliners (target tunas) |
| TWLL_SW | 12 | SW | Southwest Taiwan,China and assimilated longliners and handlines (mixed target) |
| UJPLL_NW | 13 | NW | *JPN CPUE series (1976-2015) |
| UJPLL_NE | 14 | NE | *JPN CPUE series (1976-2015) |
| UJPLL_SW | 15 | SW | *JPN CPUE series (1976-2015) |
| UJPLL_SE | 16 | SE | *JPN CPUE series (1976-2015) |
| UTWLL_NW | 17 | NW | **TWN CPUE series (1979–2015) |
| UTWLL_NE | 18 | NE | **TWN CPUE series (1979–2015) |
| UTWLL_SW | 19 | SW | **TWN CPUE series (1979–2015) |
| UTWLL_SE | 20 | SE | **TWN CPUE series (1979–2015) |
| UPOR_SW | 21 | SW | POR CPUE series (2000–2015) |
| UESP_SW | 22 | SW | ESP CPUE series (2000–2015) |
| UIND_NE | 23 | NE | IND CPUE series (2005-2015) |

\* JPN CPUE series were standardised for 1976–1993 and 1994–2015 separately, and were treated as two separate series in the assessment

\*\* TWN CPUE series were treated as two separate series: 1979–1993 and 1994–2015 in the assessment.

## 2.1 Catch history

Catch by year, fishery and area are shown in Figure 1. It is assumed that the catch in tonnes provided by the CPCs are the most reliable catch data available. While the total catch data are not perfect, they are derived primarily from the industrial fleets in the Indian Ocean and are thought to be more reasonable than for the other billfish species. Swordfish are caught by industrial longliners, gillnets and, to a lesser extent, other artisanal or recreational fisheries.

The nominal catches are not always reported by species and/or gear by the responsible institutions in each country. The catches reported under species and/or gear aggregates are decomposed by the IOTC secretariat using alternate sources of information (if available), or a pre-defined criteria so that all catches are separated into individual gears and species (IOTC 2004). The swordfish catch from the Indonesian Fresh Tuna Longliners was estimated using the Taiwanese fresh longline as a proxy for gear/species disaggregation. As the TWN fresh longline catch had a (more than) twofold increase from 2013 to 2014, the Indonesian catch increased significantly. As a result, the estimated swordfish catch for the LL_NE fishery increased from 10210 t in 2013 to 17 484t in 2014, and 18 998 t in 2015. This

appears very unlikely. Therefore in the assessment we used the average catch between 2011 and 2013 as an estimate for the Indonesian Fresh Tuna Longline catch for the last two years. Accordingly the catch estimates for the LL_NE fishery were reduced to 10 156 t and 11 460 t for 2014 and 2015. The disaggregation estimates were used in a sensitivity run instead. (Note: there is also concern that the catches of swordfish for the fresh tuna longline fishery of Indonesia may have been underestimated in recent years, as the majority of the catches of albacore and swordfish are stored and unloaded frozen and are seldom sampled in port.)

The effects of discarding and depredation are not included in the catch statistics, and it is estimated that this may account for up to 30% of the Reunion catch covered by observers (it was unclear whether the units were mass or numbers, P. Bach, IRD, Reunion, pers. comm.).  In addition, the estimates of catches of swordfish are thought to be more uncertain since the mid 1990's due to:

- To date, Iran has not reported catches of swordfish for the gillnet fishery. In recent years, many Iranian vessels have moved on to the high seas, using drifting gillnets to catch tunas and other species. The fleet is operating in the northwest Indian Ocean, which is the area that has recorded the highest catches of swordfish in recent years. The Secretariat has little information on the activities of this fleet which has made it impossible to estimate catches of swordfish for the fleet. The catches of swordfish by this fleet may represent as much as 5,000 t in recent years.

- Poor reports from IOTC CPC's: The catches of swordfish recorded for the longline fleet of India were estimated by the IOTC Secretariat, as India has never reported catches for its commercial longline fleet (around 100 vessels operating since 2004). Malaysia and Indonesia do not report catches for longliners under their flags that are not based in these countries. The catches for this component were also estimated by the IOTC Secretariat.

- Non-reporting industrial longliners (NEI): The amount of non-reporting longliners targeting swordfish was high during the 1990's and early 2000's due to the shift of vessels from the Atlantic Ocean to the Indian Ocean. The catches of the vessels were estimated by the Secretariat using information from various sources. There are also conflicting catch reports: the catches for South Korean longliners reported as nominal catches are different from the catches reported in the catch and effort data, with higher catches recorded in the CE table for some years. The Secretariat revised the catches of swordfish for the Korean fleet for the period concerned.

## 2.2  Relative abundance estimates

Eleven standardized CPUE series (Table 2, Figure 3) were submitted to WPB for the assessment, including the Japanese fleet (Ijima et al. 2017), Taiwanese fleet (Wang 2017), Spanish fleet (Ferndandez-Costa 2017), Portuguese fleet (Coelho 2017 et al.), and Indonesian fleet (Setyadjy et al. 2017).  The CPUE series are included in the assessment as relative abundance indices.

The CPUE series were somewhat different from those estimated previously: in each region, the Japanese CPUE series were standardised as two separate series: 1979–1993 and 1994–2015, because there were the significant differences between the two periods in terms of hooks between Floats, proportion of zero-catch sets and targeting practices (Ijima et al. 2017).

The Taiwanese indices were standardised for 1979 to 2016 (the index in 2016 was not used). In most areas, the early indices exhibited some large fluctuations, which can hardly be explained by the population dynamics. Some of the fishing practices for swordfish by longliners (the use of squid baits with light sticks, setting shallower at night) were widely adopted in the late 1980s, probably resulted in significant improvements in swordfish catch rates (Campbell 1998). Similarly to the Japanese CPUE, the Taiwanese CPUE is also considered as two separate series: 1979–1993 and 1994–2015 in each region.

The Portuguese pelagic longline fishery in the Indian Ocean started in the late 1990's, targeting mainly swordfish in the southwest, also catches relatively high quantities of sharks as bycatch in certain areas and seasons (Coelho 2017 et al). The swordfish CPUE indices from the Portuguese pelagic longline fishery were standardised using generalized Linear Mixed Models (GLMMs) using year, quarter, area, ratios and area * season interactions. The vessel effects were used as random variables. The Portuguese series 2000–2015 is assigned to the south-west region in the assessment model.

The Spanish series from 2000 to 2015 is included in the model for the south-west region. Shifting targeting (i.e. shark vs swordfish) is very important in this fishery. Earlier analysis demonstrated that the inclusion or exclusion of the species ratio factor makes very little difference to the annual time series in this case, suggesting that the seasonal targeting shifts are probably not introducing any consistent bias to the time series (e.g. targeting changes are probably consistent among years).

The Indonesian series covering 2006 to 2015 is included in the model for the north-east region. The indices appears very noisy and has an overall flat trend.

The CPUE series from the different LL fleets suggest very different abundance trends. In the north-west, Japanese indices show a large decline since the mid-1990s the Taiwanese indices show an overall flat trend; in the south-east, Japanese CPUE had a steeper decline than Taiwanese CPUE; In the north-east, Japanese and Taiwanese CPUE show opposite trends. In the south-west, Japanese CPUE is sharply increasing, Taiwanese CPUE series is steeply decreasing, and CPUE series from Spain is relatively stable over the last few years. Some of these conflicts could be attributed to the over-interpretation of noise.
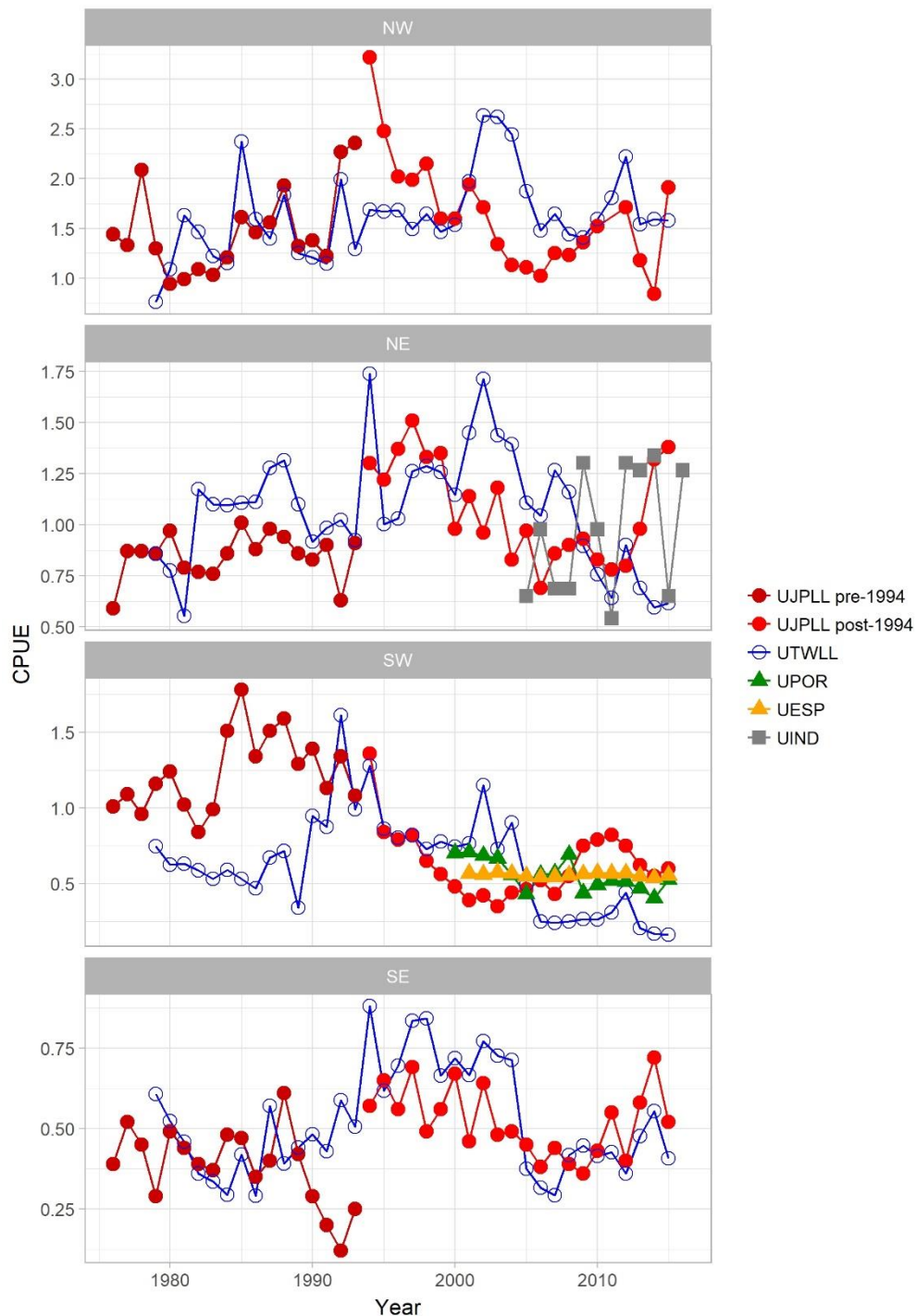
**Figure 3: Standardized CPUE by area for Japanese, Taiwanese, Portuguese, Spanish, and Indonesian longline fleets by sub-region based on papers submitted to WPB15. All series have been rescaled so that they are visually comparable for relevant periods of overlap. Note that this re-scaling does not reflect the relative weighting across areas that is applied to the Japanese fleet. Also note that Japanese indices were standardised for 1979–1993 and 1994–2015 separately.**

## 2.3 Length frequency data

Size data are available for 8 of the 12 fleets. Size composition data quality is often poor, with small sample size and non-random sampling for many fleets/strata, and changes in coverage over time (Figure 4). The size data from Japan and Taiwan were historically provided to the IOTC Secretariat at a very coarse resolution of 10° lat X 20° lon, but this has changed to 5° X 5° in recent years. This

11

creates an additional problem in that the Secretariat has to artificially partition these observations to fit the WPB spatial structure. There is also a pooling of data from different fleets, and it is noted that most of the Japanese size composition data is derived from the 'school' fleets, while most of the catch is derived from the commercial fleet, and the two fleets operate in different regions. Aggregated size distributions and time series of mean size are shown in Figure 5.

In 2009 and 2010, attempts were made to examine the size composition trends of the different fleets to resolve conflicting signals and different sources of data in relation to the plausibility of the data. Since 2011, the WPBhas agreed that all of the size composition data should be down-weighted for several reasons:

- 1950-1969: The total catches of swordfish estimated for this period are low (below 1,500t in most years). No size frequency data are available for this period. The majority of the catches of swordfish for the period come from the Japanese and Taiwanese longline fleets.

- 1970-1979: The total catches of swordfish estimated for this period range between 2,000t and 3,000t. Size frequency data is only available for the longline fishery of Japan. Between 3-16% of the total catches estimated (in number) are covered through sampling (i.e. 3-16% of the quarter x 10 x 20° strata includes some level of sampling). Samples are not available for the longline fishery of the Taiwanese fleet during this period.

- 1980-1991: The total catches of swordfish estimated for this period range from 2,000t to 8,000t. Samples are available for the majority of the strata having catches of swordfish, representing 55-90% of the total catches of swordfish estimated (in number), depending on the year.

- 1992-2012: The total catches of swordfish estimated for this period range between 14,000t and 35,000t. Between 40-60% of the total catches estimated (in number) come from fisheries for which samples are available. The main problems are: poor sample sizes and time-area coverage for the longline fishery of Japan; lack of length samples for the longline fisheries of India, Oman and various other flags (NEI); and lack of samples or poor quality samples from gillnet and other artisanal fisheries.
- In 2011, there were inconsistencies among different reported sources of data (nominal catches reported in the landing statistics, logbook catch and effort data, and size)

Size trends differ among LL fleets in the same area. According to Herrera and Pierre (2014), in recent years the majority of the samples available from the longline fishery of Japan come from training vessels. The representativeness of the samples collected on training vessels is uncertain, as these vessels do not necessarily operate in the same areas or use the same fishing techniques as the commercial vessels from Japan that tend to catch larger swordfish.

Swordfish are known to have complex geographical distributions depending on size and sex and there is evidence for spatial heterogeneity in size/sex composition in other oceans (Ward and Elscot 2000). Larger, predominantly female fish are observed in the more southern latitudes of the South Pacific. In Atlantic, medium and large-sized swordfish tend to dominate longline catches in temperate waters and smaller swordfish are more common in warmer waters. However, sex data are rare for the Indian Ocean.The sex ratio information is not available in the size data.
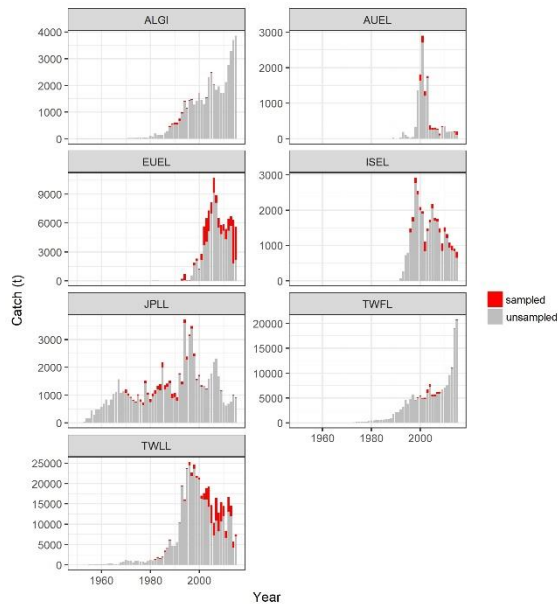
**Figure 4: Proportion of catch sampled over time by fleet.**
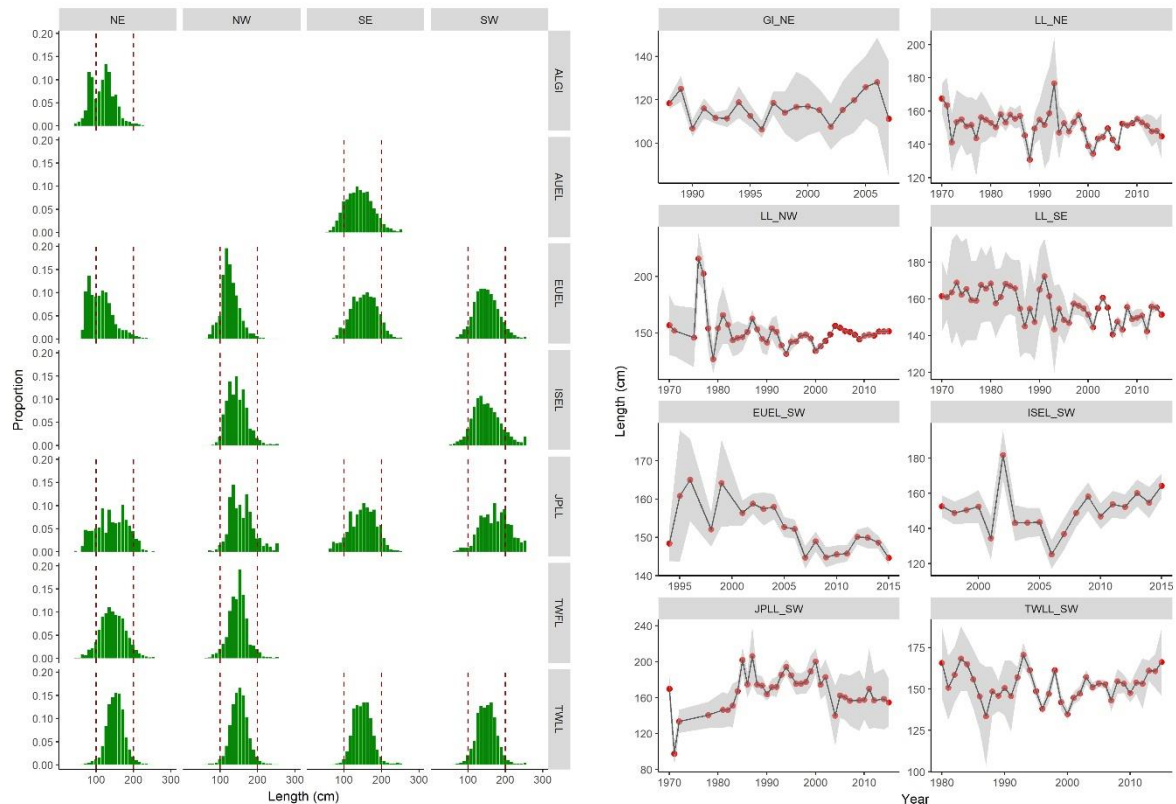


**Figure 5: Swordfish size composition data aggregated over time by fleet and area (left panels), and mean length over time by fisheries defined for the assessment (right panels). Grey shading in the right panels represents the 95% Confidence interval (based on the reported sample size, capped at 200).**

13

## 3. ASSESSMENT MODEL DESCRIPTION

The most important model assumptions are described in the following sections. The analysis was undertaken with Stock synthesis SS V3.24, 64 bit version (Methot and Wetzel 2013, Methot 2013). Standard population dynamics are described below, and equations can be found in Methot & Wetzel (2013). The template SS3 specification files for all of the models are archived with the IOTC Secretariat (The template control file is given in Appendix B). Table 2 lists the assumption options that were explored in exploratory runs, as well as combined in a balanced "grid" design (i.e. all possible combinations of a specified set of listed assumption options).

The analysis was undertaken with Stock synthesis SS 3.24z (Methot & Weltz 2013, Methot 2013).

**Table 3: Summary of SS3 specification options for the Indian Ocean assessment models. Other assumptions were constant for all models or specified separately for a particular model. The options below were applied in exploratory and balanced design (all possible combinations of a specified set of listed assumption options, see Figure 5 for the details of grid run configurations).**

| Assumption | Option |
|---|---|
| **Spatial domain** | *io;* Indian Ocean with 4 sub-regions<br>*nw;* only NW region<br>*ne;* only NE region<br>*sw;* only SW region<br>*se;* only SE region |
| **Beverton-Holt SR Steepness (h)** | *h55;* h=0.55<br>*h75;* h=0.75<br>*h95;* h=0.95 |
| **Growth, Natural Mortality and Maturity** | *GtMf;* Mixed Indian Ocean (Taiwan)<br>*GaMf;* Eastern Indian Ocean (CSIRO)<br>*GhMf;* Hawai'i (NMFS)<br>*GfMf;* SW Pacific Ocean fin ray (CSIRO)<br>*GoMf;* SW Pacific Ocean otolith (CSIRO) |
| **CPUE\*** | *NT0;* JPN 1994–2015<br>*NT1;* JPN 1976-2015<br>*NTP;* JPN 1994–2015, replace by POR 2000–2015 in SW<br>*TW0;* TWN 1994–2015<br>*TW1;* TWN 1979–2015<br>*TWP;* TWN 1994–2015, replace by POR 2000–2015 in SW<br>*A1\*\*;* JPN 1994–2015 ; *TWN* 1994–2015 ; POR; ESP;IND<br>*rNTP;* same as *NTP,* but with alternative regional weighting |
| **Recruitment**<br>$\sigma$=SD(log(devs)) | *R0;* $\sigma$=0<br>*R2;* $\sigma$=0.2<br>*R4;* $\sigma$=0.4 |
| **Catch-at-Length (SS=assumed sample)** | *CL200; SS = min(N, 200)*<br>*CL020; SS = min(N/10, 20)*<br>*CL002; SS = min(N/100, 2)* |
| **Catch estimates** | Indonesian FL catch 2014-2015 used IOTC estimates;<br>Indonesian FL catch 2014-2015 used 2011-2013 average |

\* CPUE variances were adjusted using a weighting factor ($\lambda$) applied to the individual likelihood term, such that a lognormal likelihood with $\sigma_1 = 0.1$, combined with a down-weighting factor $\lambda = 0.001$ is equivalent to the original likelihood with $\sigma_2 = \text{sqrt}(\sigma_1^2/ \lambda) = 3.16$. CPUE series included in each option were assigned $\sigma_1 = 0.1$, those not included were assigned $\sigma_1 = 3.16$
\*\* TWN CPUE variances were assigned $\sigma_1 = 0.2$

## 3.1 Spatial structure and migration

The appropriate spatial structure for the assessment remains uncertain. Different hypotheses have been proposed, various options have been explored for IO swordfish to date, including (1) one or more discrete stocks (2) two or more populations that are produced from a common spawning ground, but have foraging grounds site fidelity (i.e. while this is a single population genetically, depletion can differ in different regions at different rates) 3) discrete spawning populations with mixing in common foraging grounds (Figure 6).

Some evidence suggests that there may be genetic distinction within the IO, and this was the subject of an investigation (IOSSS project led by IFREMER, Reunion) (Bradman et al. 2010, Bourjea et al 2011). Based on results obtained in 2013 (WPB 2013, Muths 2013), there are no differences in genetic structure obtained from the SW Region and the entire IO Region (Muths et. al. 2013). As such, the assessment is based on the single stock IO model (Shared spawning with foraging grounds site fidelity, Figure 6-C). However, one of the sensitivities used sub-regional models to examine alternative regional weighting (see below as well as section 4.1). The sub-regional models essentially assumes multiple populations in the Indian Ocean (Figure 6-B).

**Indian Ocean Model (IO)**
The model is disaggregated into 4 areas corresponding to those used in the JPN and TWN catch rate standardization analyses in recent years (Figure 2). Given the vast size of the Indian Ocean, and the migration rate inferences that have been made from tagging studies to date, it seems unlikely that there would be rapid mixing processes across the whole basin, even if the population was genetically homogeneous (but we note that a few trans-Atlantic swordfish migrations have been recorded (Kadagi et al 2011)). As such, localised overfishing could result in negative local consequences even if the population is genetically homogenous. The 4-area structure is a pragmatic disaggregation that conveniently partitions most of the national fleets.

There are very few direct observations of swordfish migration in the Indian Ocean. The few conventional tag recaptures and satellite GPS tag deployments near the Australian coast provided no indication of large scale movements (but these studies are limited by biased recovery effort and short deployment times respectively) (Karen Evans, CSIRO, Australia, pers. comm.). Tagging studies from other oceans suggested residency or homing behaviour amongst components of populations (Carey and Robinson 1981), and it seems unlikely that there would be rapid mixing processes across the whole basin, even if the population was genetically homogeneous.

We can indirectly infer that there are probably some relatively large seasonal migrations. Swordfish can be caught at least as far south as 45° S, however, the spawning regions (and larval distributions) have all been identified in the tropical regions. In the southern hemisphere at least, this suggests substantial directed seasonal migrations. The spawning season also seems to be several months out of phase between the northern and southern regions. It is not clear whether this represents a single annual migration between north and south, or whether distinct populations independently move between lower and higher latitudes in each hemisphere. However, in many cases, resolving the directed seasonal migration patterns is not required in an assessment.

In principle, SS3 can be used to estimate movement rates among areas, however, these estimates are generally of little value in the absence of tagging data. In all of the models, migration rates were fixed at very low levels (<< 1% per year), which essentially creates 4 populations except for the shared spawning and recruitment dynamics (foraging grounds site-fidelity).

**Sub-Region Models (NW, NE, SW, SE)**.
The sub-regional models assume that each region is a single stock. Four models were developed (NW, NE, SW, SE), one for each region, and each model included catch and observational data for that region only (see section 4.1 for more details). These models are used to derive alternative regional scaling factors for the Japanese CPUE indices. We note that the approach employed here is different to the SW

model by Kolody (2011), which was mainly used for assessing the stock status and providing management advice for the south-west swordfish fishery.

## 3.2 Population Dynamics

The stock assessment model partitioned the Indian Ocean swordfish population into four areas, two sex groups, and age groups 1–30 years with the last age a plus group (in unfished equilibrium, <0.25% of the population survives to reach the plus-group with the lowest M value considered).

The swordfish population is sex-structured to (potentially) account for a number of sex-specific population features that may be worth describing. Notably, growth curves differ by sex, and it is useful to be able to represent the two distributions (or aggregated of the two distributions) in the catch-at-length likelihoods (or it would be useful in principle, if we were confident about the growth curves, size composition data, mortality estimates and stationary selectivity assumptions). Spatial distributions often differ by sex (e.g. large females are disproportionately found in cooler temperate waters in the south Pacific). Selectivity may differ by sex due to the differing spatial distributions, and there also may be direct size biases in some fisheries (e.g. commercial fishers report that large swordfish may be less vulnerable to circle hooks). Natural mortality may also be sex-specific, but no distinction was made in these models. However, there is no evidence that the sex structure is contributing much to the behaviour of the model in its current form.

The population was assumed to be in unfished equilibrium in 1950, the start of the catch data series. The model was iterated from 1950-2015 using an annual time-step. The nominal unit of time in the model is one year during which population processes (e.g., recruitment, spawning, and ageing) were applied in sequence according to the dynamics implemented within the Stock Synthesis model (Methot 2013). Observations were fitted to model predictions within the year. The main population dynamics processes are as follows:

A) Fast mixing –
single population model
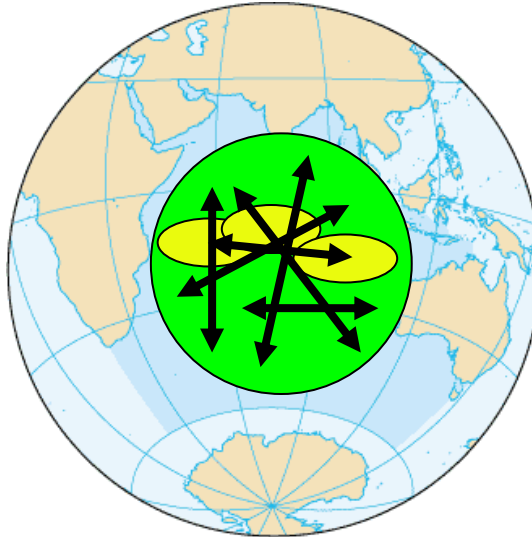
B) Very slow mixing –
multiple separate population models
(used in the  sub-regional models)
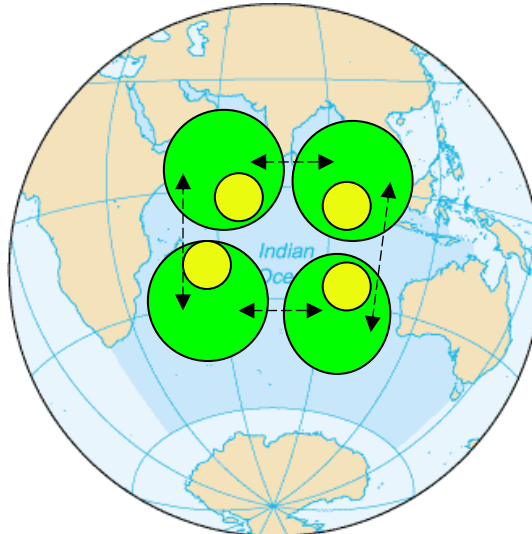
C) Shared spawning with
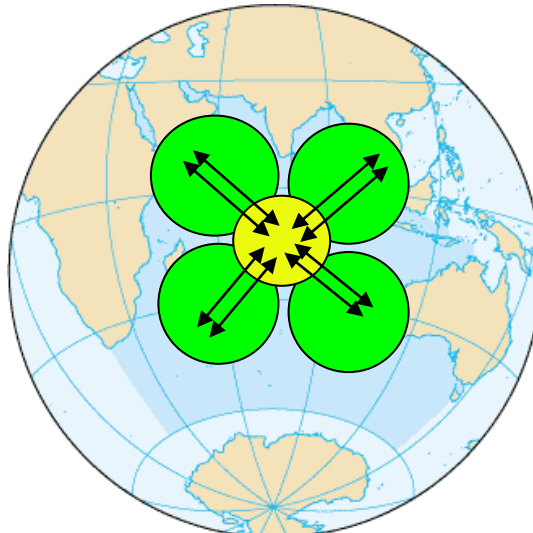foraging grounds site fidelity
(IO model)

**Figure 6: Cartoon of some alternative Indian Ocean swordfish population spatial hypotheses. Green circles represent foraging grounds, yellow circles represent spawning grounds, and arrows indicate movements to the larger green circles.**

### 3.3 Growth

Swordfish exhibit phenomenal growth in the first year of life and there is a marked difference in growth rate between male and female. The strong evidence for sex dimorphism in swordfish can be potentially important in the right-hand tail of the size distribution, which is often estimated to consist predominantly of large mature females. In previous studies three alternative sets of growth curves were explored to allow for uncertainty due to potential area-specific growth rates, and ongoing concerns about age estimation from fin spines.

- CSIRO estimated very slow growth based on South-East Indian Ocean fin rays samples (Young and Drake 2004).
- NMFS estimated higher growth from Hawaiian samples (DeMartini et al. 2007).
- Wang et al. (2010) described an intermediate growth curve (pooled western and eastern samples from the Indian Ocean equatorial region).

Visually, it appears that the NMFS growth curve cannot adequately account for the largest fish in the Indian Ocean very well (but it still might accurately reflect the high growth rates for young individuals).

More recently CSIRO has undertaken a growth study for swordfish in South-West Pacific waters comparing the use of both fin-rays and otoliths samples (Farley et al. 2016). The study found that age estimates from fin rays and otoliths produce different growth curves in the SW Pacific, with discrepancies evident in age classes >7 years for females and >4 years for males. The otolith-based growth curves indicate slower growth and a higher maximum age for both males and females, compared to the ray-based growth curves of Young & Drake (2004) and DeMartini et al. (2007). Although direct validation of the ageing method was not carried out in the study, age estimates from otoliths are likely to be more reliable than fin- rays, especially in larger/older fish, as fin-rays are subject to resorption and vascularisation of the core (Farley et al. 2016).

The biological characteristics of the Hawaiian and Southwest Pacific swordfish may differ considerably from the Indian Ocean, but the methodological differences could also explain the different growth parameter estimates obtained by these studies. Farley et al. (2016) show that the uncertainty in growth estimates that arises from different ageing methodology and protocols are influential in the Southwest Pacific swordfish assessment. Therefore this assessment considered the following five alternative growth estimates (**Figure 7**):

- GaMf – CSIRO estimates from South-East Indian Ocean fin rays samples (Young and Drake 2004).
- GtMf – Taiwan estimates from the Indian Ocean equatorial region fin ray samples (Wang et al. 2010).
- GhMf – NMFS estimates Hawaiian fin rays samples
- GrMf – CSIRO estimates based on SW pacific fin ray samples (Farley el al. 2016).
- GoMf – CSIRO estimates based on SW pacific otolith samples (Farley el al. 2016).

However, the final grid models only included the estimates by Young and Drake (2004) and Wang et al. (2010) because the samples were from the Indian Ocean, and the otolith-based estimates from South-West Pacific by Farley et al. (2016) because the otoliths estimates are likely to be more reliable than fin-rays.

The growth estimates by Farley et al. (2016) were based on orbital fork length (OFL), which were converted to lower jaw fork length (LJFL) units to be consistent with the length data in the assessment. The conversion was based on the relationship used in Davies et al. (2013), where LJFL = 1.0753(OFL + 6.898).

Length-at-age was assumed to be normally distributed around the mean length-at-age relationship with a CV of 15% at age 0, decreasing linearly (in proportion to length) to 10% at age 30+.
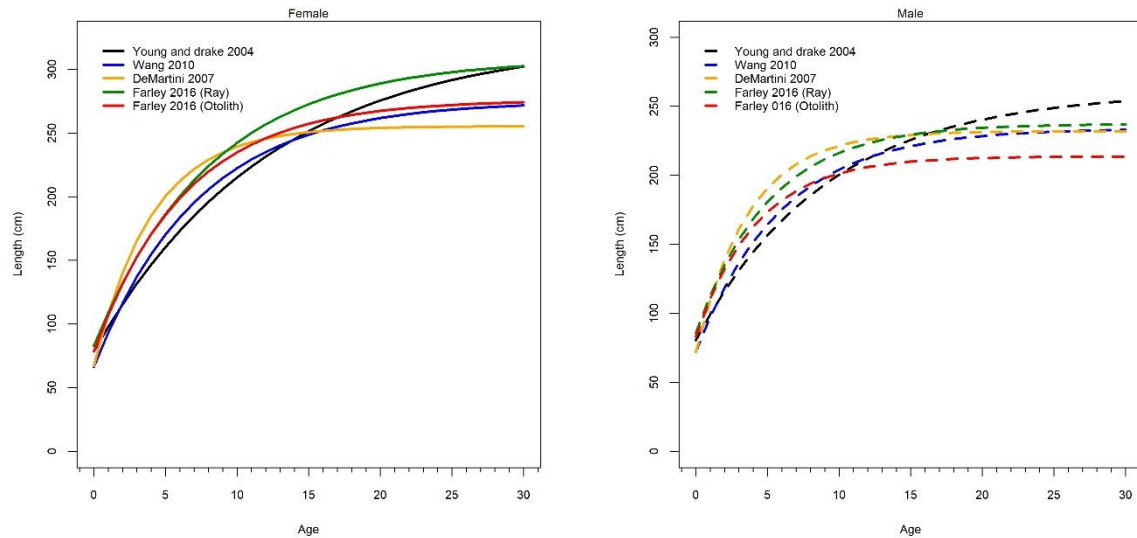


**Figure 7: Growth for female (left) and male (right) swordfish for the five options considered in the assessment: NMFS Hawaii (GhMf), Taiwan Indian Ocean (GtMf) and CSIRO Indian Ocean (GaMf), CSIRO SW Pacific fin rays (GfMf), and CSIRO SW Pacific otolith (GoMf).**

## 3.4 Natural Mortality

Natural mortality estimates for swordfish are highly uncertain given the current methods of age estimation are poorly validated. There are a broad range of M values assumed in other swordfish assessments worldwide, ranging from at least 0.2 – 0.5 (Davies et al. 2013). The value of M=0.25 (constant over ages) was adopted for the Taiwanese Indian Ocean estimates and the two new CSIRO south-west Pacific estimates, to maintain consistency with Wang and Nishida (2010). For the slow growth curve scenario (CSIRO Indian Ocean), M was assumed to be 0.2, and for the fast growth curve scenarios (Demartini et al. 2007), M was assumed to be 0.4.

## 3.5 Maturity

While a number of studies quantify the relationship between size and maturity (and there is some uncertainty here as well, also discussed in Young et al. 2008), the uncertainty of age estimation that undermines the growth relationships also undermines the maturity/fecundity by age relationship. Five relationships were assumed, one for each growth curve (Figure 8):

* GaMf – 50% maturity ~age 10, corresponding to the CSIRO study (mostly based on SW Pacific samples, Young and Drake 200).
* GhMf – 50% maturity ~age 4, logistic function, corresponding with one of the youngest age at maturity schedules used in swordfish assessment, and applied to the NMFS growth curve
* GtMf – 50% maturity ~age 6, logistic function, applied to the Taiwanese growth.
* GrMf – 50% maturity ~age 4.34, logistic function, applied to the CSIRO fin-based growth from SW pacific
* GoMf – 50% maturity ~age 4.42, logistic function, applied to the CSIRO otolith-based growth from SW pacific

The new fin-ray based and otolith based estimates are very similar because the divergence observed in length-at-age from fin-rays and otoliths occurs well after estimated maturity age in females (Farley et al. 2016). These estimates are also similar to the NMFS estimates. There is a clear difference between

the maturity schedule for Young and Drake (2002) and the other studies, but the discrepancy remains unresolved to date.
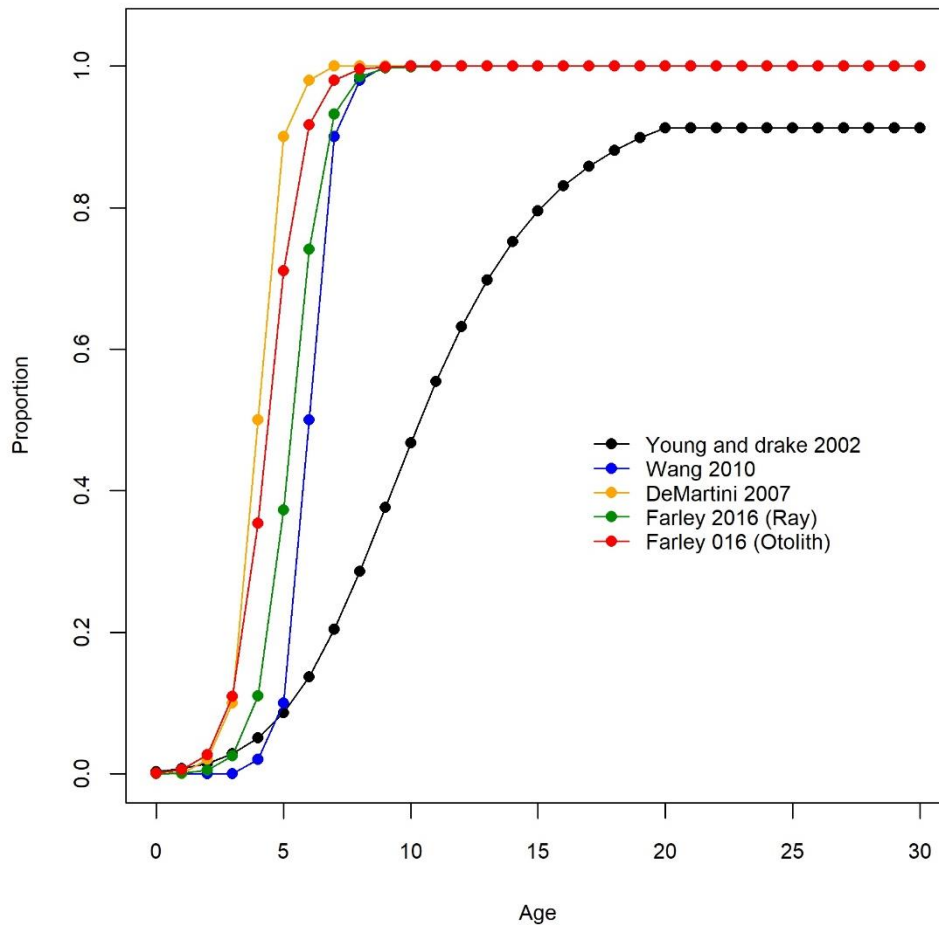


**Figure 8: Maturity for the five growth options: NMFS Hawaii (GhMf), Taiwan Indian Ocean (GtMf) and CSIRO SW Pacific by Young and Drake (2002) (GaMf), CSIRO SW Pacific fin rays by Farley et al. (2016) (GfMf), and CSIRO SW Pacific otolith by Farley et al. (2016) (GoMf).**

## 3.6 Selectivities

Previous assessments found results were insensitive to the selectivity assumptions (age-based vs pseudo-length-based). In 2016 (following 2014 and 2011), only two different size-based "double normal" selectivity curves were estimated, one for longline fleets, and one for the gillnet (and other associated) fleets. The double normal selectivity has considerable freedom to represent a dome-shape, or an approximately logistic curve that either reaches a plateau or is monotonically increasing.

Selectivity was parameterized as a pseudo-length-based function, i.e. the length-based curve is internally converted to an age-based function based on the length-at-age relationship. In this application, the potential benefit of this arises as a result of the sex dimorphism (i.e. two sex-specific age-based selectivity functions are derived from a single length-based selectivity function because of the difference in length-at-age). While the length-based selectivity function often exhibits a very steep ('knife-edge') slope, this is deceptive because there is considerable overlap in length-at-age.

## 3.7 Recruitment

Recruitment was assumed to occur annually at the start of the year. New recruits enter into the population as age-class 1 fish (averaging approximately 70 cm). Annual recruitment deviates from the recruitment relationship were estimated in the model.

A Beverton-Holt stock recruitment relationship was assumed with steepness fixed at a range of options. Spawning biomass was calculated as the biomass of mature females. In the spatially disaggregated model, this represents the sum across all regions. The three steepness options below reflect the fact that steepness is notoriously difficult to estimate, and using a wide range of options probably results in a more realistic representation of the real uncertainty:

- h55: steepness (h=0.55)
- h75: steepness (h=0.75)
- h95: steepness (h=0.95)

There is anecdotal evidence to suggest that spawning (and recruitment) may be out of phase in the southern and northern hemispheres, however, the growth, size sampling and selectivity assumptions are such that the quarterly model explored in 2010 could not provide much insight into recruitment processes. Three different levels of recruitment variability were explored in the uncertainty grid:

- r0: $\sigma_R$ = SD(log(deviates)) = 0, i.e. deterministic recruitment from the stock-recruitment relationship
- r2: $\sigma_R$ = 0.2
- r4: $\sigma_R$ = 0.4

The r4 value has previously been adopted for SWO stock assessments (e.g. Martell 2010, Kolody et al. 2008). However, in this case, we are concerned that this flexibility can result in an over-fitting to poor quality size composition data. Swordfish are often assumed to have lower recruitment variability than tuna populations, and the recent summary of tuna populations suggest that the estimated (annual) variability is often lower than has been a priori assumed in the tuna assessments (ISSF 2011 reports values of 0.2 – 0.5). Complex integrated stock assessments often infer that important population trends are driven by recruitment patterns rather than depletion, and sometimes this inference can be made for the wrong reasons. The r0 option was included to help identify whether this is a concern that requires further investigation. The r0 option is obviously not realistic, but the inferences are useful for understanding the influence of recruitment variability, and the results may be more robust than the stochastic recruitment models in some cases. The r2 option was adopted as an intermediate level of variability.

Recruits in the final two years were deterministic from the stock recruitment relationship, because these cohorts are only weakly observed by the data (and dev vectors constrained to a mean of 0 can take large liberties with unconstrained deviates). The lognormal bias correction term was applied only to the unconstrained recruitment deviates.

Area-specific parameters were estimated to distribute the mean recruitment among regions. In 2010, it was assumed that the distribution among areas remained constant over time. However, the spatial model could not explain the steep CPUE decline in the SW region. Recruitment anomalies by region were estimated with a very high CV (lognormal prior with SD(log(sigma))=99, such that the spatial distribution of recruits was only indirectly constrained by the overall recruitment CV).

## 3.8 CPUE and Catchability

The annual CPUE indices were assumed to be directly proportional to selected abundance mid-year (biomass for the ESP fishery, numbers for all others). It was generally assumed that each informative

CPUE series was highly (unrealistically) informative with observation errors SD(log) = 0.1. We do not really have this much confidence in any of the CPUE series, however, we have even less confidence in the size composition data and other structural assumptions. When a particular CPUE series was assumed to be uninformative, it was heavily down-weighted (lambda = 0.001, or equivalently σ=3.2), but still included in the model, so that the fit of the series could be examined (even though the series would have minimal influence on the parameter estimation).

The following options were explored:
- NT0: Japanese CPUE 1994–2015 treated preferentially (σ = 0.1), others down-weighted (σ = 3.1)
- NT1: Japanese CPUE 1976–1993 and 1994–2015 treated preferentially (σ = 0.1), others down-weighted (σ = 3.1)
- NTP: Japanese CPUE 1994–2015 treated preferentially (σ = 0.1), but indices 2000–2015 in South-west are replaced by Portuguese indices, others down-weighted (σ = 3.1)
- TW0: Taiwanese CPUE 1994–2015 treated preferentially (σ = 0.1), others down-weighted (σ = 3.1)
- TW1: Taiwanese CPUE 1976–1993 and 1994–2015 treated preferentially (σ = 0.1), others down-weighted (σ = 3.1)
- TWP: Taiwanese CPUE 1994–2015 treated preferentially (σ = 0.1), but indices 2000–2015 in South-west are replaced by Portuguese indices, others down-weighted (σ = 3.1)
- A1: Japanese CPUE 1994–2015, Portuguese, Spanish, Indonesian CPUE treated preferentially (σ = 0.1), Taiwanese less so (σ = 0.2)

The rationale for these options are: i) Japanese and Taiwanese CPUE have different trends, it is appropriate to admit them into the assessment as alternatives, ii) the comparison between NT0 and NT1 (and TW0 and TW1) is to illustrate that exclusion or inclusion of early CPUE indices has little effect on the overall model results; iii) NTP and TWP are intended to address the concern of the declining stock abundance in south-west, and we have more confidence in the short Portuguese series than the Japanese and Taiwanese indices (the later submitted CPUE from South African show a very similar trend to the Portuguese indices), iv) A1 is intended to illustrate the effect of including the Spanish and Indonesian series, and the Taiwanese series have generally been given less preferential weight.

The pre-1994 indices between Japanese and Taiwanese indices are not consistent. The large inter-annual fluctuations in both series are not credible. The catch efficiency for swordfish has experienced dramatic changes in the late 1980s and early 1990s with the deveopment of fresh-chill longline fleets which are able to target regions where tuna and swordfish aggregate by deploying shorter sets. The very steep increase in Tanwanese CPUE (and catch) between 1991 and 1992, which is not observed in the JPN fleet, is known to be a shift toward targeting SWO (Kolody 2011). The pre-1994 indices are down-weighted in the reference cases.

All options are examined in exploratory models. Option NTP, TWP, and A1 are considered as reference cases and are included in the final assesssment grid.

Catchability was assumed to be constant over time for all CPUE series. An area-specific scaling was applied to the Japanese CPUE series to convert the density indices to relative abundance indices that are comparable among areas (i.e. CPUE = 1 in the NW region and CPUE =1 in the SW region implies that the two regions have identical abundance, not simply identical density). The scaling factor used are 0.26, 0.27, 0.16, and 0.33 for NW, NE, SW, and SE, respectively (Nishida 2008). This allows catchability to be shared among areas for all of the Japanese fisheries. The shared catchability constraint is often useful for preventing bizarre localised behaviour in spatial models. Note that for models mainly fitted to the Taiwanese series (TW0, TW1, and TWP), the Taiwanese CPUE was adjusted to the mean of the Japanese series in each region and the shared catchability was applied to the Taiwanese CPUE instead.

The common catchability implies that the Japanese CPUE are essentially density estimates (and

abundance if scaled by the area). However, the validity of the assumption that density is uniform within each large sub-region is questionable. Given the nature of the swordfish fishery, it may be unrealistic to expect that swordfish catchability in a northern bigeye fishery has much relation to swordfish catchability in a southern SBT fishery, and the implications of these types of assumption warrant further investigation. The changes in the CPUE standardisation methodologies resulted in very different regional weighting being applied between assessments (see Figure 17 of Sharma (2014) and Figure 13 of Kolody (2011)). In this assessment, sensitivity was conducted to evaluate this assumption. However, the evaluation cannot be done by using separate catchability for each region. It would result in most biomass allocated to one region – a common issue often observed in some multi-area assessments with SS3. Instead, we derived alternative scaling factors using biomass estimated from the sub-regional models (see section 4.1).

## 3.9  Assumptions about the Catch-at-Size data

Size composition was partitioned into 24 bins of width 9 cm (except the first and last), from <45cm to >252 cm). Some of the swordfish sample sizes appear to be very large for some fleets. In the context of separable models (stationary selectivity), a literal interpretation of these very large sample sizes could be misleading in the assessment for a number of reasons, including: i) sampling is probably not truly random, ii) selectivity is probably not stationary (e.g. the spatial distribution of many fleets change over time, and most fleets change targeting practices), and iii) there is considerable uncertainty in the length-at-age relationships and M. To partially account for these problems, each length distribution with fewer than 10 fish was discarded. The input sample sizes (i.e. assumed number of purely random samples in the likelihood terms) were capped at 200 or less (see below). A somewhat arbitrary proportion (0.01) was added to each of the predicted and observed length bins to reduce the influence of outliers.

The influence of the size composition samples on the model behaviour and stock status was examined with 3 options in the exploratory runs

- CL200, sample sizes capped at 200,
- CL020, sample sizes down-weighted by factor of 10, and capped at 20
- CL002, sample sizes down-weighted by factor of 100, and capped at 2.

Francis (2012) developed a method to determine effective sample sizes for composition data in integrated stock assessments. The method was attempted in early model runs, which suggested option CL020 is appropriate. Hence the length-composition data were down-weighted with option CL020 for most models so that it informs the selectivity but the influence on the fit to the abundance data is minimised. Only options CL020 and CL002 were used in final grid models.

## 3.10  Modelling methods, parameters, and likelihood

The model is conditioned on catch (weight), such that it is assumed to be known without error, and extracted perfectly. The SS3 "hybrid" fishing mortality parameterisation was used, where SS3 starts with Pope's approximation and then conducts a fixed number (4) of iterations to approximate instantaneous F from the Baranov catch equation.

Parameters were estimated by minimising the objective function consisting of the following terms:
- Likelihoods
  - Relative abundance indices with lognormal observation errors. Depending on the CPUE option, some of these CPUE series may have been down-weighted to the point that they were uninformative.
  - Length frequencies – multinomial sampling assumptions (with assumed sample sizes << reported sample sizes depending on the option)

- Prior distributions and Penalties:
  - o Annual recruitment deviates (lognormal) from the stock-recruitment relationship.
  - o Every estimated parameter for selectivity, catchability, and R0, requires a prior probability distribution. For these parameters, the prior adopted was very diffuse, such that a bound was likely to be hit before the prior would exert an appreciable influence (e.g. SD = 99).
  - o Weak penalty (e.g. SD = 99) on the spatial distribution of the recruitment deviates in the 4 area model.
  - o Smooth penalties for parameters approaching bounds were adopted, however, bounds were not approached for any of the models discussed here (i.e. presumably because the parameters that are most difficult to estimate were generally fixed (i.e. growth, M, steepness).

The informative parameters estimated by the model included:
- Catchability for the informative CPUE series
- Selectivity parameters
- Virgin recruitment
- Annual recruitment deviations from the stock recruitment relationship
- Annual area-specific recruitment deviations (IO models only)
- Recruitment distribution by area ( IO models only)

Note that SS3 lists additional parameters as being estimated, but they should not have any significant influence on the estimated dynamics (e.g. forecast recruitment deviates).


## 4.  ASSESSMENT MODEL RUNS

The approach we have taken here is to explore a wide range of model assumptions to establish reference cases that represent key model assumptions and plausible parameter configurations, and to identify areas of uncertainty that would impact assessment results. The reference cases are used for examining model fits and diagnostics. Uncertainties are quantified using a grid of models running over permutations of parameters and/or assumption options (an approach commonly used by t-RFMOs in the context of stock assessment, and in the development of operating models for Management Strategy Evaluation).

### 4.1  Exploratory and reference models

Exploratory runs were undertaken to examine the options on:  1) choice of CPUE series as relative abundance indices, 2) growth/maturity/natural mortality, 3) stock-recruitment relationship steepness, 4) recruitment variability, 5) size-frequency sample size. The description of all the models are given in Table 4, including three reference cases and two sensitivity models.

Models 1–6 evaluate options for CPUE series (each is labelled according to the CPUE option). Models NTP, TWP, and A1 are three reference models, with h = 0.75, sigmaR = 0.2, CSIRO Indian Ocean growth estimate (GaMf), size frequency sample size capped at 20 (CL020). NTP is considered as the basic reference case.

Models 7–16 examine options of growth, steepness, recruitment variability and size frequency sample size. Each model usually represents a single change on the aforementioned parameters to the basic reference model.

Models 17–21 are a few additional sensitivities which will be discussed in the results section. M21 used the IOTC disaggregation estimates for the Indonesia fresh tuna longline catch in 2014–2015, and is considered as a sensitivity model.

Models 21–25 are used to evaluate alternative regional weighting of Japanese CPUE, with the following processes:

- Sub-regional models (22–25) were fitted to the catch and observational data in each region. Each model included only the fisheries in that region (e.g. GI and LL fisheries for NW, NE, SE, and six fisheries for SW), and the corresponding Japanese CPUE series 1994–2015. There is no spatial structure within each region, and the Japanese catchability is not constrained. The unfished spawning biomass is estimated for each model.

- The Japanese series 1994–1995 are then rescaled so that the mean of each series is proportional to the unfished spawning biomass estimate from the sub-regional model.

- Model 21 is fitted to the reweighted Japanese CPUE series with a common catchability (similar to the NTP model, the indices 2000–2015 in SW are replaced with Portuguese indices). The model is labelled as rNTP and is also considered as a sensitivity model.

**Table 4: Names and descriptions of the exploratory and reference model runs. The Reference and sensitivity models are in bold and all other runs are one-off sensitivities.**

| Run | Label | Domain | CPUE | Growth | steepness | SigmaR | LF sample Size | Comments |
|-----|-------|--------|------|--------|-----------|--------|----------------|----------|
| M0 | NT0 | IO | NT0 | GaMf | h75 | r2 | CL020 | |
| M1 | NT1 | IO | NT1 | GaMf | h75 | r2 | CL020 | |
| M2 | NTP | IO | NTP | GaMf | h75 | r2 | CL020 | **Reference model** |
| M3 | TW0 | IO | TW0 | GaMf | h75 | r2 | CL020 | |
| M4 | TW1 | IO | TW1 | GaMf | h75 | r2 | CL020 | |
| M5 | TWP | IO | TWP | GaMf | h75 | r2 | CL020 | **Reference model** |
| M6 | A1 | IO | A1 | GaMf | h75 | r2 | CL020 | **Reference model** |
| M7 | GtMf | IO | NTP | GtMf | h75 | r2 | CL020 | |
| M8 | GhMf | IO | NTP | GhMf | h75 | r2 | CL020 | |
| M9 | GrMf | IO | NTP | GrMf | h75 | r2 | CL020 | |
| M10 | GoMf | IO | NTP | GoMf | h75 | r2 | CL020 | |
| M11 | h55 | IO | NTP | GaMf | h55 | r2 | CL020 | |
| M12 | h95 | IO | NTP | GaMf | h95 | r2 | CL020 | |
| M13 | r0 | IO | NTP | GaMf | h75 | r0 | CL020 | |
| M14 | r4 | IO | NTP | GaMf | h75 | r4 | CL020 | |
| M15 | CL002 | IO | NTP | GaMf | h75 | r2 | CL002 | |
| M16 | CL200 | IO | NTP | GaMf | h75 | r2 | CL200 | |
| M17 | selectivity | IO | NTP | GtMf | h75 | r2 | CL020 | separate selectivity for JPLL_SW |
| M18 | GtMf-f | IO | NTP | GtMf | h75 | r2 | CL020 | Young and Drake (2002) maturity |
| M19 | GoMf-f | IO | NTP | GoMf | h75 | r2 | CL020 | Young and Drake (2002) maturity |
| M20 | IND catch | IO | NTP | GaMf | h75 | r2 | CL020 | **sensitivity model**, IOTC catch estimates for IND |

| | | | | | | | | |
|---|---|---|---|---|---|---|---|---|
| M21 | rNTP | IO | rNTP | GaMf | h75 | r2 | CL020 | **sensitivity model**, JPN indices rescaled |
| M22 | NW | NW | UJPLL_NW | GaMf | h75 | r2 | CL020 | |
| M23 | NE | NE | UJPLL_NE | GaMf | h75 | r2 | CL020 | |
| M24 | SW | SW | UJPLL_NE | GaMf | h75 | r2 | CL020 | |
| M25 | SE | SE | UJPLL_SE | GaMf | h75 | r2 | CL020 | |

## 4.2 Quantification of uncertainty

For each of the reference and sensitivity models, an examination of uncertainty in the model structure was integrated into a single analysis that explored the interactions of the assumptions tested in the exploratory runs. In each case, these interactions were tested in a grid of 54 combinations of the various options for each of the four parameter factors (steepness, growth, recruitment variability, and catch-at-length sample size), i.e. a separate model was run for each combination in the grid. This is useful to determine if there are particular interactions between model assumptions. Reference cases NTP, TWP, and A1 were also integrated into a larger assessment grid (IO-grid, 162 models) so that the uncertainly in CPUE series can also be expressed in the estimated stock status. The Grid-IO is considered to be the main assessment grid for summarising model outputs. Model configuration combinations for these assessment grids are summarised in Table 5.

It is clear that there are large uncertainties in the biology and data that underpin this assessment, such that it would be difficult to defend the selection of a unique model to adequately represent the stock status. The models in the assessment grid were not assumed to have equal plausibility, and relative weight was predefined for the factors examined, or the options within each. Table 6 shows the weighting scheme adopted for the synthesis of stock status results and the Kobe 2 Strategy Matrix. The weighting is unavoidably subjective.

**Table 5: Model configuration combinations used in assessment grids (where a grid represents the list of models with a balanced design of all possible permutations of the indicated options). Grid-catch has the same configuration as grid-NTP except that it used the IOTC disaggregated catch estimates in 2014-2015 for the Indonesian fresh tuna longline fleets.**

| | | | | | Assessment Grid | | |
|---|---|---|---|---|---|---|---|
| Configuration | | Grid-NTP | Grid-TWP | Grid-A1 | Grid-IO | Grid-rNTP | Grid-catch |
| Domain | | IO | IO | IO | IO | IO | IO |
| CPUE option | | NTP | TWP | A1 | NTP TWP A1 | *rNTP | NTP |
| Growth | | GaMf, GtMf, GoMf | GaMf, GtMf, GoMf | GaMf, GtMf, GoMf | GaMf, GtMf, GoMf | GaMf, GtMf, GoMf | GaMf, GtMf, GoMf |
| steepness | | h55, h75, h95 | h55, h75, h95 | h55, h75, h95 | h55, h75, h95 | h55, h75, h95 | h55, h75, h95 |
| SigmaR | | r0, r2, r4 | r0, r2, r4 | r0, r2, r4 | r0, r2, r4 | r0, r2, r4 | r0, r2, r4 |
| LF sample Size | | CL020, CL002 | CL020 CL002 | CL020, CL002 | CL020, CL002 | CL020, CL002 | CL020, CL002 |

* The Japanese series 1994–1995 rescaled so that the mean of each series is proportional to the unfished spawning biomass estimate from the corresponding sub-regional model.

**Table 6: Weighting scheme for the models represented in the final stock status synthesis for the assessment grids and used in the Kobe-2 Strategy Matrix.**

| | | | | | | | Assessment grid |
|---|---|---|---|---|---|---|---|
| Configuration | | Grid-NTP | Grid-TWP | Grid-A1 | Grid-IO | Grid-rNTP | Grid-catch |
| Steepness | h55 | 0.2 | 0.2 | 0.2 | 0.2 | 0.2 | 0.2 |
| | h75 | 0.6 | 0.6 | 0.6 | 0.6 | 0.6 | 0.6 |
| | h95 | 0.2 | 0.2 | 0.2 | 0.2 | 0.2 | 0.2 |
| Growth | GaMf | 0.4 | 0.4 | 0.4 | 0.4 | 0.4 | 0.4 |
| | GtMf | 0.4 | 0.4 | 0.4 | 0.4 | 0.4 | 0.4 |
| | GoMf | 0.2 | 0.2 | 0.2 | 0.2 | 0.2 | 0.2 |
| CPUE | NTP | 1 | | | 0.5 | | 1 |
| | TWP | | 1 | | 0.2 | | |
| | A1 | | | 1 | 0.3 | | |
| | rNTP | | | | | 1 | |
| SigmaR | r0 | 0.2 | 0.2 | 0.2 | 0.2 | 0.2 | 0.2 |
| | r2 | 0.4 | 0.4 | 0.4 | 0.4 | 0.4 | 0.4 |
| | r4 | 0.4 | 0.4 | 0.4 | 0.4 | 0.4 | 0.4 |
| LF sample size | CL020 | 0.8 | 0.8 | 0.8 | 0.8 | 0.8 | 0.8 |
| | CL002 | 0.2 | 0.2 | 0.2 | 0.2 | 0.2 | 0.2 |

## 4.3  Projections and Kobe 2 Strategy Matrix

Projections were conducted from the MPD estimates of all grid models at catch levels of 60%, 80%, 100%, 120% and 140% of 2015 levels (assuming 2015 selectivity and catch allocations among fisheries). The projections used deterministic recruitment from the stock recruitment relationship (starting in 2013). This approach ignores two important sources of uncertainty: statistical uncertainty in the parameter estimates, and recruitment variability. However, the approach does incorporate the model selection uncertainty, which is usually greater than both of these sources of uncertainty in most cases. However, if the model selection process results in a very small subset of heavily weighted models, or important decision are required in relation to the tails of the distribution, the additional sources of uncertainty should be considered. Three and ten year projection results are summarised in a management decision table (Kobe 2 Strategy Matrix), i.e. The projections are summarised in terms of a weighted average of results that describe the proportion of scenarios in which SPB(2015)<SPB(MSY), SPB(2025)<SPB(MSY)  F(2015)>F(MSY), F(2025)>F(MSY)

## 5. RESULTS

We discuss the main results of exploratory and reference model runs below. Given the large number and complexity of the models, it is not possible to show all the details, we mainly address the key aspects or emphasise the main points of interest. Most diagnostics plots including model comparisons are given in Appendix A, and those related to reference and sensitivity models are given in the section below. Estimates of management quantities for the exploratory, reference and sensitivity models are shown in Table 7.

### 5.1 Exploratory and reference models

The profile likelihood on R0 from the reference model NTP did not suggest minimisation failure, and there is no apparent conflict among various sources of likelihood components, more importantly between the abundance and length frequency data (Figure 9).

CPUE and LF weighting
Both NT0 (Japanese CPUE 1994–2015) and NT1 (Japanese CPUE 1979–2015, as two series) fitted the indices very well (Figure A1). In some areas pre-1994 indices do not seem to be consistent with SWO reproductive dynamics, the large inter-annual changes in abundance are not explained by the catch but rather by recruitment anomalies. This is also the case for models fitted mainly to the Taiwanese series (TW0 and TW1, see Figure A2). In these models, inclusion or exclusion of the early CPUE doesn't appear to have a significant impact on current stock status (it does alter the biomass trend prior to 1994). In view of these results, reference models NTP (Figure 10), TWP (Figure A3), and A1 (Figure A4) have down-weighted the pre-1994 CPUE for both Japanese and Taiwanese fleet ($\sigma$=3.2).

Model NTP fitted both the Japanese and Portuguese CPUE series reasonably well, but it is generally not able to fit the large initial drop in the north-west and south-west, nor the large increase in north-east over the last two years (Figure 10–left). The standardised residuals show no apparent pattern (Figure 10-right). Model TWP also showed good fits to the Taiwanese series (Figure A3). Apparently allowing for time-varying distribution of recruits by area help the model to explain the different trend amongst regions. Model A1 has worse fits to most CPUE series than other models, and the fits appear to be driven mostly by the Japanese CPUE (Figure A4).

For Model NTP, the fits to the catch-at-length capture the gross features of the data, but the fits are not great (Figure 11–left). In general, the fits for the EU and IS fleets were much better. The model tend to over-estimate annual mean length for the GI, LL_NW, and LL_NE fleets, but underestimate the mean length for the JPLL_SW fleet (Figure 11–right). If we increase the sample size for GI fleet, and use a separate selectivity for JPLL_SW (exploratory model 'selectivity'), the model can improve the fits to the gillnet data, and also reduce the bias in the predicted mean length for the LL_NW, LL_NE, and JPLL_SW fisheries (Figure A5), but the fit to the actual length distribution for JPLL_SW is worse. The JPLL_SW length samples appear to have a wider distribution, with proportionally more fish greater than 200 cm. Maybe a more flexible selectivity should be used for JPLL_SW, but we do not expect this to change the assessment results much because the swordfish catch by the Japanese longline fleet in the south-west was very small.

We also would not want to increase the sample size for the size data. A large sample size (CL200) generated more recruitment anomalies (Figure A6–right), indicating that the model may have over-fitted to the noise in the data. When sample size is capped at 20 or smaller (CL020, CL002), the recruitment deviations are mostly driven by the CPUE trend; when the sample size is capped at 200, the recruitment deviations are driven by the size frequency data (see Figure A6). This is also evident in Figure A7, which shows that although more weight on the LF data can reduce the bias in the predicted mean annual length (Figure A7–left), it will lead to poor fits to the CPUE series (Figure A7–right). Therefore option CL200 is not considered further in the assessment grid.

Estimated recruitment deviations are shown in Figure 12. There is a very strong signal suggesting that recruitment was very high immediately prior to the start of the targeted fishery in the 1990s, followed by anomalously low recruitment. This trend is suspicious, but without the recruitment anomalies, the model could not provide a reasonable fit to the CPUE series. It was expected that the recruitment signal might be corroborated by the size data, but there was not a strong signal in mean sizes, except that the observed mean size for EUEL_SW and LL_SE fleet showed some decline through the 2000s (see Figure 11–left)). The distribution of recruits show very similar patterns among regions (see Figure 11-right).

Figure 13 showed typical size-based selectivity estimates for the longline and gillnet associated fisheries. The dome-shaped pattern may be consistent with the size/sex-based partitioning of the species, in which the largest, predominantly female individuals tend to be caught in the extremes of the range (at least in the south Pacific). However, the dome shape can also arise as an artefact of errors in the specification of growth and natural mortality (including variability in M by age). The selectivity estimates were stable across the model runs examined.

This model (NTP) suggests that the population in the southern regions is considerably lower than the northern regions (Figure 14). The most notable features are the big increase in the population estimated around the early 1990s (the beginning of the targeted fishery), the general decline in all regions over the next 20 years, and the decline in the SW region that seems to have continued over the last five years (apparently it depends on which CPUE series are used for SW, e.g. see Figure A8–left). Models based on Taiwanese indices estimated much lower biomass for all regions (Figure A8–right), and both TW0 and TW1 estimated that the current spawning biomass in south west is less than 10% of the unfished level.

Growth and maturity

The five different growth options resulted in very different biomass estimates (Figure A9-left). Both the fin-ray based and otolith-based growth from SW Pacific samples resulted in much higher biomass estimates than the other growth options. Estimated spawning biomass using the otolith-based growth (GoMf) is more than twice the SSB using the CSIRO Indian Ocean growth (GaMf). However, further investigation showed that the difference is mostly caused by the discrepancy in maturity schedule associated with those options. The difference in estimated SSB between these models is much smaller if the same maturity schedule is used (Figure A9-right)

Alternative catch estimates

The sensitivity model (INDcatch) that used a higher catch estimate for 2014–2015 for the LL_NE fishery, estimated a biomass trend very similar to the model that used a lower catch estimate. The result is not too surprising, as catch is the 'scalar' of biomass, and the use of higher catch estimates has increased the biomass across all regions (Figure 16), mitigating the effect on stock status of using higher catch estimates (Note that the Japanese CPUE indices are high in 2014 and 2015 in the North east region). Additional analyses show that if we exclude the Japanese CPUE indices in 2014 and 2015, the model using the higher catch estimate will have almost identical biomass estimate to the model with the lower catch estimate up to year 2014, but the biomass at the beginning of 2015 will be approximately 7000t less (Figure A10). The effect of using the higher catch estimate is more pronounced in the projection period (see Figure A10), assuming future catches remains at the 2015 level.

CPUE regional weighting

The four sub-regional models (NW, NE, SW, SE, see Table 4) fitted the Japanese indices reasonably well although some lack of fit is also evident in the last few years (Figure A11–left). These independent models suggest NE has the highest biomass overall, followed by NW, SW, and SE. Model rNTP, based on the re-scaled Japanese CPUE, estimated very similar biomass to the sub-regional models (Figure A11–right), but much lower biomass than the NTP model in all regions, and the current spawning biomass is estimated to be less than 30% B0 (Figure 17, Table 7)
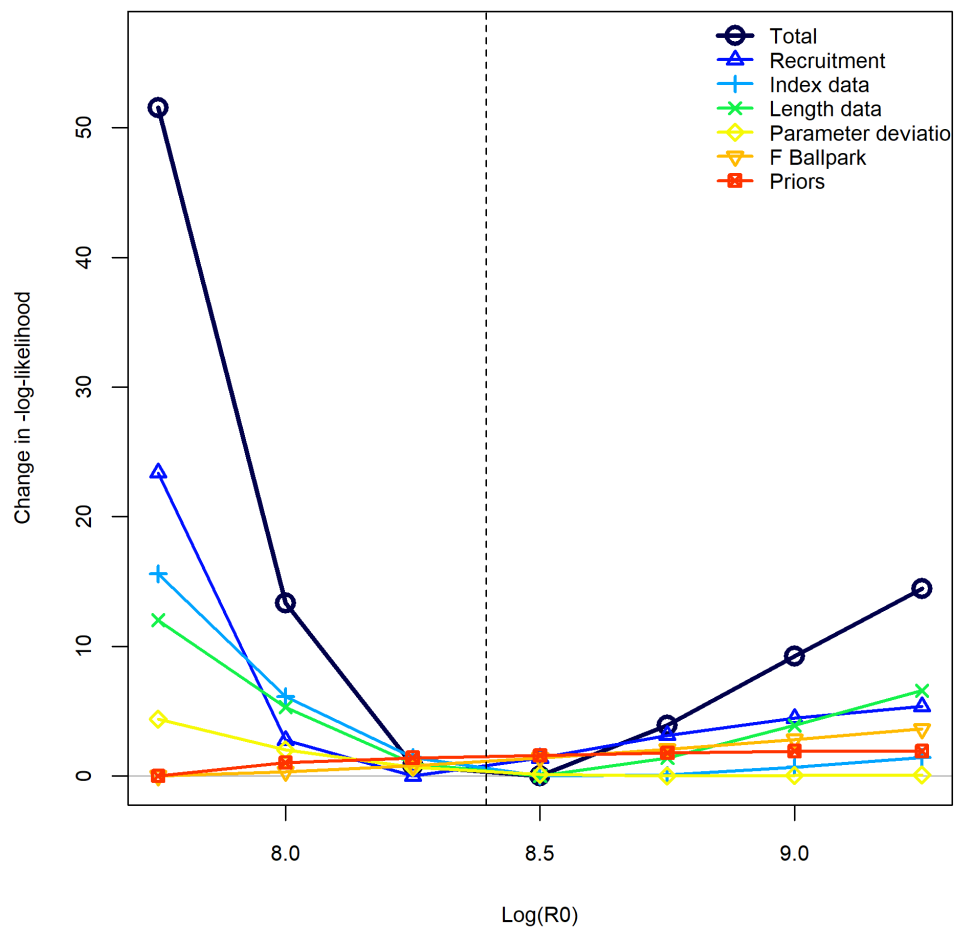
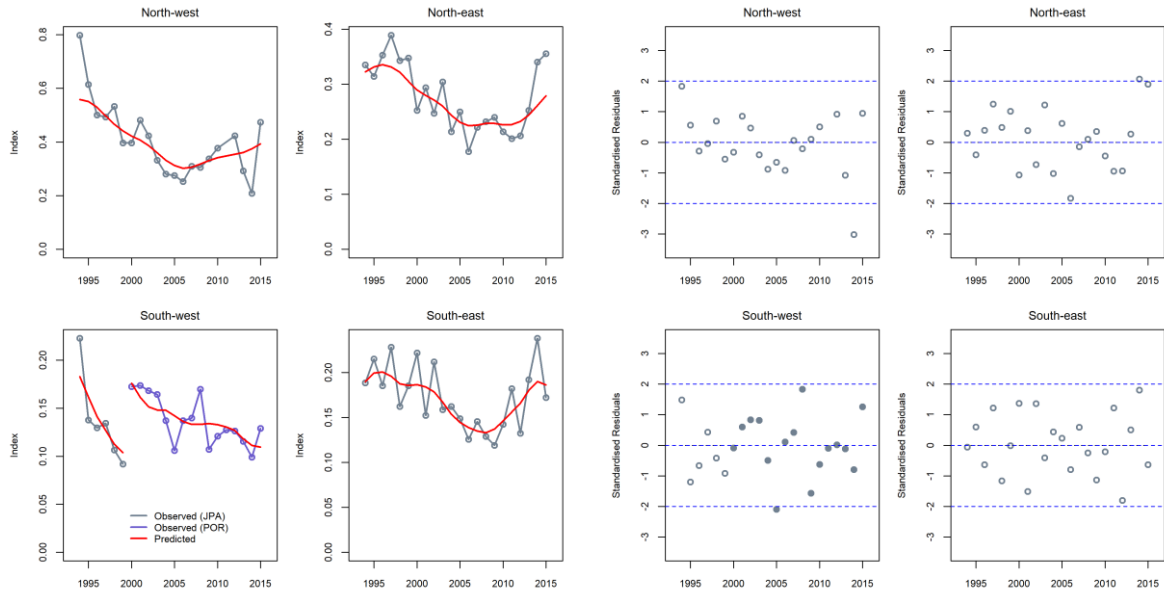**Figure 9: Likelihood profile on R0 from reference model NTP.**

**Figure 10: Fits to Japanese and Portuguese CPUE series by region for reference model NTP (left), and the standardised residuals from the fits (right).**
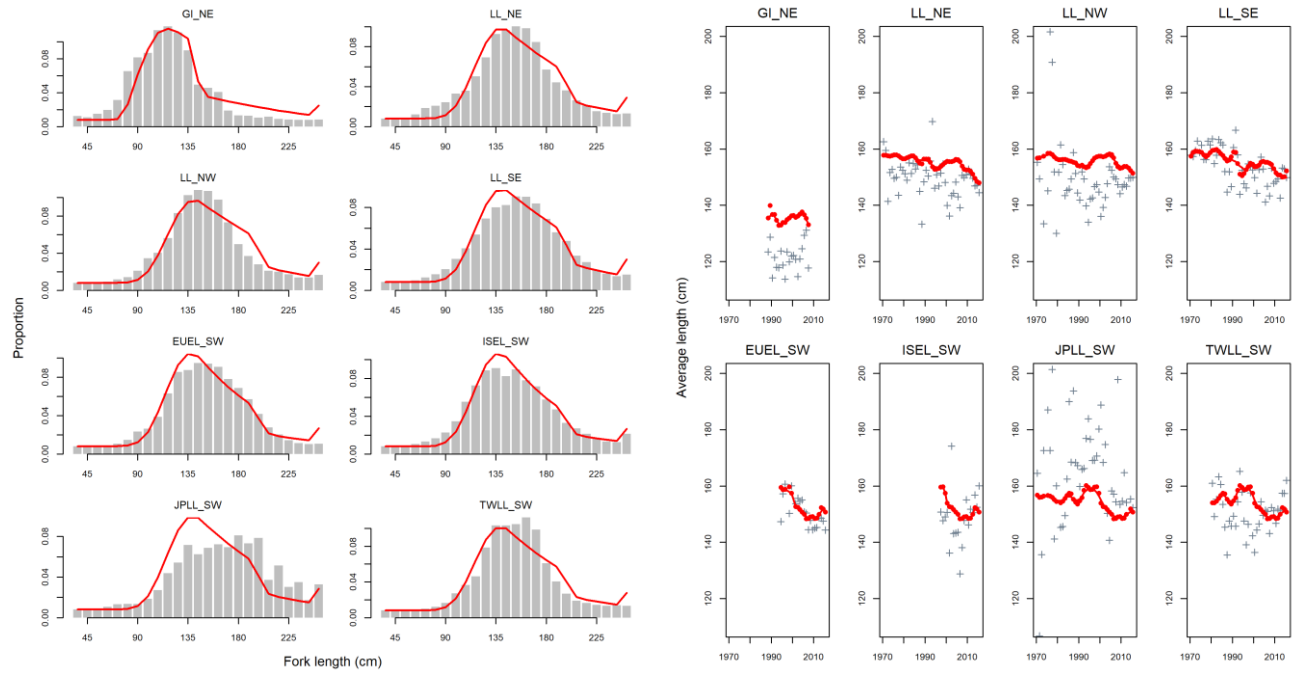


**Figure 11: Fits to aggregated length frequency (left) and to the mean length distribution (right) by fishery (left) for reference model NTP.**
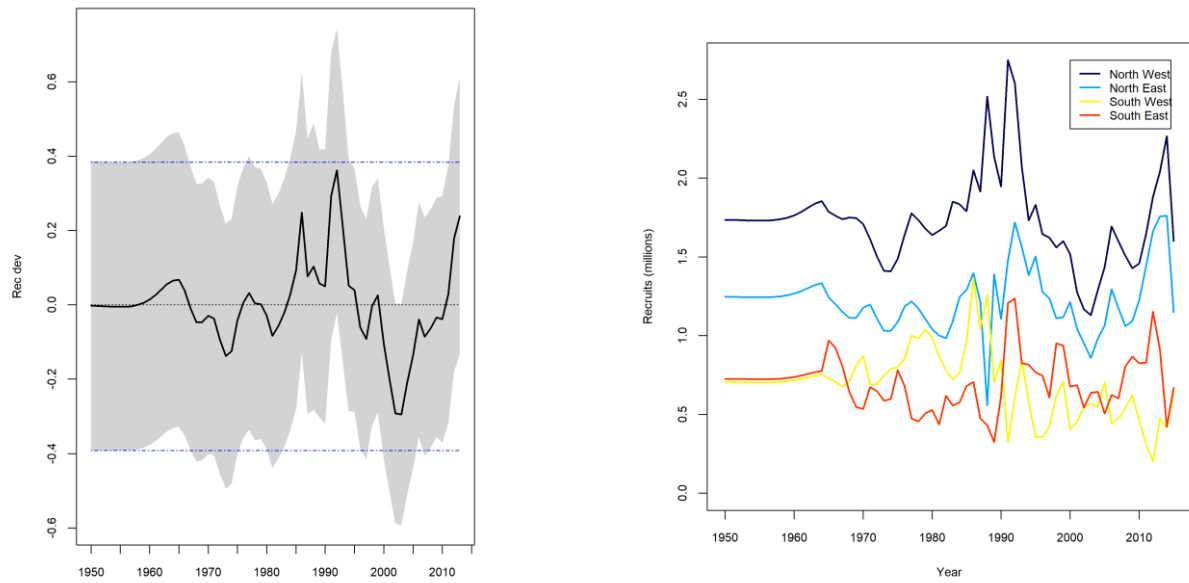
**Figure 12: Estimated recruitment deviations for reference model NTP (left) and estimated annual recruits by region (right). The shaded area represents uncertainty estimates from the MPD model fits.**
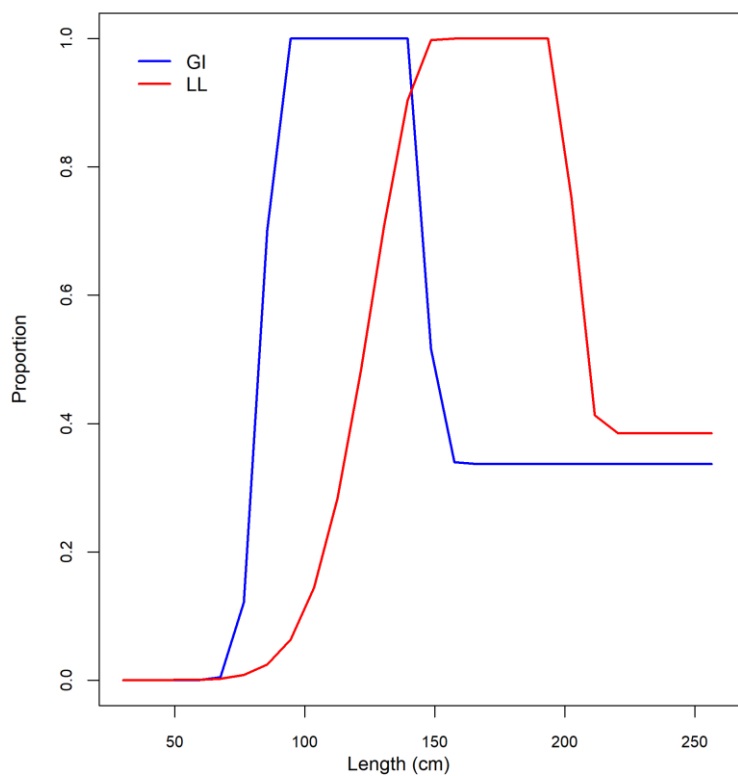


**Figure 13: Estimated double-normal selectivity for the Gillnet and Longline fleets for model NTP.**
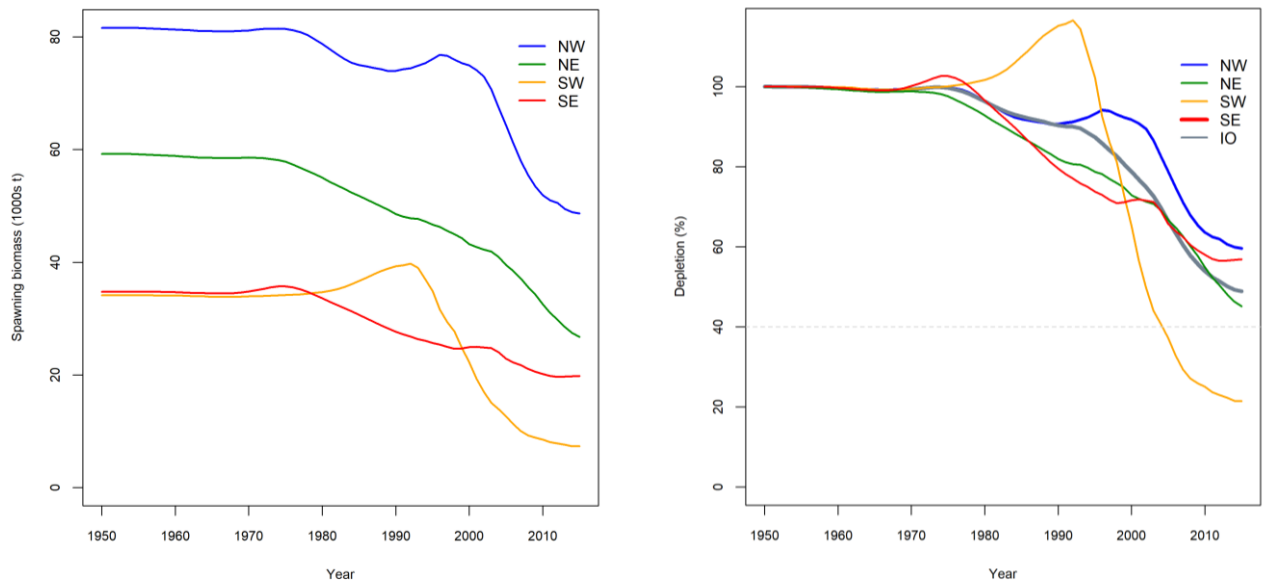
**Figure 14: Estimated Spawning biomass by region (left), and estimated depletion by region as well as overall depletion for the Indian Ocean for reference model NTP (right).**
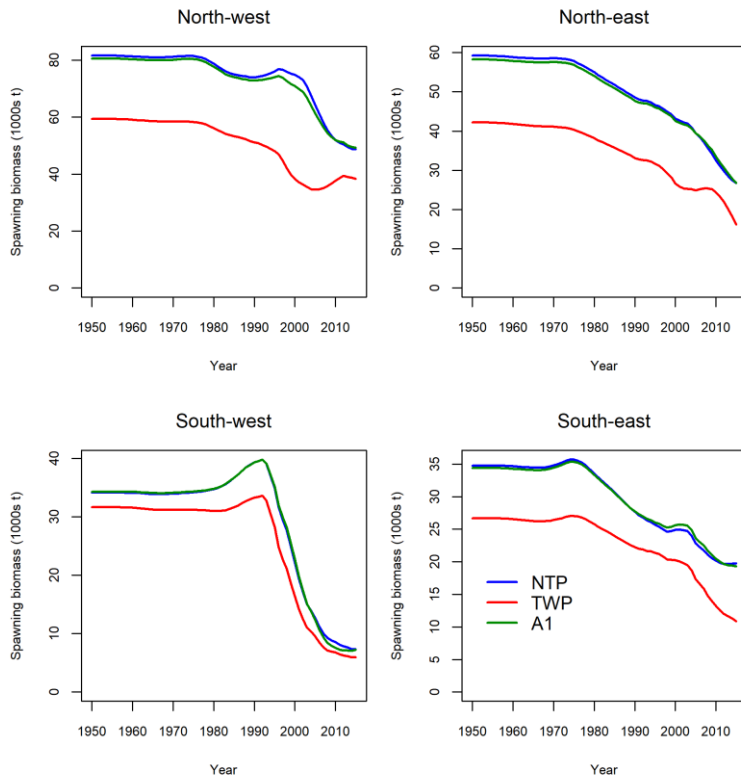


**Figure 15: Comparison of estimated Spawning biomass by region between reference models NTP, TWP, and A1.**
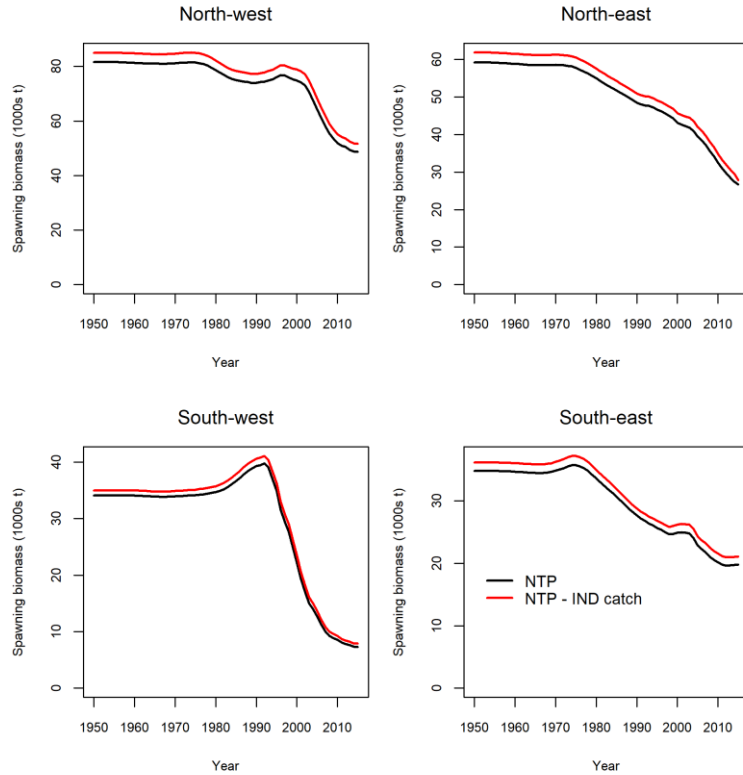
**Figure 16: Comparison of estimated spawning biomass by region between reference model NTP (lower catch estimate) and sensitivity IND catch (higher catch estimate).**
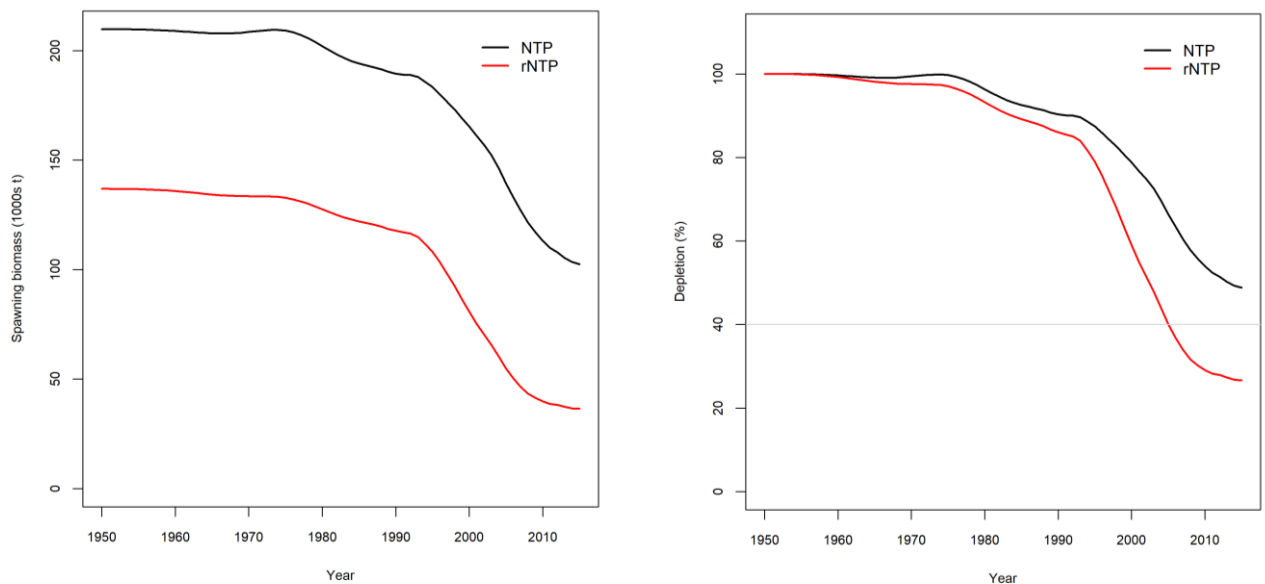


**Figure 17: Comparison of estimated total spawning biomass (left) and depletion (right) for the Indian Ocean between reference model NTP and sensitivity rNTP.**

**Table 7: Estimates of management quantities for the reference case and key model runs. Shaded rows are reference models.**

| Run | Label | Likelihood | C2015 (000) | MSY (000) | C2015 /MSY | F2015 | Fmsy | F2015 /Fmsy | SSB2015 (000) | SSBmsy (000) | SSB0 (000) | SSB2015 /SSBmsy | SSB2015 /SSB0 | SSBmsy/ SSB0 | B2015 (000) | B0 (000) | B2015 /B0 |
|-----|-------|-----------|------|------|------|------|------|------|------|------|------|------|------|------|------|------|------|
| M0 | NT0 | 535.9 | 34 | 39 | 0.89 | 0.05 | 0.11 | 0.47 | 110 | 51 | 217 | 2.17 | 0.51 | 0.23 | 650 | 992 | 0.66 |
| M1 | NT1 | 497.6 | 34 | 40 | 0.85 | 0.05 | 0.11 | 0.44 | 120 | 53 | 228 | 2.26 | 0.53 | 0.23 | 695 | 1039 | 0.67 |
| M2 | NTP | 536.3 | 34 | 37 | 0.92 | 0.05 | 0.11 | 0.50 | 102 | 49 | 210 | 2.09 | 0.49 | 0.23 | 604 | 957 | 0.63 |
| M3 | TW0 | 573.2 | 34 | 28 | 1.20 | 0.09 | 0.11 | 0.79 | 71 | 38 | 160 | 1.89 | 0.44 | 0.23 | 376 | 731 | 0.51 |
| M4 | TW1 | 576.8 | 34 | 29 | 1.17 | 0.08 | 0.11 | 0.73 | 80 | 39 | 165 | 2.06 | 0.48 | 0.24 | 413 | 753 | 0.55 |
| M5 | TWP | 512.4 | 34 | 28 | 1.20 | 0.08 | 0.11 | 0.78 | 71 | 37 | 160 | 1.90 | 0.45 | 0.23 | 387 | 730 | 0.53 |
| M6 | A1 | 598.2 | 34 | 37 | 0.93 | 0.05 | 0.11 | 0.52 | 103 | 49 | 208 | 2.11 | 0.49 | 0.23 | 589 | 947 | 0.62 |
| M7 | GtMf | 496.5 | 34 | 44 | 0.77 | 0.06 | 0.14 | 0.41 | 146 | 67 | 279 | 2.19 | 0.52 | 0.24 | 574 | 861 | 0.67 |
| M8 | GhMf | 500.2 | 34 | 86 | 0.40 | 0.04 | 0.21 | 0.18 | 206 | 72 | 308 | 2.86 | 0.67 | 0.23 | 841 | 1068 | 0.79 |
| M9 | GrMf | 545.9 | 34 | 58 | 0.59 | 0.04 | 0.14 | 0.27 | 283 | 114 | 455 | 2.47 | 0.62 | 0.25 | 831 | 1176 | 0.71 |
| M10 | GoMf | 528.9 | 34 | 68 | 0.50 | 0.03 | 0.15 | 0.23 | 337 | 131 | 519 | 2.57 | 0.65 | 0.25 | 949 | 1294 | 0.73 |
| M11 | h55 | 536.8 | 34 | 28 | 1.23 | 0.05 | 0.06 | 0.80 | 108 | 72 | 225 | 1.51 | 0.48 | 0.32 | 625 | 1028 | 0.61 |
| M12 | h95 | 536.3 | 34 | 50 | 0.68 | 0.05 | 0.20 | 0.27 | 101 | 24 | 203 | 4.29 | 0.50 | 0.12 | 600 | 926 | 0.65 |
| M13 | r0 | 626.1 | 34 | 28 | 1.22 | 0.09 | 0.11 | 0.82 | 61 | 37 | 156 | 1.67 | 0.39 | 0.23 | 372 | 713 | 0.52 |
| M14 | r4 | 545.0 | 34 | 40 | 0.86 | 0.05 | 0.11 | 0.45 | 112 | 52 | 223 | 2.14 | 0.50 | 0.23 | 670 | 1019 | 0.66 |
| M15 | CL002 | -30.6 | 34 | 32 | 1.07 | 0.07 | 0.10 | 0.67 | 70 | 42 | 176 | 1.68 | 0.40 | 0.24 | 460 | 804 | 0.57 |
| M16 | CL200 | 4818.3 | 34 | 50 | 0.68 | 0.03 | 0.11 | 0.33 | 178 | 68 | 290 | 2.61 | 0.61 | 0.24 | 929 | 1322 | 0.70 |
| M17 | selectivity | 4228.5 | 34 | 54 | 0.63 | 0.03 | 0.10 | 0.29 | 208 | 76 | 321 | 2.74 | 0.65 | 0.24 | 1088 | 1463 | 0.74 |
| M18 | GtMf-f | 554.4 | 34 | 37 | 0.91 | 0.05 | 0.11 | 0.48 | 87 | 42 | 172 | 2.10 | 0.51 | 0.24 | 600 | 989 | 0.61 |
| M19 | GoMf-f | 542.1 | 34 | 44 | 0.77 | 0.04 | 0.11 | 0.39 | 131 | 56 | 233 | 2.33 | 0.56 | 0.24 | 757 | 1132 | 0.67 |
| M20 | IND catch | 538.7 | 42 | 39 | 1.08 | 0.06 | 0.11 | 0.59 | 108 | 51 | 218 | 2.12 | 0.50 | 0.23 | 634 | 995 | 0.64 |
| M21 | rNTP | 527.6 | 42 | 24 | 1.71 | 0.11 | 0.11 | 1.09 | 36 | 32 | 137 | 1.14 | 0.27 | 0.23 | 281 | 624 | 0.45 |
| M22 | NW | 169.4 | 11 | 6 | 1.67 | 0.18 | 0.10 | 1.75 | 8 | 9 | 36 | 0.89 | 0.21 | 0.24 | 59 | 166 | 0.36 |
| M23 | NE | 161.3 | 13 | 8 | 1.53 | 0.12 | 0.10 | 1.11 | 15 | 11 | 47 | 1.39 | 0.33 | 0.23 | 111 | 216 | 0.52 |
| M24 | SW | 364.5 | 4 | 6 | 0.63 | 0.06 | 0.11 | 0.54 | 8 | 7 | 31 | 1.16 | 0.27 | 0.23 | 65 | 143 | 0.45 |
| M25 | SE | 136.6 | 5 | 4 | 1.09 | 0.07 | 0.10 | 0.71 | 10 | 6 | 24 | 1.71 | 0.40 | 0.23 | 66 | 111 | 0.59 |

## 5.2 Summary of stock status

A time series of stock status and other management reference values estimated from the reference and sensitivity grids are shown in Figure 18 (all models equally weighted). Each plot shows the summary of 54 models (Grid-IO is combination of Grid-NTP, Grid-TWP, and Grid-A1, and consists of 162 models in total). Using the weighting scheme from Table 6, the biomass and F time series are shown with the Kobe plots in Figure 19. Common stock status reference points are summarized in Table 8 and the projection results are summarised in the Kobe 2 Strategy Matrix in Table 9.

It is clear that the MPD estimates from almost all the runs suggest that SSB2015>SSBMSY, and most (considerable more than 50%) suggest that F2015<FMSY. However, most models for sensitivity Grid-rNRP, suggest that F2015>FMSY (more than 50%).

The CPUE options A1, NT resulted in very similar stock status estimates in general, but option TWP resulted in slightly more pessimistic stock status. Most models from Grid-NTP and Grid-A1 suggested that biomass will increase slightly and fishing mortality will remain relatively stable if 2015 catch level is maintained (Figure 18). Grid-TWP suggested that biomass will decrease and fishing mortality will increase at the current catch level. For Grid-catch and Grid-rNTP also suggested that biomass will decrease and fishing mortality will increase if the catch remains the same.

Kobe plots for each assessment grid are presented in Figure 19, after the models are weighted by a plausibility scheme (see Table 6). The Kobe plots for five of the six assessment grids suggest that the stock is not overfished and overfishing has not occurred. For Grid-IO, SSB2015/SSBMSY is estimated to be 2.30 with a 90% quantile range 1.32–4.52, and F2015/FMSY is estimated to be 0.57 with a 90% quantile range 0.22–1.09 (Table 8). The Kobe plot for grid-rNTH suggest that the stock is not overfished but overfishing has occurred, with SSB2015/SSBMSY estimated to be 1.40 (0.92–2.54), and F2015/FMSY estimated to be 1.07 (0.62–1.51).

The estimates of MSY, F(T)/FMSY) and SSB(T)/SSBMSY were generally influenced by the same assumptions in the same direction. More pessimistic results were generally associated with lower steepness, slower growth/low M, reduced recruitment variability and lower assumed size composition sample sizes (Figure 20). Time series of SSB(T)/SSBMSY formed into a few distinctive clusters as separated by a combination of steepness and growth parameters (Figure 21). However, the estimated level of depletion is least sensitive to the steepness assumption.

It is well known that a key parameter determining the value of the ratio SSBMSY/SSB0 is the shape of the stock-recruitment relationship (e.g. Punt et al., 2008). SSBMSY/SSB0 was estimated to be 0.23 for h=0.75. With h=0.55, the SSBMSY occurred at about 35%B0; with h=0.95, SSBMSY occurred at about 10% B0 (Figure 22). The SWO assessment in the South West Pacific (Davies et al. 2013) estimated that SSBMSY ranged between 0.15 and 0.30 of B0.
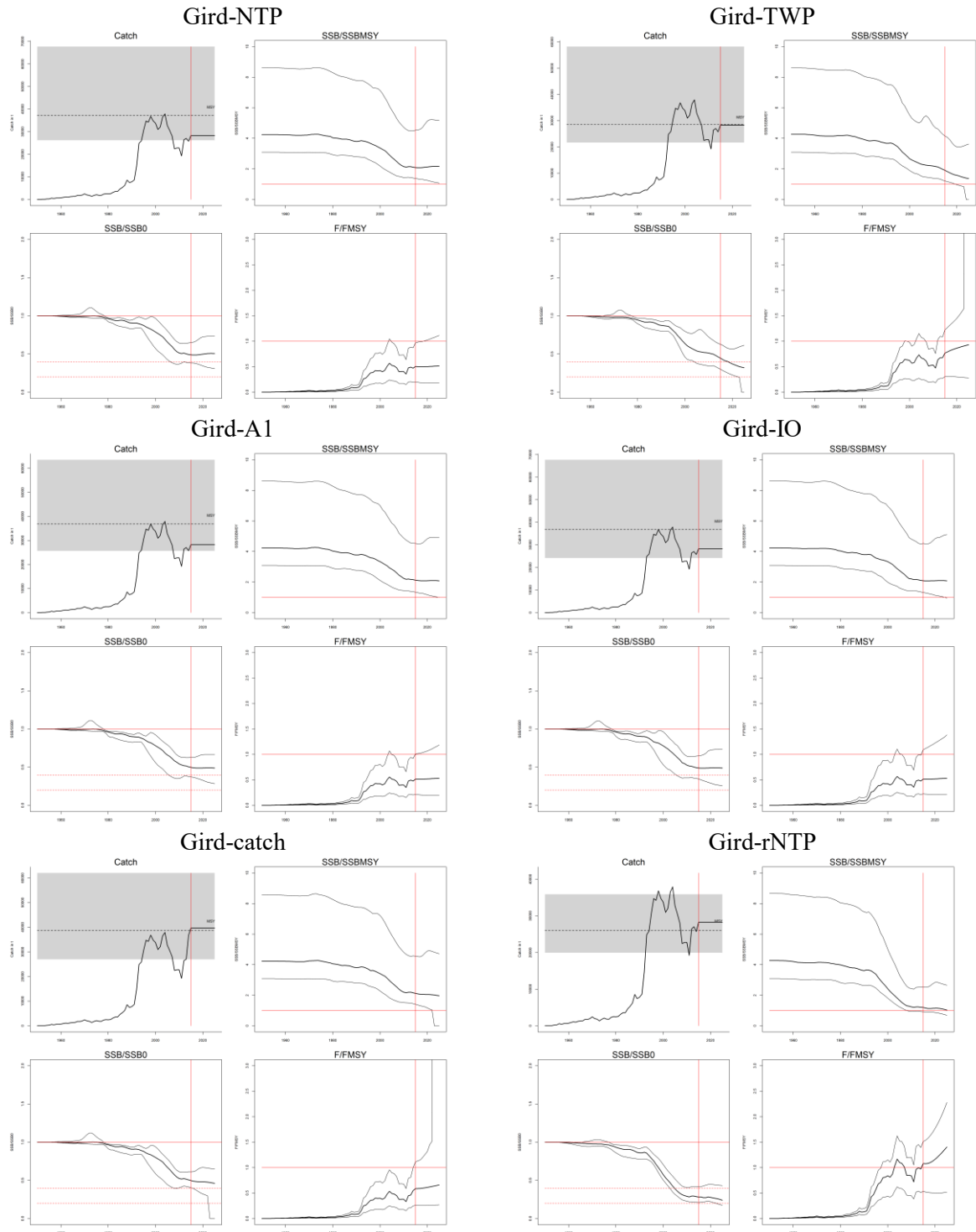
**Figure 18: Stock status summary for the whole Indian Ocean for each of the assessment grids. Thick black lines in the time series plots represent the median of the weighted aggregate results, thin lines represent 5th and 95th percentiles. In the catch plot, dotted lines represent weighted mean MSY, the shaded area represents 5th and 95th percentiles. The red vertical line indicate the start of projection years (10 year projection at current catches).**
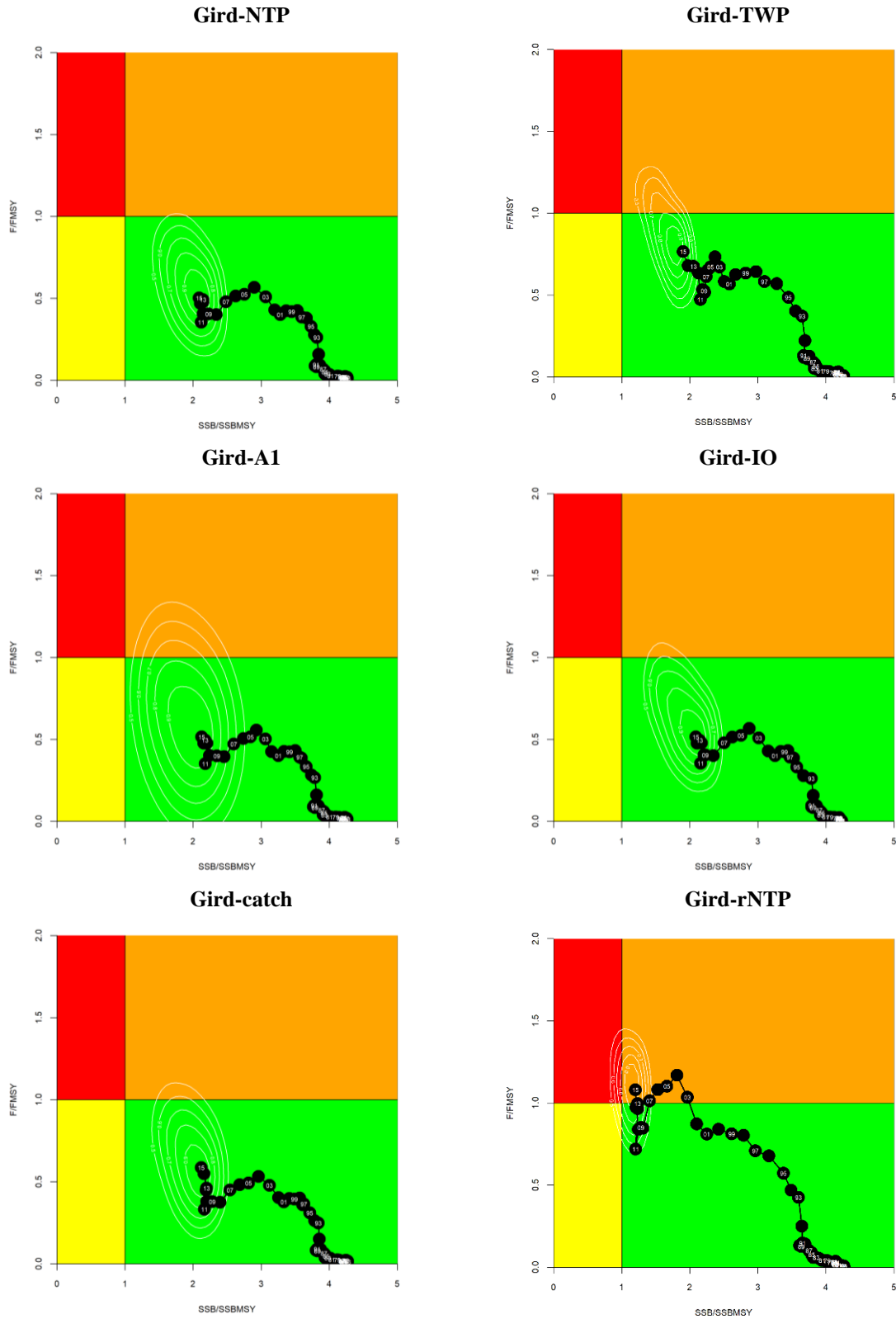
**Figure 19: Weighted average Kobe stock status plot for the whole Indian Ocean for each of the assessment grid. Black circles represent the annual medians of the weighted aggregate distributions. Contours represent the smoothed probability distribution for 2015 (isopleths are probability relative to the maximum).**
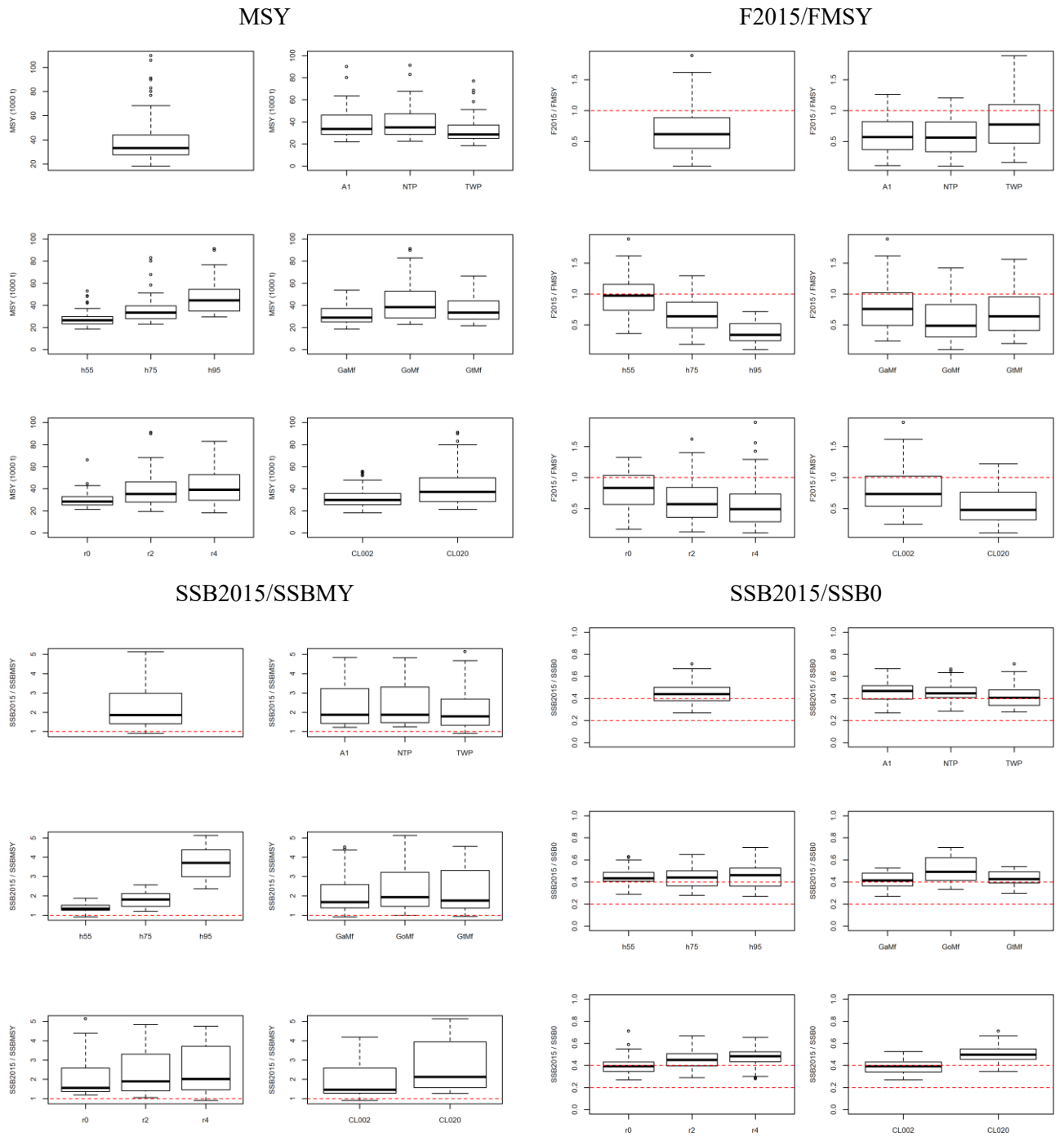
MSY

F2015/FMSY

SSB2015/SSBMY

SSB2015/SSB0

**Figure 20: Key management quantities estimates (MSY, F2015/FMSY, SSB2015/SSBMSY, SSB2015/SSB0) for the 162 models included in grid-IO, partitioned by assessment options.**
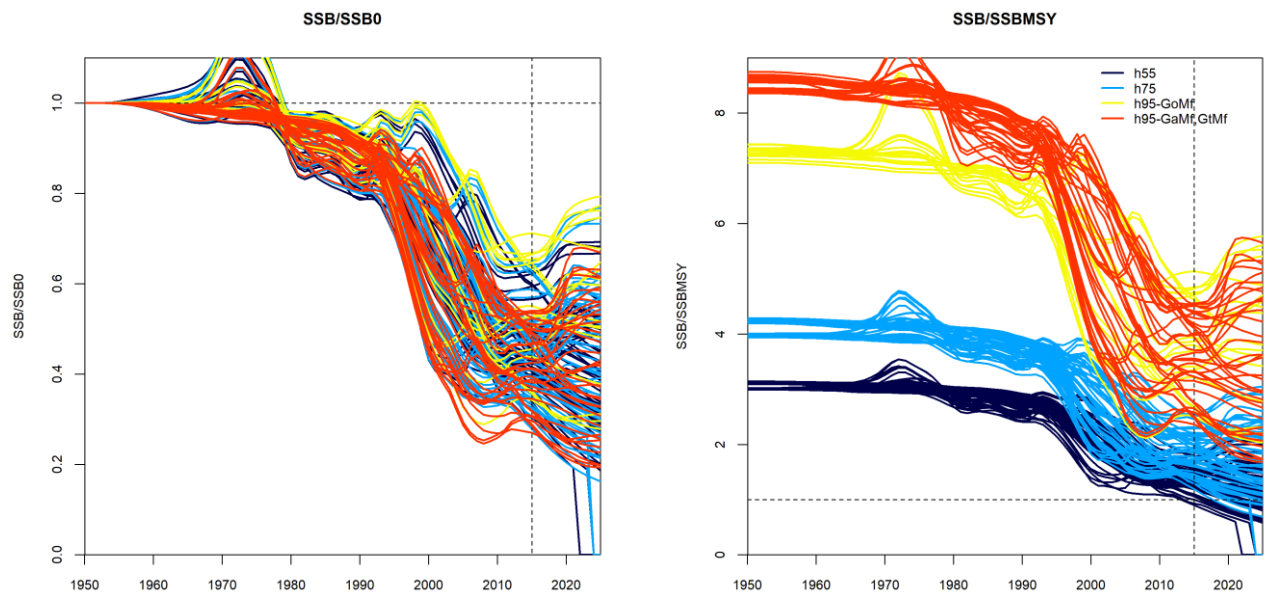
39

**Figure 21: Estimated time series SSB/SSB0 (left) and SSB/SSBMSY (right) for all models included in the grid-IO.**
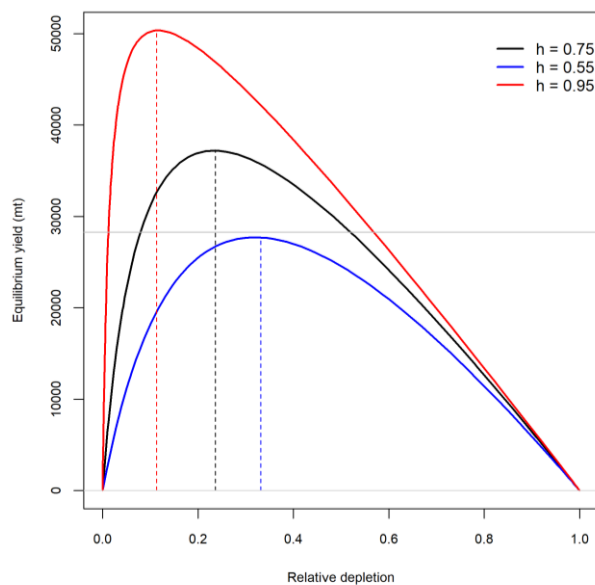


**Figure 22: Equilibrium yield curves for exploratory models h55, NTP, and h95, illustrating the effect of steepness on estimated depletion level corresponding to SSBMSY**

**Table 8: Stock status summary table for each of the assessment grid, based on the weighted combination of MPD models as defined in Table 6.**

| Management Quantity | Grid-NTP |
|---|---|
| Curren catch | 34 144 |
| Mean catch over last 5 years | 30 503 |
| MSY (1000 t) | 42 000 (26 184–67 660 ) |
| Current Data Period | 1950–2015 |
| F(Current)/F(MSY) | 0.52 (0.20–0.65 ) |
| B(Current)/B(MSY) | |
| SB(Current)/SB(MSY) | 2.33 (1.38– 4.53) |
| B(Current)/B(0) | |
| SB(Current)/SB(0) | 0.49 (0.38–0.65 ) |

| Management Quantity | Grid-TWP |
|---|---|
| Curren catch | 34 144 |
| Mean catch over last 5 years | 30 503 |
| MSY (1000 t) | 33 164 (21 638–58 179) |
| Current Data Period | 1950–2015 |
| F(Current)/F(MSY) | 0.75 (0.31– 1.222) |
| B(Current)/B(MSY) | |
| SB(Current)/SB(MSY) | 2.16 (1.20– 4.15) |
| B(Current)/B(0) | |
| SB(Current)/SB(0) | 0.45 (0.30–0.63) |

| Management Quantity | Grid-A1 |
|---|---|
| Curren catch | 34 144 |
| Mean catch over last 5 years | 30 503 |
| MSY (1000 t) | 39 930 (25 630–63 500 ) |
| Current Data Period | 1950–2016 |
| F(Current)/F(MSY) | 0.56(0.22–1.01 ) |
| B(Current)/B(MSY) | |
| SB(Current)/SB(MSY) | 2.32 (1.34– 4.52) |
| B(Current)/B(0) | |
| SB(Current)/SB(0) | 0.48 (0.37– 0.62 ) |

| Management Quantity | Grid-IO |
|---|---|
| Curren catch | 34 144 |
| Mean catch over last 5 years | 30 503 |
| MSY (1000 t) | 39 610 (24 170–67 660 ) |
| Current Data Period | 1950–2017 |
| F(Current)/F(MSY) | 0.57 (0.22–1.09 ) |
| B(Current)/B(MSY) | |
| SB(Current)/SB(MSY) | 2.30(1.32–4.52 ) |
| B(Current)/B(0) | |
| SB(Current)/SB(0) | 0.47(0.34–0.65 ) |

| Management Quantity | Grid-rNTP |
|---|---|
| Curren catch | 34 144 |
| Mean catch over last 5 years | 30 503 |
| MSY (1000 t) | 25 696 (19 935–35 210 ) |
| Current Data Period | 1950–2018 |
| F(Current)/F(MSY) | 1.07  (0.62– 1.51) |
| B(Current)/B(MSY) | |
| SB(Current)/SB(MSY) | 1.17 (0.90–1.65) |
| B(Current)/B(0) | |
| SB(Current)/SB(0) | 0.30 (0.23–0.42 ) |

| Management Quantity | Grid-catch |
|---|---|
| Curren catch | 41 682 |
| Mean catch over last 5 years | 33 476 |
| MSY (1000 t) | 42 078 (26 955–62 000 ) |
| Current Data Period | 1950–2019 |
| F(Current)/F(MSY) | 0.61 (0.26–1.11 ) |
| B(Current)/B(MSY) | |
| SB(Current)/SB(MSY) | 2.36 (1.41–4.56 ) |
| B(Current)/B(0) | |
| SB(Current)/SB(0) | 0.49 (0.40–0.61 ) |

**Table 9: Kobe 2 Strategy Matrix for Indian Ocean SWO assessment grids. Probability (expressed as a percentage of the distribution of models weighted as in Table 6) of exceeding the MSY-based spawning biomass and fishing mortality reference points.**

| Grid-NTP | | | Catch Level (relative to 2015) | | |
|---|---|---|---|---|---|
| | 60% | 80% | 100% | 120% | 140% |
| SSB(2018) <SSB(MSY) | 0 | 0 | 0 | 0 | 0 |
| F(2018) >F(MSY) | 0 | 0.004 | 0.0456 | 0.136 | 0.2416 |
| SSB(2025) <SSB(MSY) | 0 | 0 | 0.008 | 0.0576 | 0.1712 |
| F(2025) >F(MSY) | 0 | 0.004 | 0.0696 | 0.2232 | 0.3808 |

| Grid-TWP | | | | | |
|---|---|---|---|---|---|
| | 60% | 80% | 100% | 120% | 140% |
| SSB(2018) <SSB(MSY) | 0.02 | 0.0272 | 0.044 | 0.044 | 0.1152 |
| F(2018) >F(MSY) | 0.016 | 0.164 | 0.276 | 0.5344 | 0.6728 |
| SSB(2025) <SSB(MSY) | 0.02 | 0.048 | 0.2376 | 0.3232 | 0.6744 |
| F(2025) >F(MSY) | 0.016 | 0.1664 | 0.336 | 0.5984 | 0.816 |

| Grid-A1 | | | | | |
|---|---|---|---|---|---|
| | 60% | 80% | 100% | 120% | 140% |
| SSB(2018) <SSB(MSY) | 0 | 0 | 0 | 0 | 0.0024 |
| F(2018) >F(MSY) | 0 | 0.004 | 0.0648 | 0.2128 | 0.3272 |
| SSB(2025) <SSB(MSY) | 0 | 0 | 0.0528 | 0.16 | 0.256 |

| | | | | | |
|---|---|---|---|---|---|
| F(2025) >F(MSY) | 0 | 0.02 | 0.1312 | 0.3256 | 0.4 |

Grid-IO

| | 60% | 80% | 100% | 120% | 140% |
|---|---|---|---|---|---|
| SSB(2018) <SSB(MSY) | 0.004 | 0.00544 | 0.0088 | 0.0088 | 0.02376 |
| F(2018) >F(MSY) | 0.0032 | 0.036 | 0.09744 | 0.23872 | 0.35352 |
| SSB(2025) <SSB(MSY) | 0.004 | 0.0096 | 0.06736 | 0.14144 | 0.29728 |
| F(2025) >F(MSY) | 0.0032 | 0.04128 | 0.14136 | 0.32896 | 0.4736 |

Grid-catch

| | 60% | 80% | 100% | 120% | 140% |
|---|---|---|---|---|---|
| SSB(2018) <SSB(MSY) | 0 | 0 | 0 | 0 | 0.0224 |
| F(2018) >F(MSY) | 0 | 0.024 | 0.1312 | 0.2392 | 0.3488 |
| SSB(2025) <SSB(MSY) | 0 | 0.0128 | 0.1152 | 0.1968 | 0.2912 |
| F(2025) >F(MSY) | 0 | 0.0504 | 0.2504 | 0.3552 | 0.5752 |

Grid-rNTP

| | 60% | 80% | 100% | 120% | 140% |
|---|---|---|---|---|---|
| SSB(2018) <SSB(MSY) | 0.092 | 0.092 | 0.1416 | 0.24 | 0.3448 |
| F(2018) >F(MSY) | 0 | 0.164 | 0.5344 | 0.7568 | 0.7752 |
| SSB(2025) <SSB(MSY) | 0.092 | 0.124 | 0.4864 | 0.7504 | 0.828 |
| F(2025) >F(MSY) | 0 | 0.2344 | 0.7288 | 0.8432 | 0.9344 |

## 6. DISCUSSION

The Indian Ocean swordfish fisheries present a number of unique problems in the development of a stock population model: there is a lack of good information on recruitment; there is considerable uncertainty on growth, maturity, and natural mortality; there are good time series of CPUE, but their reliability to track abundance is highly uncertain, given the conflicts between these time series; there is also a large amount of data on size structure, but the sampling may be not random. As with earlier assessments, the models presented here, while fairly representing some of the data (e.g., the biomass indices), also show some signs of poor fit. The assessment tested various combinations of assumptions to explore the sensitivity and describe the uncertainty in the stock status. It is unlikely the estimates of historical stock size are accurate, given assumptions about annual recruitment and the reliance on the historical catch-effort indices of abundance. Current stock status as estimated here should thus be treated with caution.

Stock status was estimated for 162 models based on 3 reference cases (NTP, TWP, and A1) running a permutation of the parameters including growth, steepness, recruitment variability, and effective sample size for size composition data. Estimates from the majority of models suggested the Indian Ocean Swordfish stock as a whole is currently not overfished, and not subject to overfishing. SSB2015/SSBMSY is estimated to be 2.30 (weighted average of the 162 models), with a 90% quantile range 1.32–4.52, and F2015/FMSY estimated to b 0.57 with a 90% quantile range 0.22–1.09. The 10-year projections for these models suggest the risk of the spawning biomass falling below the target (SSBMSY) is less than 10% by 2025 if the catch remains at the current level.

A sensitivity model using alternative regional weighting factors for the Japanese CPUE indices produced more pessimistic results. The sensitivity running over a grid of 54 models estimated SSB2015/SSBMSY to be 1.17 (0.90–1.65), and F2015 / FMSY to be 1.07 (0.62– 1.51), suggesting that the stock is not overfished, but is probably subject to overfishing.

There is considerable uncertainty on growth estimates. The assessment explored five alternative sets of growth curves to admit the uncertainty due to potential area-specific growth rates and ongoing concerns about methods of age estimation from fin-rays. The new age estimation from otoliths (Farley et al 2016) appear promising, but the samples are from SW Pacific and the biological characteristics of Southwest Pacific swordfish may differ considerably from the Indian Ocean. The otolith-based growth curves indicate slower growth and a higher maximum age for both males and females, compared to the fin-ray based growth curves of Young & Drake (2004) and age estimates from otoliths are likely to be more reliable than for fin-rays, especially in larger/older fish, as fin-rays are subject to resorption and vascularisation of the core, although fin-ray based growth estimation is more practical for younger fish (Farley et al. 2016). The biomass estimates are very different between the model using the fin-ray based growth from the Indian Ocean, and that using the otolith based growth. It was found that the difference is mostly due to the discrepancy of maturity estimates between the two studies, which remains unresolved.

The Japanese and Taiwanese longline fleets have traditionally been used to generate the abundance indices for Indian Ocean swordfish stocks. These fleets have an extensive history, broad spatial coverage, and substantive logbook programmes. However, the operations of these fleets have changed historically, with large shifts in targeting that are poorly quantified. Conventional fisheries theory suggests that the depletion estimated by the Japanese series has been more consistent with the swordfish exploitation history than the Taiwanese series, and this interpretation has generally been given more weight in the assessment and management advice (Kolody 2011). However, the trend in the early CPUE series (pre-1994) for both fleets cannot be explained by the catch or other plausible dynamics. It is widely known that the catch efficiency of swordifih has experienced dramatic changes in the late 1980s and early 1990s with the deveopment of fresh-chill longline fleets which have further improved on catch rates through refinements to fishing gear such as the the introduction of light sticks and monofilament longlines in this period (Ward & Elscot 2000).

The abrupt decline in the JPN CPUE in the early 1990s is the strongest signal in the assessment that drives the inference of very high depletion in the SW region. The drop is so steep that the assessment models can only explain it through a combination of fishery depletion and anomalous recruitment (Martell 2010, Kolody 2010). However, the WPB also recognized that the Japanese fleet underwent some dramatic changes in the 1990s that might be exaggerating the estimated level of swordfish depletion at that time (Kolody 2011)

The conflicts in the SW region represent a particular concern, because there is a perception that this region may be excessively depleted. The recent Japanese CPUE is sharply increasing, while the SW Taiwanese CPUE series is steeply decreasing. In contrast, the CPUE series from Spain appeared to be relatively stable over the last few years At least one of the JPN or TWN series must be grossly misleading. Both TW0 and TW1 (models mainly fitted to Taiwanese CPUE) estimated that the current abundance in south-west is below 10% of the virgin level. The effort from the Taiwanese fleet since 2005 in the region is very low, and this casts serious doubt on the reliability of the apparent population collapse. We would tend to trust the Portuguese and Spanish series more than the others because: i) these fleets seem to have operated consistently over the recent time period, and ii) the standardisation analyses were very robust to different assumptions. The CPUE from the South African domestic fleet (not used in the assessment) showed a declining trend between 2006 and 2016, more similar to the Portuguese CPUE.

Indonesian CPUE was used for the first time in the swordfish assessment. The CPUE series appears very noisy and shows an overall flat trend. The Indonesian CPUE had little influence on the assessment results.

The steepness value appear to have little influence to the fits of data, but is very influential on estimates of MSY-related reference quantities. The stock-recruit function alone is not sufficient to explain the recruitment pattern, and the pattern of anomalous recruitment is similar regardless whether steepness is

low or high. The lower h55 value seems to be too low given the life history of this species. The h95 option seems to be at the higher end of results generally found for tuna stocks (ISSF 2011), and seems unlikely, but more likely than h55. Observations of other SWO populations which have experienced a decrease in fishing effort seem to show a rapid population rebound (North Atlantic, SW Pacific), and this may currently be happening in the western Indian Ocean. Together with life history considerations, this suggests that the higher steepness values are probably more likely for this species.

The model seems to be very sensitive to the size composition assumptions, even when the maximum sample size is less than 200. Given the concerns about the non-random sampling, changing distributions of effort and data irregularities, the length composition data is unlikely to be representative of the size structure of SWO population, which is known to depend on area and sex. Therefore we are inclined to down-weight the length composition data.

A common catchability coefficient was estimated in the assessment model, thereby, linking the Japanese CPUE indices among regions. This significantly increases the power of the model to estimate the relative (and absolute) level of biomass among regions (Langley 2016). The approach was to determine regional scaling factors that incorporated both the size of the region and the relative catch rate to determine the relative level of exploitable longline biomass among regions. This essentially assumes that the Japanese CPUE are a measure of regional swordfish density/abundance. Of all the assumptions examined, this assumption appears to be most influential to the assessment results. Sub-regions in Indian Ocean are unlikely to have a homogeneous distribution of swordfish density, some coastal regions clearly have higher CPUE than offshore regions (Kolody 2011). The relative magnitude of the mean CPUE also differs substantially among areas for each of the JPN and TWN fleets. The sensitivity model (rNTP) suggested that the regional weighting applied to the Japanese CPUE is important to this assessment. But the use of sub-regional models to determine alternative weighting factors may not be appropriate as it assumes each region constitutes a biological stock. The uncertainty regarding the scaling factor cannot be fully evaluated in a single stock assessment. We recommend that the uncertainty should be addressed more formally using a structured approach within a management strategy evaluation framework, and also that CPUE standardisation should continue to be improved to develop more robust regional weighting estimates (see an example of the potential improvement proposed by Hoyle & Langley (2013).

## 7. ACKNOWLEDGMENTS

## 8. REFERENCES

Anon. 2006. Report of the Fifth session of the IOTC working party on billfish. Colombo, Sri Lanka, 27-31 MAR 2006.

Bourjea, J., Le Couls S., Grewe P., Evano H. and Muths D. 2011. Preliminary results of the Indian Ocean swordfish stock structure project – IOSSS – focus on the population genetic approach. IOTC-2011-WPB-09-info-5.

Bradman, H., Grewe, P. and Appleton, B. 2010. Direct comparison of mitochondrial markers for the analysis of swordfish population structure. Fisheries Research 109: 95–99.

Campbell, R. 1998. Longline effort in the eastern AFZ. Unpublished paper presented at the Eastern Tuna and Billfish Fishery Effort Setting Workshop, Canberra, 20 November 1998.

Carey, F.G., Robinson, B.H. 1981. Daily patterns in the activities of swordfish, Xiphias gladius, observed by acoustic telemetry. Fisheries Bulletin 79(2), pp.277-292.

Coelho, R., Lino, P.G., Rosa, D. 2017. SWORDFISH CATCHES BY THE PORTUGUESE PELAGIC LONGLINE FLEET IN 1998-2016 IN THE INDIAN OCEAN: CATCH, EFFORT AND STANDARDIZED CPUES. IOTC–2017–WPB15–14.

Davies, N., Pilling, G., Harley, S., Hampton, J. 2013. Stock assessment of swordfish (*Xiphias gladius*) in the southwest Pacific Ocean. WCPFC-SC9-2013/SA-WP-05.

FERNANDEZ-COSTA, J., GARCIA-CORTES, B., RAMOS-CARTELLE, A., MEJUTO, J. 2017. UPDATED STANDARDIZED CATCH RATES OF SWORDFISH (XIPHIAS GLADIUS) CAUGHT BY THE SPANISH SURFACE LONGLINE FLEET IN THE INDIAN OCEAN DURING THE 2001-2015 PERIOD. IOTC–2017–WPB15–16.

Farley, J., Clear, Naomi., Kolody, D., Krusic-Golub, K,. Eveson, Paige., Young, Jock. 2016. Determination of swordfish growth and maturity relevant to the southwest Pacific stock. R 2014/0821.

Kadagi, N.I., Harris, T., and Conway, N. 2011. East Africa billfish Conservation and Research: Marlin, Sailfish and Swordfish Mark-Recapture field studies. IOTC-2011-WPB09-10.

IJIMA ET.AL. 2017. CPUE STANDARDIZATION OF THE INDIAN OCEAN SWORDFISH (XIPHIAS GLADIUS) BY JAPANESE LONGLINE FISHERIES: USING NEGATIVE BINOMIAL GLMM AND ZERO INFLATED NEGATIVE BINOMIAL GLMM TO CONSIDER VESSEL EFFECT. IOTC–2017–WPB15–19.

IOTC secretariat. 2004. DISAGGREGATION OF CATCHES RECORDED UNDER AGGREGATES OF GEAR AND SPECIES IN THE IOTC NOMINAL CATCHES DATABASE. IOTC-2004-WPTT-06.

ISSF 2011. Report of the 2011 ISSF stock assessment workshop, Rome, Italy, March 14-17. Unpublished report. 18pp.

Kolody, D. 2009. Exploratory Modelling of the Indian Ocean Swordfish Fishery, using an age-structured, sex-structured and spatially-disaggregated implementation of Stock Synthesis software.

Kolody, D. 2010. A Spatially-Structured Stock Synthesis Assessment of the Indian Ocean Swordfish Fishery 1950-2008, including Special Emphasis on the SW Region. Working paper for the IOTC Billfish Working Party July 2010: IOTC-2010-WPB-05.

Kolody, D. 2011. Review of CPUE Issues for the 2011 Indian Ocean Swordfish Stock Assessment. IOTC-2011-WPB09-13.

Kolody, D.; Herrera, M. 2011. An Age-, Sex- and Spatially-Structured Stock Assessment of the Indian Ocean Swordfish Fishery 1950-2009, including Special Emphasis on the South-West Region. OTC-2011-WPB-17.

Kolody, D., R. Campbell, and N. Davies. 2008. A MULTIFAN-CL stock assessment of south-Pacific swordfish 1952-2007, WCPFC-SC4-2008/SA-WP-6 (Revision 1).

Langley, A. 2016. Stock assessment of bigeye tuna in the Indian Ocean for 2016 — model development and evaluation. IOTC-2016-WPTT18-20.

Lu, C,P., Chen, C.A., Hui, C.F., Tzeng, T.D., Yeh, S.Y. 2006. Population genetic structure of the swordfish, *Xiphias gladius* (Linnaeus 1758), in the Indian Ocean and West Pacific inferred from the

complete DNA sequence of the mitochondrial control region. Zoological studies 45(2): 269-279.

Martell, S. 2010. SCAM Swordfish Stock Assessment. Working Party IOTC-2010-WPB-14.

Methot Jr, R.D., Wetzel, C.R. 2013. Stock synthesis: A biological and statistical framework for fish stock assessment and fishery management. Fisheries Research, 142(0): 86-99.

Methot Jr, R.D. 2014. User Manual for Stock Synthesis. Model Version 3.24s. Available from https://vlab.ncep.noaa.gov/group/stock-synthesis

Nishikawa, Y., Honma, M., Ueyanagi, S., Kikawa, S. 1985. Average distribution of larvae of oceanic species of scombrid fishes, 1956–1981. Far Seas Fisheries Research Laboratory, Shimizu. S Series 12. WPTT-04-06.

Nishida, T. 2008. Notes on the standardized swordfish CPUE of tuna longline fisheries (Japan and Taiwan) in WPB6 (1980-2006 and 1992-2006). IOTC-2008-WPB-INF04.

Francis, R.I.C.C. 2012. Data weighting in statistical fisheries stock assessment models. Canadian Journal of Fisheries and Aquatic Sciences, 2011, 68(6): 1124-1138,

SETYADJI, B., FAHMI, Z., ANDRADE, H. 2017. STANDARDISED CPUE INDICES FOR SWORDFISH (XIPHIAS GLADIUS) FROM THE INDONESIAN TUNA LONGLINE FISHERY. IOTC–2017–WPB15–15.

Sharma, R., Herrera, M. 2016. An Age-, Sex- and Spatially-Structured Stock Assessment of the Indian Ocean Swordfish Fishery 1950-2012, USING STOCK SYNTHESIS. IOTC–2014–WPB12–26_Rev2.

WANG, S.P. 2017. CPUE STANDARDIZATION OF SWORDFISH (XIPHIAS GLADIUS) CAUGHT BY TAIWANESE LONGLINE FISHERY IN THE INDIAN OCEAN. IOTC–2017–WPB15–17.

Hoyle, S., Langley, A. 2007. REGIONAL WEIGHTING FACTORS FOR YELLOWFIN TUNA IN WCP-CA STOCK ASSESSMENTS. WCPFC-SC3-ME SWG/WP-1.

Penny, A.J., Griffiths, M.H. 1998. A first description of the developing South African pelagic longline fishery. Working paper SCRS/98 presented at the SCRS Swordfish Working Meeting. ICCAT, Mardrid.

Punt, A. E., Dorn, M.W., and Haltuch, M.A. 2008. Evaluation of threshold management strategies for groundfish off the USWest Coast. Fisheries Research, 94: 251–266.

Punt, A. E., Smith, A. D. M., Smith, D. C., Tuck, G. N., and Klaer, N. L. 2014. Selecting relative abundance proxies for BMSY and BMEY. – ICES Journal of Marine Science, 71: 469–483.

Wang, S.P., Chi-Hong, L., Chiang, W.C. 2010. Age and growth analysis of swordfish (Xiphias gladius) in the Indian Ocean based on the specimens collected by Taiwanese observer program. Working paper IOTC-2010-WPB-08 (revision 1).

Ward, P., Elscot, S. 2000. Broadbill swordfish: Status of world fisheries: Bureau of Rural Sciences, Canberra.

WPB 2009. Indian Ocean Tuna Commission Report on Billfish 2009. Report of the 7th Session of the IOTC Working Party on Billfish. Seychelles, July 6-10, 2009.

Young, J. and A. Drake. 2002. Reproductive dynamics of broadbill swordfish (Xiphius gladius) in the domestic longline fishery off eastern Australia. Final report for project 1999/108, Fisheries Research Development Corporation, Canberra, Australia.

Young, J., Drake, A. 2004. Age and growth of broadbill swordfish (Xiphius gladius)from Australian waters. Final report for project 2001/014, Fisheries Research Development Corporation, Canberra, Australia.

Young, J., Humphreys, R., Uchiyama, J., Clear, N. 2008. Comparison of swordfish maturity and ageing from Hawaiian and Australian waters. WCPFC-SC3-BI SWG/WP-1.

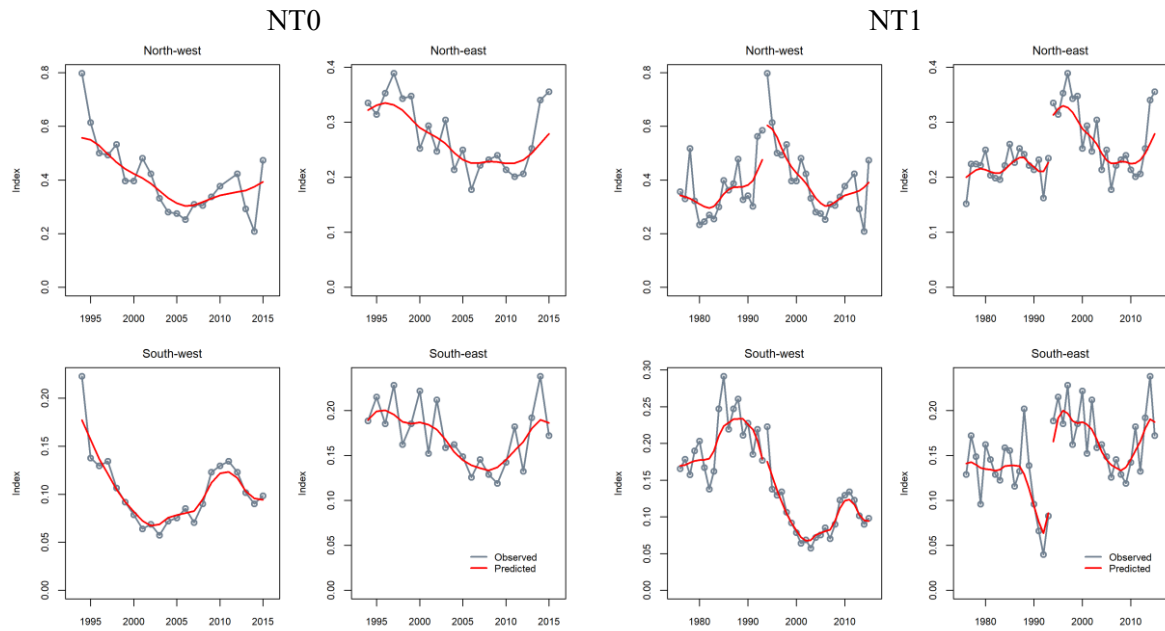## APPENDIX A: SELECTED EXPLORATORY MODEL OUTPUTS



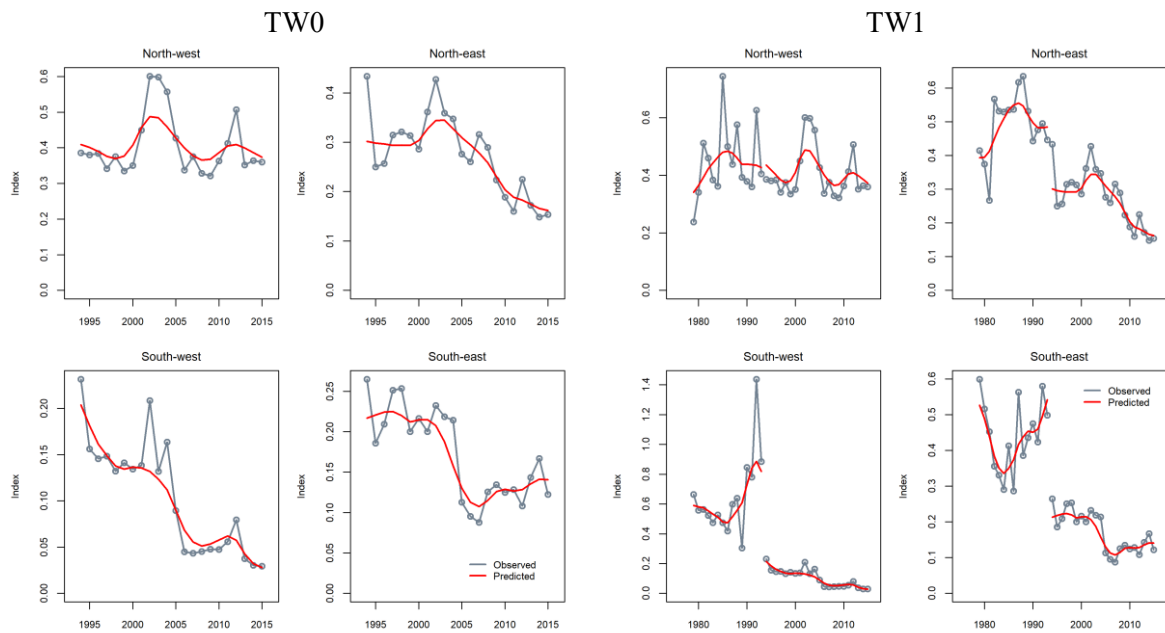**Figure A1: Fits to Japanese CPU for exploratory run NT0 (left) and NT1 (right).**



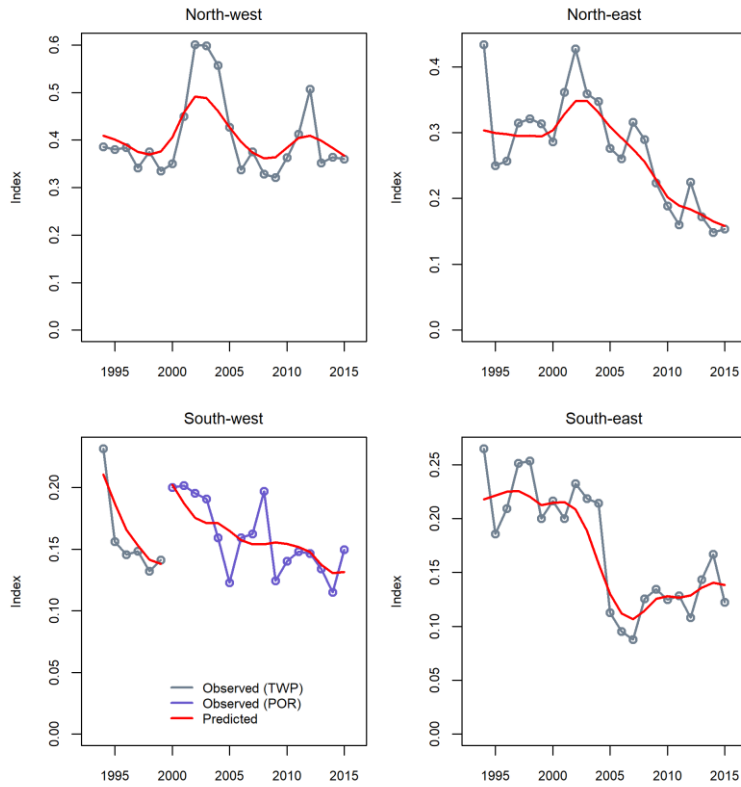**Figure A2: Fits to Taiwanese CPUE for exploratory run TW0 (left) and TW1 (right).**

**Figure A3: Fits to Taiwanese and Portuguese CPUE for reference model run TWP**.
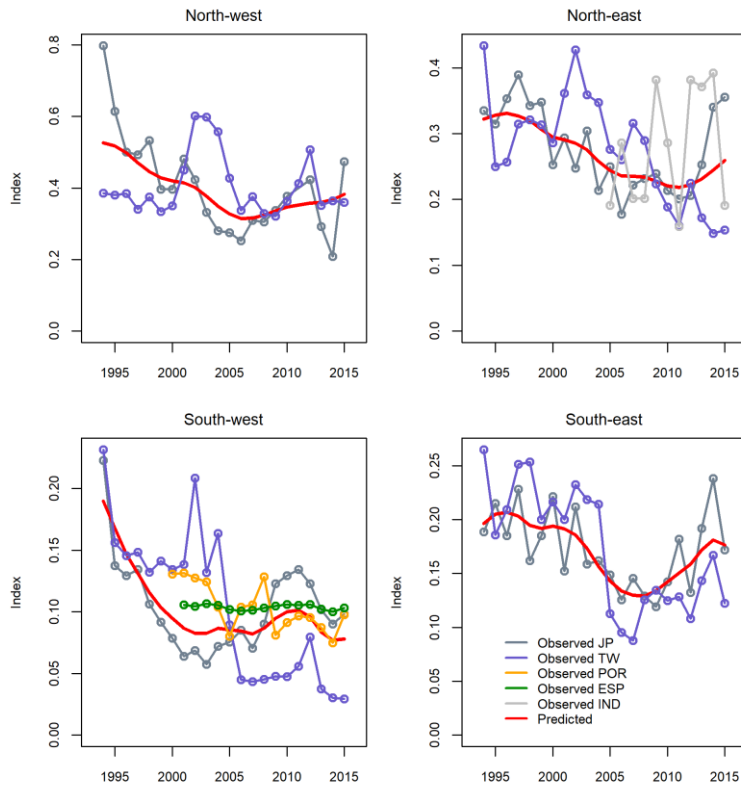


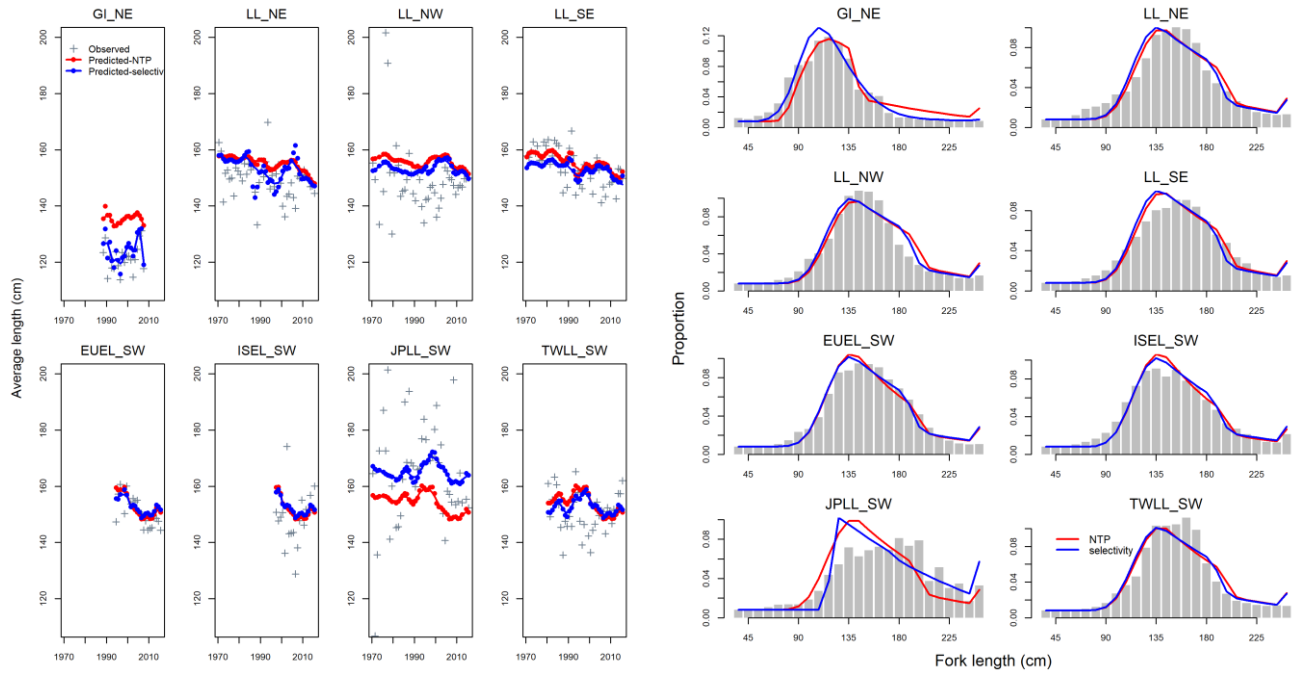**Figure A4: Fits to all CPUE series for reference model run A1.**

**Figure A5: Comparison of fits to the mean length distribution (left) and aggregated length frequency (right) between model NTP (M2) and model selectivity (M17).**
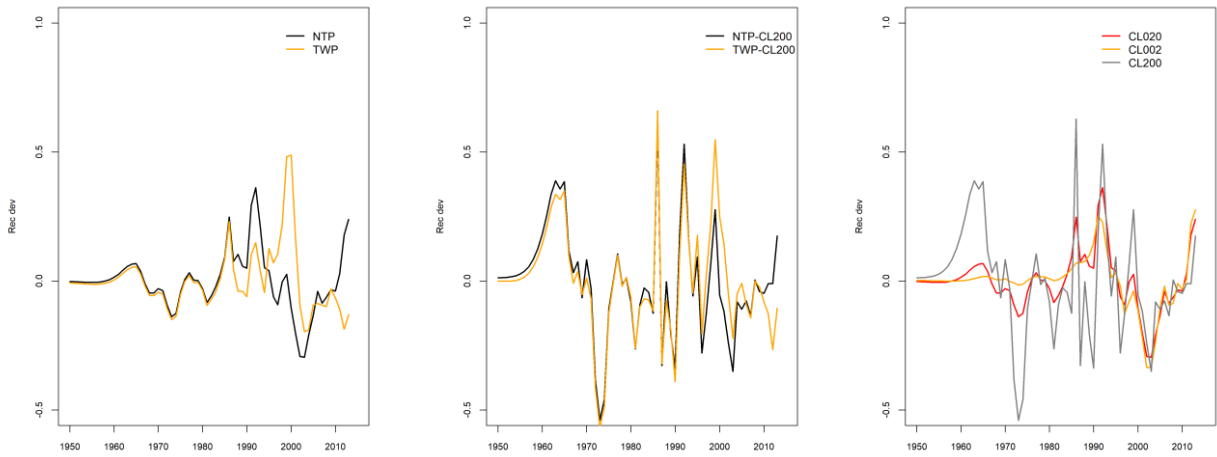


**Figure A6: Comparison of recruitment deviations among model NTP and TWP (left), between model NTP-CL200 and TWP-CL200 (middle), and between models CL002, CL020, and CL200 (right)**
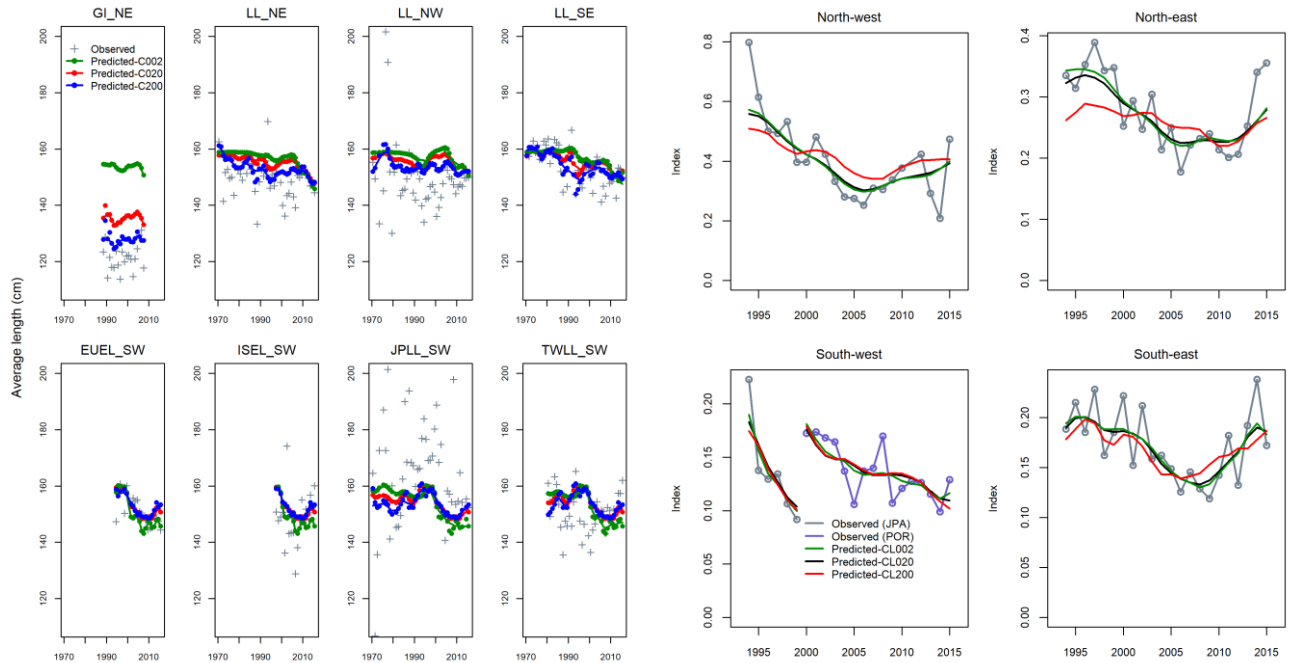
**Figure A7: Comparison of fits to the mean length distribution (left) and fits to the Japanese and Portuguese CPUE (right) between model CL002, CL020, and CL200.**
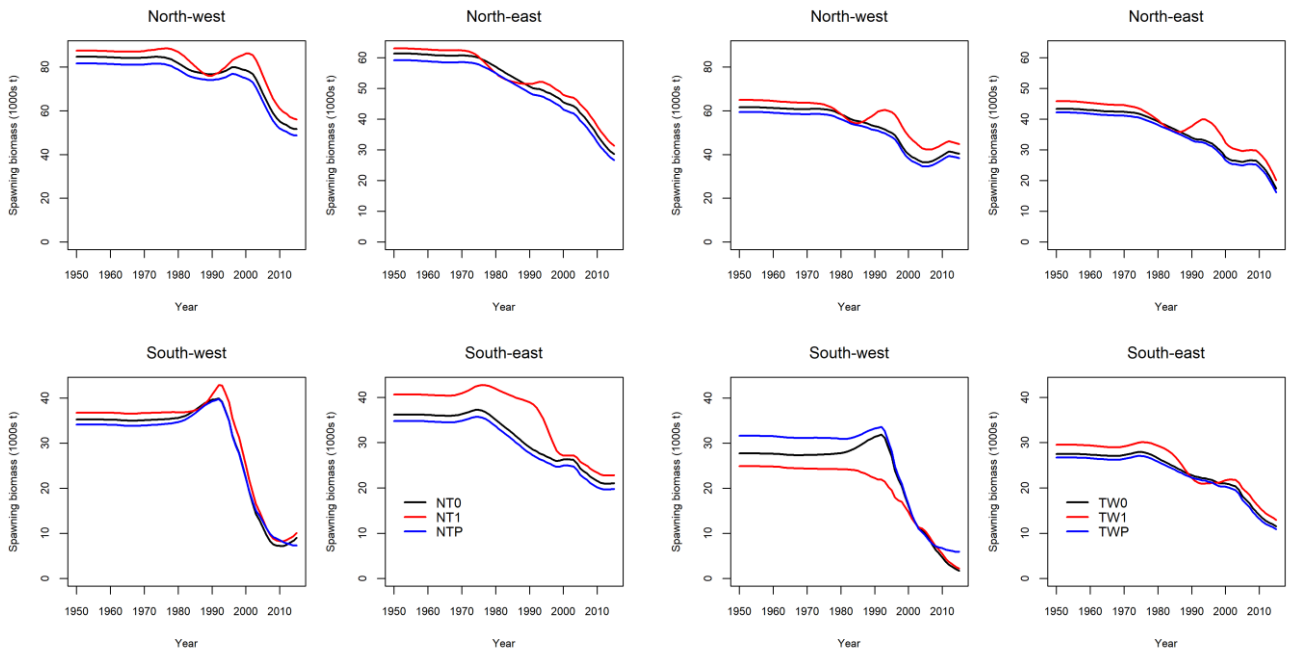


**Figure A8: Comparison of estimated biomass by region between models NT0, NT1, and NTP (left), and between models TW0, TW1, and TWP (right).**
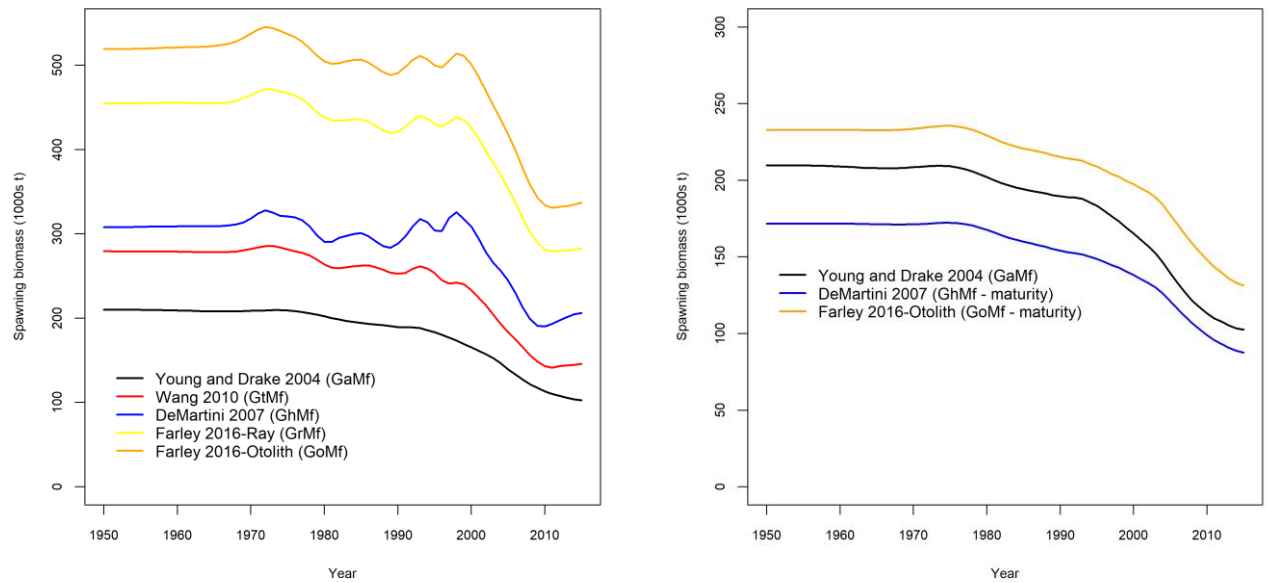
**Figure A9: Comparison of estimated total spawning biomass for the Indian ocean between models with different growth/maturity: GaMf, GtMf, GhMf, GrMf, and GoMf (left); between models with different growth but the same maturity: GaMf, GhMf-maturity, and GoMf-maturity (right).**
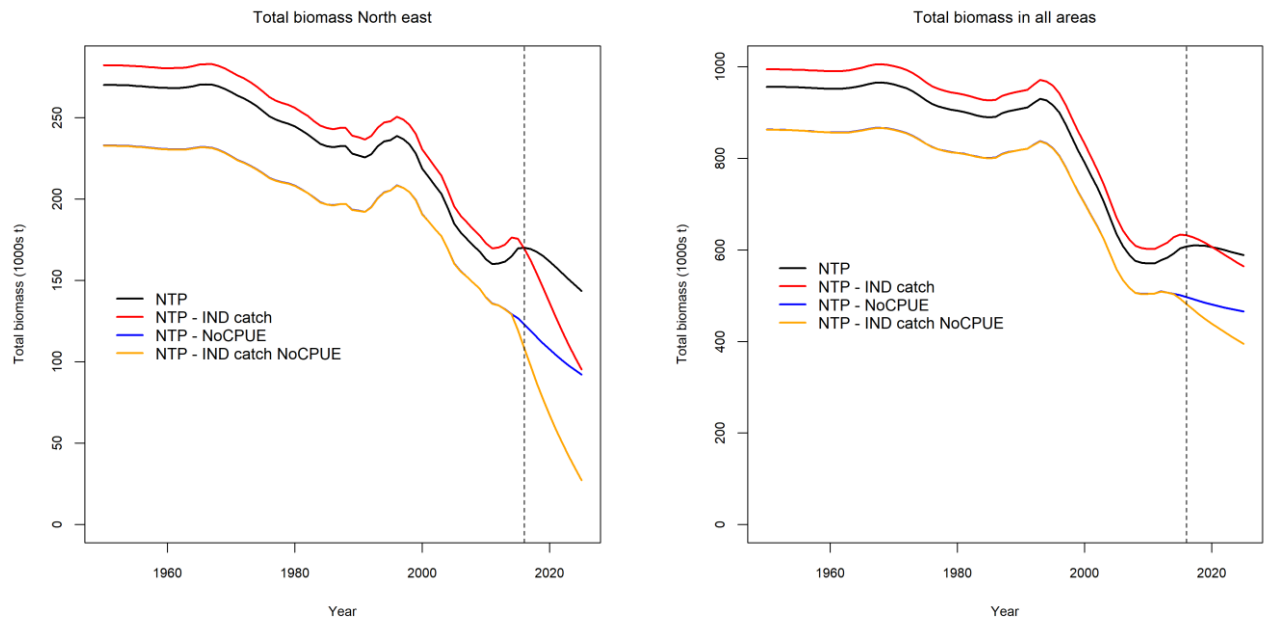


**Figure A10: Comparison of estimated total biomass for the north east region (left) and for all areas (right) between four models: reference model NTP (lower catch estimate), sensitivity IND catch (higher catch estimate), model NTP but with Japanese CPUE in 2014 and 2015 excluded (NTP – NoCPUE), and model NTP – IND catch but the with Japanese CPUE in 2014 and 2015 excluded (NTP – IND catch NoCPUE)**

**Figure A11: Estimated spawning biomass from the sub-regional model fitted to NW, NE, SW, and SE data, overlaid with the Japanese indices each model is fitted to (left); a comparison of spawning biomass by region between the sub-regional model, model rNTP, and NTP.**

## APPENDIX B. SS3 CONTROL.SS FILE TEMPLATE

# Each model assumption from Table 5 is created by the automated removal of flagged comment markers (e.g. for option 'io4', the full 4 area Indian Ocean model, '# xxx io4' is stripped out of the file).
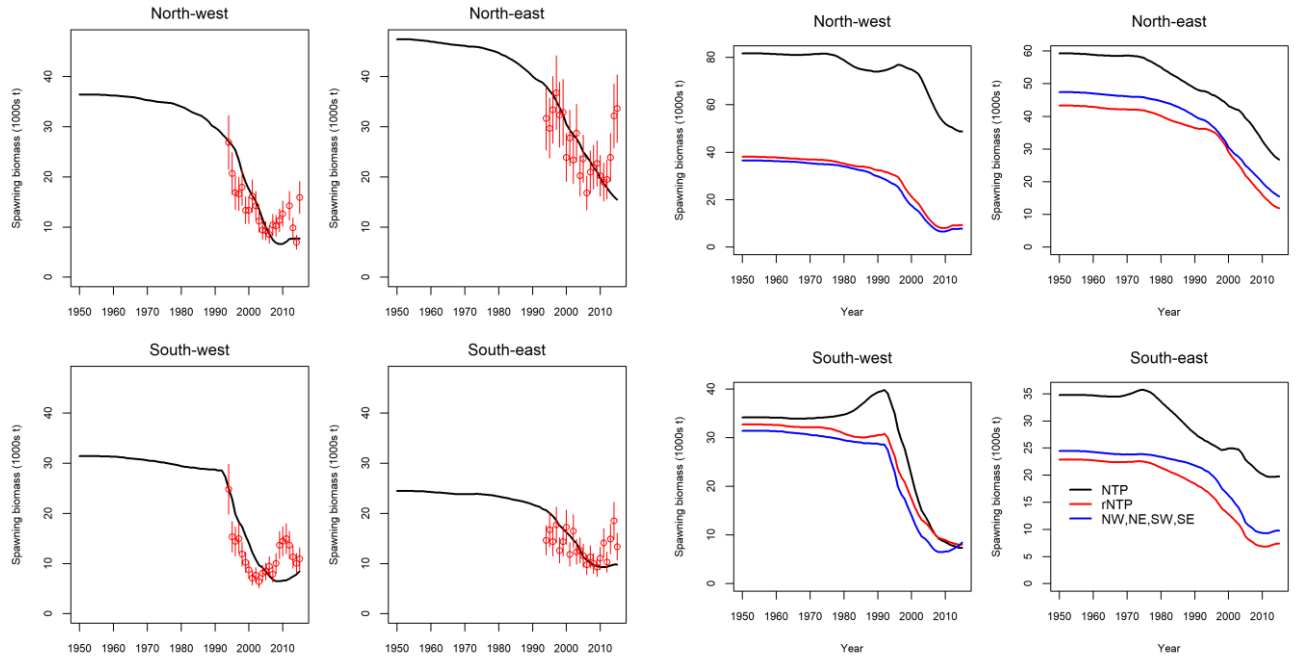
```
#V3.24z
#_data_and_control_files: DATA.SS // CONTROL.SS
1 #_N_Growth_Patterns
1 #_N_Morphs_Within_GrowthPattern
#_Cond  1 #_Morph_between/within_stdev_ratio (no read if N_morphs=1)
#_Cond  1 #vector_Morphdist_(-1_in_first_val_gives_normal_approx)
#
# xxx io4 4 #  number of recruitment assignments (overrides GP*area*seas parameter values)
# xxx io4 0 # recruitment interaction requested
#GP seas area for each recruitment assignment
# xxx io4   1 1 1
# xxx io4   1 1 2
# xxx io4   1 1 3
# xxx io4   1 1 4

# xxx io4 8 #_N_movement_definitions
# xxx io4 0.6 # first age that moves (real age at begin of season, not integer)
# seas,GP,source_area,dest_area,minage,maxage
# xxx io4  1 1 1 2 9 30
# xxx io4  1 1 1 3 9 30
# xxx io4  1 1 2 1 9 30
# xxx io4  1 1 2 4 9 30
# xxx io4  1 1 3 1 9 30
# xxx io4  1 1 3 4 9 30
# xxx io4  1 1 4 2 9 30
# xxx io4  1 1 4 3 9 30
#
0 #_Nblock_Patterns
#_Cond 0 #_blocks_per_pattern
# begin and end years of blocks
#
0.5 #_fracfemale
0 #_natM_type:_0=1Parm;
1=N_breakpoints;_2=Lorenzen;_3=agespecific;_4=agespec_withseasinterpolate
  #_no additional input for selected M option; read 1P per morph
1 # GrowthModel: 1=vonBert with L1&L2; 2=Richards with L1&L2; 3=not implemented; 4=not
implemented
0.01 #_Growth_Age_for_L1
999 #_Growth_Age_for_L2 (999 to use as Linf)
0 #_SD_add_to_LAA (set to 0.1 for SS2 V1.x compatibility)
0 #_CV_Growth_Pattern: 0 CV=f(LAA); 1 CV=F(A); 2 SD=F(LAA); 3 SD=F(A); 4 logSD=F(A)
3 #_maturity_option:  1=length logistic; 2=age logistic; 3=read age-maturity matrix by
growth_pattern; 4=read age-fecundity; 5=read fec and wt from wtatage.ss
#_Age_Maturity by growth pattern


# xxx GaMf 0.00325603 0.007115515 0.014569273 0.028013449 0.050623862 0.085939643
0.136874216 0.20429726 0.285874625 0.376104793 0.467854808 0.554549562 0.631738337
0.69745447 0.751682329 0.795546622 0.830633963 0.858568952 0.880806505 0.898561132
```

0.912807328 0.912807328 0.912807328 0.912807328 0.912807328 0.912807328 0.912807328
0.912807328 0.912807328 0.912807328 0.912807328 # CSIRO maturity 50% age 10
# xxx GtMf 0 0 0 0 0.02 0.1 0.5 0.9 0.98 1 1 1 1 1 1 1 1 1 1 1 1 1 1 1 1 1 1 1 1 1 # TWN/Hawai'i
Maturity 50% age 4
# xxx GhMf 0 0 0.02 0.1 0.5 0.9 0.98 1 1 1 1 1 1 1 1 1 1 1 1 1 1 1 1 1 1 1 1 1 1 1 # NMFS
L_at_Amin_Fem_GP_1_
# xxx GrMf 0.001 0.005 0.025 0.110 0.373 0.741 0.932 0.985 0.997 0.999 1 1 1 1 1 1 1 1 1 1 1 1 1 1
1 1 1 1 1 1 1 # Farley 2016 Ray
# xxx GoMf 0.001 0.006 0.027 0.109 0.354 0.711 0.917 0.98 0.996 0.999 1 1 1 1 1 1 1 1 1 1 1 1 1 1 1
1 1 1 1 1 1 1 # Farley 2016 Ootlith

1 #_First_Mature_Age
1 #_fecundity option:(1)eggs=Wt*(a+b*Wt);(2)eggs=a*L^b;(3)eggs=a*Wt^b; (4)eggs=a+b*L;
(5)eggs=a+b*W
0 #_hermaphroditism option: 0=none; 1=age-specific fxn
1 #_parameter_offset_approach (1=none 2= M G CV_G as offset from female-GP1 3=like SS2
V1.x)
1 #_env/block/dev_adjust_method (1=standard; 2=logistic transform keeps in base parm bounds;
3=standard w/ no bound check)
#
#_growth_parms
#_LO HI INIT PRIOR PR_type SD PHASE env-var use_dev dev_minyr dev_maxyr dev_stddev
Block Block_Fxn


# xxx GaMf 0.1 0.6 0.2 0.2 0 1 -8 0 0 0 0 0.5 0 0 # NatM_p_1_Fem_GP_1
# xxx GtMf 0.1 0.6 0.25 0.25 0 1 -8 0 0 0 0 0.5 0 0 # NatM_p_1_Fem_GP_1
# xxx GhMf 0.1 0.6 0.4 0.25 0 1 -8 0 0 0 0 0.5 0 0 # NatM_p_1_Fem_GP_1
# xxx GrMf 0.1 0.6 0.25 0.25 0 1 -8 0 0 0 0 0.5 0 0 # NatM_p_1_Fem_GP_1
# xxx GoMf 0.1 0.6 0.25 0.25 0 1 -8 0 0 0 0 0.5 0 0 # NatM_p_1_Fem_GP_1

# xxx GaMf 70 90 78.5 78.5 0 0.1 -2 0 0 0 0 0.5 0 0     # CSIRO L_at_Amin_Fem_GP_1_
# xxx GaMf 310 340 323.4 323.4 0 0.1 -2 0 0 0 0 0.5 0 0     # CSIRO L_at_Amax_Fem_GP_1_
# xxx GaMf 0.05 0.1 0.08148 0.08148 0 0.1 -3 0 0 0 0 0.5 0 0 # CSIRO VonBert_K_Fem_GP_1_

# xxx GtMf 70 90 66.2     66.2 0 0.1 -2 0 0 0 0 0.5 0 0   # Wang IO L_at_Amin_Fem_GP_1
# xxx GtMf 310 340 274.9 274.9 0 0.1 -2 0 0 0 0 0.5 0 0   # Wang IO L_at_Amax_Fem_GP_1
# xxx GtMf 0.05 0.26 0.138 0.138 0 0.1 -3 0 0 0 0 0.5 0 0 # Wang IO VonBert_K_Fem_GP_1

# xxx GhMf 70 90 72.6 72.6 0 0.1 -2 0 0 0 0 0.5 0 0     # NMFS L_at_Amin_Fem_GP_1_
# xxx GhMf 250 340 255.3 255.3 0 0.1 -2 0 0 0 0 0.5 0 0   # NMFS L_at_Amax_Fem_GP_1_
# xxx GhMf 0.24 0.26 0.246 0.246 0 0.1 -3 0 0 0 0 0.5 0 0   # NMFS VonBert_K_Fem_GP_1_


# xxx GrMf 70 90 83.22 83.22 0 0.1 -2 0 0 0 0 0 0 0     # Farley Ray L_at_Amin_Fem_GP_1_
# xxx GrMf 300 340 308.0713 308.0713 0 0.1 -2 0 0 0 0 0 0 0     # Farley Ray Ray
L_at_Amax_Fem_GP_1_
# xxx GrMf 0.05 0.2 0.123 0.123 0 0.1 -3 0 0 0 0 0 0 0     # Farley Ray Ray
VonBert_K_Fem_GP_1_

# xxx GoMf 70 90 78.70 78.70 0 0.1 -2 0 0 0 0 0 0 0     # Farley Otolith
L_at_Amin_Fem_GP_1_
# xxx GoMf 310 340 275.8123 275.8123 0 0.1 -2 0 0 0 0 0 0 0     # Farley Otolith Ray
L_at_Amax_Fem_GP_1_
# xxx GoMf 0.05 0.2 0.157 0.157 0 0.1 -3 0 0 0 0 0 0 0     # Farley Otolith Ray

VonBert_K_Fem_GP_1_

 0.05 0.25 0.15 0.15 0 0 0.15 -3 0 0 0 0 0.5 0 0 # CV_young_Fem_GP_1
 0.05 0.25 0.1 0.15 0 0.15 -3 0 0 0 0 0.5 0 0 # CV_old_Fem_GP_1

# xxx GaMf  0.1 0.6 0.2 0.2 0 1 -8 0 0 0 0 0.5 0 0   # NatM_p_1_Mal_GP_1
# xxx GtMf  0.1 0.6 0.25 0.25 0 1 -8 0 0 0 0 0.5 0 0 # NatM_p_1_Mal_GP_1
# xxx GhMf  0.1 0.6 0.4 0.25 0 1 -8 0 0 0 0 0.5 0 0  # NatM_p_1_Mal_GP_1
# xxx GrMf  0.1 0.6 0.25 0.25 0 1 -8 0 0 0 0 0.5 0 0 # NatM_p_1_Mal_GP_1
# xxx GoMf  0.1 0.6 0.25 0.25 0 1 -8 0 0 0 0 0.5 0 0 # NatM_p_1_Mal_GP_1


# xxx GaMf   70 90 80.6 80.6 0 0.1 -2 0 0 0 0 0.5 0 0         # CSIRO L_at_Amin_Mal_GP_1_
# xxx GaMf   240 280 260.47 260.47 0 0.1 -2 0 0 0 0 0.5 0 0   # CSIRO L_at_Amax_Mal_GP_1_
# xxx GaMf   0.07 0.13 0.1096 0.1096 0 0.1 -3 0 0 0 0 0.5 0 0 # CSIRO VonBert_K_Mal_GP_1_

# xxx GtMf  70 90 72.1 72.1 0 0.1 -2 0 0 0 0 0.5 0 0 # Wang IO L_at_Amin_Mal_GP_1
# xxx GtMf  230 280 234 234 0 0.1 -2 0 0 0 0 0.5 0 0 # Wang IO L_at_Amax_Mal_GP_1
# xxx GtMf  0.26 0.28 0.169 0.169 0 0.1 -3 0 0 0 0 0.5 0 0 # Wang IO VonBert_K_Mal_GP_1

# xxx GhMf  70 90 77.1 77.1 0 0.1 -2 0 0 0 0 0.5 0 0         # NMFS L_at_Amin_Mal_GP_1_
# xxx GhMf  230 280 232.04 232.04 0 0.1 -2 0 0 0 0 0.5 0 0   # NMFS L_at_Amax_Mal_GP_1_
# xxx GhMf  0.26 0.28 0.271 0.271 0 0.1 -3 0 0 0 0 0.5 0 0   # NMFS VonBert_K_Mal_GP_1_

# xxx GrMf 70 90 86.17 86.17 0 0.1 -2 0 0 0 0 0 0 0          # Farley Ray L_at_Amin_Mal_GP_1_
# xxx GrMf 200 280 237.3166 237.3166 0 0.1 -2 0 0 0 0 0 0 0       # Farley Ray
L_at_Amax_Mal_GP_1_
# xxx GrMf 0.07 0.30 0.197 0.197 0 0.1 -3 0 0 0 0 0 0 0          # Farley Ray
VonBert_K_Mal_GP_1_

# xxx GoMf 70 90 83.57 83.57 0 0.1 -2 0 0 0 0 0 0 0          # Farley Otolith
L_at_Amin_Mal_GP_1_
# xxx GoMf 200 280 213.7675 213.7675 0 0.1 -2 0 0 0 0 0 0 0      # Farley Otolith
L_at_Amax_Mal_GP_1_
# xxx GoMf 0.07 0.30 0.235 0.235 0 0.1 -3 0 0 0 0 0 0 0          # Farley Otolith
VonBert_K_Mal_GP_1_


 0.05 0.25 0.15 0.15 0 0.15 -3 0 0 0 0 0.5 0 0 # CV_young_Mal_GP_1
 0.05 0.25 0.1 0.15 0 0.15 -3 0 0 0 0 0.5 0 0 # CV_old_Mal_GP_1
 -3 3 3.815e-006 3.815e-006 -1 99 -3 0 0 0 0 0.5 0 0 # Wtlen_1_Fem
 -3 4 3.188 3.188 -1 99 -3 0 0 0 0 0.5 0 0 # Wtlen_2_Fem
 35 73 55 55 -1 99 -3 0 0 0 0 0 0 0 # Mat50%_Fem
 -3 3 -0.25 -0.25 -1 99 -3 0 0 0 0 0 0 0 # Mat_slope_Fem
 -3 3 1 1 -1 99 -3 0 0 0 0 0 0 0 # Eggs/kg_inter_Fem
 -3 3 0 0 -1 99 -3 0 0 0 0 0 0 0 # Eggs/kg_slope_wt_Fem
 -3 3 3.815e-006 3.815e-006 -1 99 -3 0 0 0 0 0.5 0 0 # Wtlen_1_Mal
 -3 4 3.188 3.188 -1 99 -3 0 0 0 0 0.5 0 0 # Wtlen_2_Mal
 -8 8 0 1 -1 99 -3 0 0 0 0 0.5 0 0 # RecrDist_GP_1
 -8 8 0 1 -1 99 -4 0 0 0 0 0.5 0 0 # RecrDist_Area_1
# xxx io4  -8 8 -0.509876 1 -1 99 4 0 1 1965 2014 0.9 0 0 # RecrDist_Area_2
# xxx io4  -8 8 -0.295335 1 -1 99 4 0 1 1965 2014 0.9 0 0 # RecrDist_Area_3
# xxx io4  -8 8 -0.187103 1 -1 99 4 0 1 1965 2014 0.9 0 0 # RecrDist_Area_4
 -8 8 0 1 -1 99 -7 0 0 0 0 0.5 0 0 # RecrDist_Seas_1

```
 1 1 1 1 -1 99 -3 0 0 0 0 0 0 0 # CohortGrowDev
# xxx io4  -8 9 -7 -5 0 5 -9 0 0 0 0 0 0 0 # MoveParm_A_seas_1_GP_1from_1to_2
# xxx io4  -8 9 -7 -5 0 5 -9 0 0 0 0 0 0 0 # MoveParm_B_seas_1_GP_1from_1to_2
# xxx io4  -8 9 -7 -5 0 5 -9 0 0 0 0 0 0 0 # MoveParm_A_seas_1_GP_1from_1to_3
# xxx io4  -8 9 -7 -5 0 5 -9 0 0 0 0 0 0 0 # MoveParm_B_seas_1_GP_1from_1to_3
# xxx io4  -8 9 -7 -5 0 5 -9 0 0 0 0 0 0 0 # MoveParm_A_seas_1_GP_1from_2to_1
# xxx io4  -8 9 -7 -5 0 5 -9 0 0 0 0 0 0 0 # MoveParm_B_seas_1_GP_1from_2to_1
# xxx io4  -8 9 -7 -5 0 5 -9 0 0 0 0 0 0 0 # MoveParm_A_seas_1_GP_1from_2to_4
# xxx io4  -8 9 -7 -5 0 5 -9 0 0 0 0 0 0 0 # MoveParm_B_seas_1_GP_1from_2to_4
# xxx io4  -8 9 -7 -5 0 5 -9 0 0 0 0 0 0 0 # MoveParm_A_seas_1_GP_1from_3to_1
# xxx io4  -8 9 -7 -5 0 5 -9 0 0 0 0 0 0 0 # MoveParm_B_seas_1_GP_1from_3to_1
# xxx io4  -8 9 -7 -5 0 5 -9 0 0 0 0 0 0 0 # MoveParm_A_seas_1_GP_1from_3to_4
# xxx io4  -8 9 -7 -5 0 5 -9 0 0 0 0 0 0 0 # MoveParm_B_seas_1_GP_1from_3to_4
# xxx io4  -8 9 -7 -5 0 5 -9 0 0 0 0 0 0 0 # MoveParm_A_seas_1_GP_1from_4to_2
# xxx io4  -8 9 -7 -5 0 5 -9 0 0 0 0 0 0 0 # MoveParm_B_seas_1_GP_1from_4to_2
# xxx io4  -8 9 -7 -5 0 5 -9 0 0 0 0 0 0 0 # MoveParm_A_seas_1_GP_1from_4to_3
# xxx io4  -8 9 -7 -5 0 5 -9 0 0 0 0 0 0 0 # MoveParm_B_seas_1_GP_1from_4to_3
#
#_Cond 0  #custom_MG-env_setup (0/1)
#_Cond -2 2 0 0 -1 99 -2 #_placeholder when no MG-environ parameters
#
#_Cond 0  #custom_MG-block_setup (0/1)
#_Cond -2 2 0 0 -1 99 -2 #_placeholder when no MG-block parameters
#_Cond No MG parm trends
#
#_seasonal_effects_on_biology_parms
 0 0 0 0 0 0 0 0 0 0 #_femwtlen1 femwtlen2 mat1 mat2 fec1 fec2 Malewtlen1 malewtlen2 L1 K
#_Cond -2 2 0 0 -1 99 -2 #_placeholder when no seasonal MG parameters
#
# xxx io4 4 #_MGparm_Dev_Phase
#
#_Spawner-Recruitment
3 #_SR_function: 1=B-H_flattop; 2=Ricker; 3=std_B-H; 4=SCAA; 5=Hockey; 6=Shepard_3Parm
#_LO HI INIT PRIOR PR_type SD PHASE
 7 18 8.42702 11 -1 100 3 # SR_R0
# xxx h55 0.2 1 0.55 0.55 1 0.1 -10 # SR_steep
# xxx h75 0.2 1 0.75 0.75 1 0.1 -10 # SR_steep
# xxx h95 0.2 1 0.95 0.95 1 0.1 -10 # SR_steep
# xxx r0 0 2 0.01 0.01 -1 0.8 -3 # SR_sigmaR
# xxx r2 0 2 0.2 0.2 -1 0.8 -3 # SR_sigmaR
# xxx r4 0 2 0.4 0.4 -1 0.8 -3 # SR_sigmaR
 -5 5 0.1 0 0 1 -3 # SR_envlink
 -5 5 0 0 0 1 -4 # SR_R1_offset
 0 0 0 0 -1 0 -99 # SR_autocorr
0 #_SR_env_link
0 #_SR_env_target_0=none;1=devs;_2=R0;_3=steepness
# xxx r4 1 #do_recdev:  0=none; 1=devvector; 2=simple deviations
# xxx r2 1 #do_recdev:  0=none; 1=devvector; 2=simple deviations
# xxx r0 0 #do_recdev:  0=none; 1=devvector; 2=simple deviations
1950 # first year of main recr_devs; early devs can preceed this era
2013 # last year of main recr_devs; forecast devs start in following year
6 #_recdev phase
1 # (0/1) to read 13 advanced options
0 #_recdev_early_start (0=none; neg value makes relative to recdev_start)
-5 #_recdev_early_phase
```

5 #_forecast_recruitment phase (incl. late recr) (0 value resets to maxphase+1)
1 #_lambda for Fcast_recr_like occurring before endyr+1
1970 #_last_early_yr_nobias_adj_in_MPD
1971 #_first_yr_fullbias_adj_in_MPD
2001 #_last_yr_fullbias_adj_in_MPD
2002 #_first_recent_yr_nobias_adj_in_MPD
1 #_max_bias_adj_in_MPD (-1 to override ramp and set biasadj=1.0 for all estimated recdevs)
0 #_period of cycles in recruitment (N parms read below)
-6 #min rec_dev
6 #max rec_dev
0 #_read_recdevs
#_end of advanced SR options
#
#_placeholder for full parameter lines for recruitment cycles
# read specified recr devs
#_Yr Input_value
#
#
#Fishing Mortality info
0.2 # F ballpark for tuning early phases
2003 # F ballpark year (neg value to disable)
3 # F_Method:  1=Pope; 2=instan. F; 3=hybrid (hybrid is recommended)
4 # max F or harvest rate  depends on F_Method
# no additional F input needed for Fmethod 1
# if Fmethod=2; read overall start F value; overall phase; N detailed inputs to read
# if Fmethod=3; read N iterations for tuning for Fmethod 3
2  # N iterations for tuning F in hybrid method (recommend 3 to 7)
#
#_initial_F_parms
#_LO HI INIT PRIOR PR_type SD PHASE
# xxx io4 0 1 0 0.01 0 99 -1 # InitF_1GI_NE
# xxx io4 0 1 0 0.01 0 99 -1 # InitF_2LL_NE
# xxx io4 0 1 0 0.01 0 99 -1 # InitF_3GI_NW
# xxx io4 0 1 0 0.01 0 99 -1 # InitF_4LL_NW
# xxx io4 0 1 0 0.01 0 99 -1 # InitF_5GI_SE
# xxx io4 0 1 0 0.01 0 99 -1 # InitF_6LL_SE
# xxx io4 0 1 0 0.01 0 99 -1 # InitF_7ALGI_SW
# xxx io4 0 1 0 0.01 0 99 -1 # InitF_8EUEL_SW
# xxx io4 0 1 0 0.01 0 99 -1 # InitF_9ISEL_SW
# xxx io4 0 1 0 0.01 0 99 -1 # InitF_10JPLL_SW
# xxx io4 0 1 0 0.01 0 99 -1 # InitF_11TWFL_SW
# xxx io4 0 1 0 0.01 0 99 -1 # InitF_12TWLL_SW


#
#_Q_setup
 # Q_type options: <0=mirror 0=median_float 1=mean_float 2=parameter 3=parm_w_random_dev
4=parm_w_randwalk 5=mean_unbiased_float_assign_to_parm
 #_Den-dep env-var extra_se Q_type
# xxx io4 0 0 0 2 # 1 GI_NE
# xxx io4 0 0 0 2 # 2 LL_NE
# xxx io4 0 0 0 2 # 3 GI_NW
# xxx io4 0 0 0 2 # 4 LL_NW
# xxx io4 0 0 0 2 # 5 GI_SE
# xxx io4 0 0 0 2 # 6 LL_SE

```
# xxx io4 0 0 0 2 # 7 ALGI_SW
# xxx io4 0 0 0 2 # 8 EUEL_SW
# xxx io4 0 0 0 2 # 9 ISEL_SW
# xxx io4 0 0 0 2 # 10 JPLL_SW
# xxx io4 0 0 0 2 # 11 TWFL_SW
# xxx io4 0 0 0 2 # 12 TWLL_SW
# xxx io4 0 0 0 2 # 13 UJPLL_NW
# xxx io4 0 0 0 -13 # 14 UJPLL_NE
# xxx io4 0 0 0 -13 # 15 UJPLL_SW
# xxx io4 0 0 0 -13 # 16 UJPLL_SE
# xxx io4 0 0 0 2 # 17 UTWLL_NW
# xxx io4 0 0 0 2 # 18 UTWLL_NE
# xxx io4 0 0 0 2 # 19 UTWLL_SW
# xxx io4 0 0 0 2 # 20 UTWLL_SE
# xxx io4 0 0 0 2 # 21 UPOR_SW
# xxx io4 0 0 0 2 # 22 UESP_SW
# xxx io4 0 0 0 2 # 23 URELL_SW
# xxx io4 0 0 0 2 # 24 UIND_NE
# xxx io4 0 0 0 2 # 25 UJPLL_NW_pre
# xxx io4 0 0 0 2 # 26 UJPLL_NE_pre
# xxx io4 0 0 0 2 # 27 UJPLL_SW_pre
# xxx io4 0 0 0 2 # 28 UJPLL_SE_pre
# xxx io4 0 0 0 2 # 29 UTWLL_NW_pre
# xxx io4 0 0 0 2 # 30 UTWLL_NE_pre
# xxx io4 0 0 0 2 # 31 UTWLL_SW_pre
# xxx io4 0 0 0 2 # 32 UTWLL_SE_pre


#_Cond 0 #_If q has random component  then 0=read one parm for each fleet with random q; 1=read
a parm for each year of index
#_Q_parms(if_any)
# LO HI INIT PRIOR PR_type SD PHASE

# xxx io4 -10 10 -0.494066 0 0 99 -1 # Q_base_1_GI_NE
# xxx io4 -10 10 -0.494066 0 0 99 -1 # Q_base_2_LL_NE
# xxx io4 -10 10 -0.494066 0 0 99 -1 # Q_base_3_GI_NW
# xxx io4 -10 10 -0.494066 0 0 99 -1 # Q_base_4_LL_NW
# xxx io4 -10 10 -0.494066 0 0 99 -1 # Q_base_5_GI_SE
# xxx io4 -10 10 -0.494066 0 0 99 -1 # Q_base_6_LL_SE
# xxx io4 -10 10 -0.494066 0 0 99 -1 # Q_base_7_ALGI_SW
# xxx io4 -10 10 -0.494066 0 0 99 -1 # Q_base_8_EUEL_SW
# xxx io4 -10 10 -0.494066 0 0 99 -1 # Q_base_9_ISEL_SW
# xxx io4 -10 10 -0.494066 0 0 99 -1 # Q_base_10_JPLL_SW
# xxx io4 -10 10 -0.494066 0 0 99 -1 # Q_base_11_TWFL_SW
# xxx io4 -10 10 -0.494066 0 0 99 -1 # Q_base_12_TWLL_SW
# xxx io4 -20 10 -7.41213  0 0 99  1 # Q_base_13_UJPLL_NW
# xxx io4 -20 10 -9.53595 0 0 99   1 # Q_base_17_UTWLL_NW
# xxx io4 -20 10 -9.0215 0 0 99    1 # Q_base_18_UTWLL_NE
# xxx io4 -20 10 -7.26104 0 0 99   1 # Q_base_19_UTWLL_SW
# xxx io4 -20 10 -10.4321 0 0 99   1 # Q_base_20_UTWLL_SE
# xxx io4 -20 10 -11.6308 0 0 99   1 # Q_base_21_UPOR_SW
# xxx io4 -20 10 -7.81646 0 0 99   1 # Q_base_22_UESP_SW
# xxx io4 -20 10 -11.6308 0 0 99   1 # Q_base_23_URELL_SW
# xxx io4 -20 10 -11.6308 0 0 99   1 # Q_base_24_UIND_NE
# xxx io4 -20 10 -7.41213  0 0 99  1 # Q_base_25_UJPLL_NW_pre
```

# xxx io4 -20 10 -7.41213  0 0 99   1 # Q_base_26_UJPLL_NE_pre
# xxx io4 -20 10 -7.41213  0 0 99   1 # Q_base_27_UJPLL_SW_pre
# xxx io4 -20 10 -7.41213  0 0 99   1 # Q_base_28_UJPLL_SE_pre
# xxx io4 -20 10 -7.41213  0 0 99   1 # Q_base_29_UTWLL_NW_pre
# xxx io4 -20 10 -7.41213  0 0 99   1 # Q_base_30_UTWLL_NE_pre
# xxx io4 -20 10 -7.41213  0 0 99   1 # Q_base_31_UTWLL_SW_pre
# xxx io4 -20 10 -7.41213  0 0 99   1 # Q_base_32_UTWLL_SE_pre


#_size_selex_types
#_Pattern Discard Male Special
 # xxx io4 24 0 0 0 # 1 GI_NE
 # xxx io4 24 0 0 0 # 2 LL_NE
 # xxx io4 5 0 0 1 # 3 GI_NW
 # xxx io4 5 0 0 2 # 4 LL_NW
 # xxx io4 5 0 0 1 # 5 GI_SE
 # xxx io4 5 0 0 2 # 6 LL_SE
 # xxx io4 5 0 0 1 # 7 ALGI_SW
 # xxx io4 5 0 0 2 # 8 EUEL_SW
 # xxx io4 5 0 0 2 # 9 ISEL_SW
 # xxx io4 5 0 0 2 # 10 JPLL_SW
 # xxx io4 5 0 0 2 # 11 TWFL_SW
 # xxx io4 5 0 0 2 # 12 TWLL_SW
 # xxx io4 5 0 0 2 # 13 UJPLL_NW
 # xxx io4 5 0 0 2 # 14 UJPLL_NE
 # xxx io4 5 0 0 2 # 15 UJPLL_SW
 # xxx io4 5 0 0 2 # 16 UJPLL_SE
 # xxx io4 5 0 0 2 # 17 UTWLL_NW
 # xxx io4 5 0 0 2 # 18 UTWLL_NE
 # xxx io4 5 0 0 2 # 19 UTWLL_SW
 # xxx io4 5 0 0 2 # 20 UTWLL_SE
 # xxx io4 5 0 0 2 # 21 UPOR_SW
 # xxx io4 5 0 0 2 # 22 UESP_SW
 # xxx io4 5 0 0 2 # 23 URELL_SW
 # xxx io4 5 0 0 2 # 24 UIND_NE
 # xxx io4 5 0 0 2 # 25 UJPLL_NW_pre
 # xxx io4 5 0 0 2 # 26 UJPLL_NE_pre
 # xxx io4 5 0 0 2 # 27 UJPLL_SW_pre
 # xxx io4 5 0 0 2 # 28 UJPLL_SE_pre
 # xxx io4 5 0 0 2 # 29 UTWLL_NW_pre
 # xxx io4 5 0 0 2 # 30 UTWLL_NE_pre
 # xxx io4 5 0 0 2 # 31 UTWLL_SW_pre
 # xxx io4 5 0 0 2 # 32 UTWLL_SE_pre


#_age_selex_types
#_Pattern ___ Male Special
 # xxx io4 10 0 0 0 # 1 GI_NE
 # xxx io4 10 0 0 0 # 2 LL_NE
 # xxx io4 10 0 0 0 # 3 GI_NW
 # xxx io4 10 0 0 0 # 4 LL_NW
 # xxx io4 10 0 0 0 # 5 GI_SE
 # xxx io4 10 0 0 0 # 6 LL_SE
 # xxx io4 10 0 0 0 # 7 ALGI_SW
 # xxx io4 10 0 0 0 # 8 EUEL_SW
 # xxx io4 10 0 0 0 # 9 ISEL_SW
 # xxx io4 10 0 0 0 # 10 JPLL_SW

```
# xxx io4 10 0 0 0 # 11 TWFL_SW
# xxx io4 10 0 0 0 # 12 TWLL_SW
# xxx io4 10 0 0 0 # 13 UJPLL_NW
# xxx io4 10 0 0 0 # 14 UJPLL_NE
# xxx io4 10 0 0 0 # 15 UJPLL_SW
# xxx io4 10 0 0 0 # 16 UJPLL_SE
# xxx io4 10 0 0 0 # 17 UTWLL_NW
# xxx io4 10 0 0 0 # 18 UTWLL_NE
# xxx io4 10 0 0 0 # 19 UTWLL_SW
# xxx io4 10 0 0 0 # 20 UTWLL_SE
# xxx io4 10 0 0 2 # 21 UPOR_SW
# xxx io4 10 0 0 2 # 22 UESP_SW
# xxx io4 10 0 0 2 # 23 URELL_SW
# xxx io4 10 0 0 2 # 24 UIND_NE
# xxx io4 10 0 0 2 # 25 UJPLL_NW
# xxx io4 10 0 0 2 # 26 UJPLL_NE
# xxx io4 10 0 0 2 # 27 UJPLL_SW
# xxx io4 10 0 0 2 # 28 UJPLL_SE
# xxx io4 10 0 0 2 # 29 UTWLL_NW
# xxx io4 10 0 0 2 # 30 UTWLL_NE
# xxx io4 10 0 0 2 # 31 UTWLL_SW
# xxx io4 10 0 0 2 # 32 UTWLL_SE


#_LO HI INIT PRIOR PR_type SD PHASE env-var use_dev dev_minyr dev_maxyr dev_stddev
Block Block_Fxn
# xxx io4 50 200 91.86 150 1 99 3 0 0 0 0 0.5 0 0 # SizeSel_1P_1_GI_NE
# xxx io4 -6 4 -1.061 -3 1 99 3 0 0 0 0 0.5 0 0 # SizeSel_1P_2_GI_NE
# xxx io4 -1 9 4.714 8.3 1 99 3 0 0 0 0 0.5 0 0 # SizeSel_1P_3_GI_NE
# xxx io4 -1 9 4.00 4 1 99 3 0 0 0 0 0.5 0 0 # SizeSel_1P_4_GI_NE
# xxx io4 -15 -5 -10 -1 1 99 -3 0 0 0 0 0.5 0 0 # SizeSel_1P_5_GI_NE
# xxx io4 -5 9 -0.730581 -1 1 99 3 0 0 0 0 0.5 0 0 # SizeSel_1P_6_GI_NE
# xxx io4 50 200 142.278 150 1 99 3 0 0 0 0 0.5 0 0 # SizeSel_2P_1_LL_NE
# xxx io4 -6 4 -0.316252 -3 1 99 3 0 0 0 0 0.5 0 0 # SizeSel_2P_2_LL_NE
# xxx io4 -1 9 6.97936 8.3 1 99 3 0 0 0 0 0.5 0 0 # SizeSel_2P_3_LL_NE
# xxx io4 -1 9 5.26149 4 1 99 3 0 0 0 0 0.5 0 0 # SizeSel_2P_4_LL_NE
# xxx io4 -15 -5 -10 -1 1 99 -3 0 0 0 0 0.5 0 0 # SizeSel_2P_5_LL_NE
# xxx io4 -5 9 -1.57659 -1 1 99 3 0 0 0 0 0.5 0 0 # SizeSel_2P_6_LL_NE
# xxx io4 -5 3 1 -4 1 0.05 -3 0 0 0 0 0.5 0 0 # SizeSel_3P_1_GI_NW
# xxx io4 -5 3 -1 -4 1 0.05 -3 0 0 0 0 0.5 0 0 # SizeSel_3P_2_GI_NW
# xxx io4 -5 3 1 -4 1 0.05 -3 0 0 0 0 0.5 0 0 # SizeSel_4P_1_LL_NW
# xxx io4 -5 3 -1 -4 1 0.05 -3 0 0 0 0 0.5 0 0 # SizeSel_4P_2_LL_NW
# xxx io4 -5 3 1 -4 1 0.05 -3 0 0 0 0 0.5 0 0 # SizeSel_5P_1_GI_SE
# xxx io4 -5 3 -1 -4 1 0.05 -3 0 0 0 0 0.5 0 0 # SizeSel_5P_2_GI_SE
# xxx io4 -5 3 1 -4 1 0.05 -3 0 0 0 0 0.5 0 0 # SizeSel_6P_1_LL_SE
# xxx io4 -5 3 -1 -4 1 0.05 -3 0 0 0 0 0.5 0 0 # SizeSel_6P_2_LL_SE
# xxx io4 -5 3 1 -4 1 0.05 -3 0 0 0 0 0.5 0 0 # SizeSel_7P_1_ALGI_SW
# xxx io4 -5 3 -1 -4 1 0.05 -3 0 0 0 0 0.5 0 0 # SizeSel_7P_2_ALGI_SW
# xxx io4 -5 3 1 -4 1 0.05 -3 0 0 0 0 0.5 0 0 # SizeSel_8P_1_EUEL_SW
# xxx io4 -5 3 -1 -4 1 0.05 -3 0 0 0 0 0.5 0 0 # SizeSel_8P_2_EUEL_SW
# xxx io4 -5 3 1 -4 1 0.05 -3 0 0 0 0 0.5 0 0 # SizeSel_9P_1_ISEL_SW
# xxx io4 -5 3 -1 -4 1 0.05 -3 0 0 0 0 0.5 0 0 # SizeSel_9P_2_ISEL_SW
# xxx io4 -5 3 1 -4 1 0.05 -3 0 0 0 0 0.5 0 0 # SizeSel_10P_1_JPLL_SW
# xxx io4 -5 3 -1 -4 1 0.05 -3 0 0 0 0 0.5 0 0 # SizeSel_10P_2_JPLL_SW
# xxx io4 -5 3 1 -4 1 0.05 -3 0 0 0 0 0.5 0 0 # SizeSel_11P_1_TWFL_SW
# xxx io4 -5 3 -1 -4 1 0.05 -3 0 0 0 0 0.5 0 0 # SizeSel_11P_2_TWFL_SW
```

```
# xxx io4 -5 3 1 -4 1 0.05 -3 0 0 0 0 0.5 0 0 # SizeSel_12P_1_TWLL_SW
# xxx io4 -5 3 -1 -4 1 0.05 -3 0 0 0 0 0.5 0 0 # SizeSel_12P_2_TWLL_SW
# xxx io4 -5 3 1 -4 1 0.05 -3 0 0 0 0 0.5 0 0 # SizeSel_13P_1_UJPLL_NW
# xxx io4 -5 3 -1 -4 1 0.05 -3 0 0 0 0 0.5 0 0 # SizeSel_13P_2_UJPLL_NW
# xxx io4 -5 3 1 -4 1 0.05 -3 0 0 0 0 0.5 0 0 # SizeSel_14P_1_UJPLL_NE
# xxx io4 -5 3 -1 -4 1 0.05 -3 0 0 0 0 0.5 0 0 # SizeSel_14P_2_UJPLL_NE
# xxx io4 -5 3 1 -4 1 0.05 -3 0 0 0 0 0.5 0 0 # SizeSel_15P_1_UJPLL_SW
# xxx io4 -5 3 -1 -4 1 0.05 -3 0 0 0 0 0.5 0 0 # SizeSel_15P_2_UJPLL_SW
# xxx io4 -5 3 1 -4 1 0.05 -3 0 0 0 0 0.5 0 0 # SizeSel_16P_1_UJPLL_SE
# xxx io4 -5 3 -1 -4 1 0.05 -3 0 0 0 0 0.5 0 0 # SizeSel_16P_2_UJPLL_SE
# xxx io4 -5 3 1 -4 1 0.05 -3 0 0 0 0 0.5 0 0 # SizeSel_17P_1_UTWLL_NW
# xxx io4 -5 3 -1 -4 1 0.05 -3 0 0 0 0 0.5 0 0 # SizeSel_17P_2_UTWLL_NW
# xxx io4 -5 3 1 -4 1 0.05 -3 0 0 0 0 0.5 0 0 # SizeSel_18P_1_UTWLL_NE
# xxx io4 -5 3 -1 -4 1 0.05 -3 0 0 0 0 0.5 0 0 # SizeSel_18P_2_UTWLL_NE
# xxx io4 -5 3 1 -4 1 0.05 -3 0 0 0 0 0.5 0 0 # SizeSel_19P_1_UTWLL_SW
# xxx io4 -5 3 -1 -4 1 0.05 -3 0 0 0 0 0.5 0 0 # SizeSel_19P_2_UTWLL_SW
# xxx io4 -5 3 1 -4 1 0.05 -3 0 0 0 0 0.5 0 0 # SizeSel_20P_1_UTWLL_SE
# xxx io4 -5 3 -1 -4 1 0.05 -3 0 0 0 0 0.5 0 0 # SizeSel_20P_2_UTWLL_SE
# xxx io4 -5 3 1 -4 1 0.05 -3 0 0 0 0 0.5 0 0 # SizeSel_21P_1_UPOR_SW
# xxx io4 -5 3 -1 -4 1 0.05 -3 0 0 0 0 0.5 0 0 # SizeSel_21P_2_UPOR_SW
# xxx io4 -5 3 1 -4 1 0.05 -3 0 0 0 0 0.5 0 0 # SizeSel_22P_1_UESP_SW
# xxx io4 -5 3 -1 -4 1 0.05 -3 0 0 0 0 0.5 0 0 # SizeSel_22P_2_UESP_SW
# xxx io4 -5 3 1 -4 1 0.05 -3 0 0 0 0 0.5 0 0 # SizeSel_23P_1_URELL_SW
# xxx io4 -5 3 -1 -4 1 0.05 -3 0 0 0 0 0.5 0 0 # SizeSel_23P_2_URELL_SW
# xxx io4 -5 3 1 -4 1 0.05 -3 0 0 0 0 0.5 0 0 # SizeSel_24P_1_UIND_NE
# xxx io4 -5 3 -1 -4 1 0.05 -3 0 0 0 0 0.5 0 0 # SizeSel_24P_2_UIND_NE
# xxx io4 -5 3 1 -4 1 0.05 -3 0 0 0 0 0.5 0 0 # SizeSel_25P_1_UJPLL_NW_pre
# xxx io4 -5 3 -1 -4 1 0.05 -3 0 0 0 0 0.5 0 0 # SizeSel_25P_2_UJPLL_NW_pre
# xxx io4 -5 3 1 -4 1 0.05 -3 0 0 0 0 0.5 0 0 # SizeSel_26P_1_UJPLL_NE_pre
# xxx io4 -5 3 -1 -4 1 0.05 -3 0 0 0 0 0.5 0 0 # SizeSel_26P_2_UJPLL_NE_pre
# xxx io4 -5 3 1 -4 1 0.05 -3 0 0 0 0 0.5 0 0 # SizeSel_27P_1_UJPLL_SW_pre
# xxx io4 -5 3 -1 -4 1 0.05 -3 0 0 0 0 0.5 0 0 # SizeSel_27P_2_UJPLL_SW_pre
# xxx io4 -5 3 1 -4 1 0.05 -3 0 0 0 0 0.5 0 0 # SizeSel_28P_1_UJPLL_SE_pre
# xxx io4 -5 3 -1 -4 1 0.05 -3 0 0 0 0 0.5 0 0 # SizeSel_28P_2_UJPLL_SE_pre
# xxx io4 -5 3 1 -4 1 0.05 -3 0 0 0 0 0.5 0 0 # SizeSel_29P_1_UTWLL_NW_pre
# xxx io4 -5 3 -1 -4 1 0.05 -3 0 0 0 0 0.5 0 0 # SizeSel_29P_2_UTWLL_NW_pre
# xxx io4 -5 3 1 -4 1 0.05 -3 0 0 0 0 0.5 0 0 # SizeSel_30P_1_UTWLL_NE_pre
# xxx io4 -5 3 -1 -4 1 0.05 -3 0 0 0 0 0.5 0 0 # SizeSel_30P_2_UTWLL_NE_pre
# xxx io4 -5 3 1 -4 1 0.05 -3 0 0 0 0 0.5 0 0 # SizeSel_31P_1_UTWLL_SW_pre
# xxx io4 -5 3 -1 -4 1 0.05 -3 0 0 0 0 0.5 0 0 # SizeSel_31P_2_UTWLL_SW_pre
# xxx io4 -5 3 1 -4 1 0.05 -3 0 0 0 0 0.5 0 0 # SizeSel_32P_1_UTWLL_SE_pre
# xxx io4 -5 3 -1 -4 1 0.05 -3 0 0 0 0 0.5 0 0 # SizeSel_32P_2_UTWLL_SE_pre


#_Cond 0 #_custom_sel-env_setup (0/1)
#_Cond -2 2 0 0 -1 99 -2 #_placeholder when no enviro fxns
#_Cond 0 #_custom_sel-blk_setup (0/1)
#_Cond -2 2 0 0 -1 99 -2 #_placeholder when no block usage
#_Cond No selex parm trends
#_Cond -4 # placeholder for selparm_Dev_Phase
#_Cond 0 #_env/block/dev_adjust_method (1=standard; 2=logistic trans to keep in base parm bounds;
3=standard w/ no bound check)
#
# Tag loss and Tag reporting parameters go next
0  # TG_custom:  0=no read; 1=read if tags exist
```

#_Cond -6 6 1 1 2 0.01 -4 0 0 0 0 0 0 0 #_placeholder if no parameters
#
1 #_Variance_adjustments_to_input_values
# xxx io4 #_fleet: 1 2 3 4 5 6 7 8 9 10 11 12 13 14 15 16 17 18 19 20 21 22 23 24 25 26 27 28 29 30 31 32
# xxx io4 0 0 0 0 0 0 0 0 0 0 0 0 0 0 0 0 0 0 0 0 0 0 0 0 0 0 0 0 0 0 0 0 #_add_to_survey_CV
# xxx io4 0 0 0 0 0 0 0 0 0 0 0 0 0 0 0 0 0 0 0 0 0 0 0 0 0 0 0 0 0 0 0 0 #_add_to_discard_stddev
# xxx io4 0 0 0 0 0 0 0 0 0 0 0 0 0 0 0 0 0 0 0 0 0 0 0 0 0 0 0 0 0 0 0 0 #_add_to_bodywt_CV

# xxx io4 # xxx CL002 0.01 0.01 0.01 0.01 0.01 0.01 0.01 0.01 0.01 0.01 0.01 0.01 1 1 1 1 1 1 1 1 1 1 1 1 1 1 1 1 1 1 1 1 #_mult_by_lencomp_N
# xxx io4 # xxx CL020 0.1 0.1 0.1 0.1 0.1 0.1 0.1 0.1 0.1 0.1 0.1 0.1 1 1 1 1 1 1 1 1 1 1 1 1 1 1 1 1 1 1 1 1 1 1 1 #_mult_by_lencomp_N
# xxx io4 # xxx CL200 1. 1. 1. 1. 1. 1. 1. 1. 1. 1. 1. 1. 1 1 1 1 1 1 1 1 1 1 1 1 1 1 1 1 1 1 1 1 #_mult_by_lencomp_N
# xxx io4 1 1 1 1 1 1 1 1 1 1 1 1 1 1 1 1 1 1 1 1 1 1 1 1 1 1 1 1 1 1 1 1 #_mult_by_agecomp_N
# xxx io4 1 1 1 1 1 1 1 1 1 1 1 1 1 1 1 1 1 1 1 1 1 1 1 1 1 1 1 1 1 1 1 1 #_mult_by_size-at-age_N

#
4 #_maxlambdaphase
1 #_sd_offset
#
# xxx io4 32 # number of changes to make to default Lambdas (default value is 1.0)
# Like_comp codes: 1=surv; 2=disc; 3=mnwt; 4=length; 5=age; 6=SizeFreq; 7=sizeage; 8=catch;
# 9=init_equ_catch; 10=recrdev; 11=parm_prior; 12=parm_dev; 13=CrashPen; 14=Morphcomp;
15=Tag-comp; 16=Tag-negbin
# lambdas like_comp fleet/survey phase value sizefreq_method

# xxx io4 # xxx NT0 1 13 1 1 1
# xxx io4 # xxx NT0 1 14 1 1 1
# xxx io4 # xxx NT0 1 15 1 1 1
# xxx io4 # xxx NT0 1 16 1 1 1
# xxx io4 # xxx NT0 1 17 1 0.001 1
# xxx io4 # xxx NT0 1 18 1 0.001 1
# xxx io4 # xxx NT0 1 19 1 0.001 1
# xxx io4 # xxx NT0 1 20 1 0.001 1
# xxx io4 # xxx NT0 1 21 1 0.001 1
# xxx io4 # xxx NT0 1 22 1 0.001 1
# xxx io4 # xxx NT0 1 23 1 0.001 1
# xxx io4 # xxx NT0 1 24 1 0.001 1
# xxx io4 # xxx NT0 1 25 1 0.001 1
# xxx io4 # xxx NT0 1 26 1 0.001 1
# xxx io4 # xxx NT0 1 27 1 0.001 1
# xxx io4 # xxx NT0 1 28 1 0.001 1
# xxx io4 # xxx NT0 1 29 1 0.001 1
# xxx io4 # xxx NT0 1 30 1 0.001 1
# xxx io4 # xxx NT0 1 31 1 0.001 1
# xxx io4 # xxx NT0 1 32 1 0.001 1

# xxx io4 # xxx NT1 1 13 1 1 1
# xxx io4 # xxx NT1 1 14 1 1 1
# xxx io4 # xxx NT1 1 15 1 1 1
# xxx io4 # xxx NT1 1 16 1 1 1

# xxx io4 # xxx NT1 1 17 1 0.001 1
# xxx io4 # xxx NT1 1 18 1 0.001 1
# xxx io4 # xxx NT1 1 19 1 0.001 1
# xxx io4 # xxx NT1 1 20 1 0.001 1
# xxx io4 # xxx NT1 1 21 1 0.001 1
# xxx io4 # xxx NT1 1 22 1 0.001 1
# xxx io4 # xxx NT1 1 23 1 0.001 1
# xxx io4 # xxx NT1 1 24 1 0.001 1
# xxx io4 # xxx NT1 1 25 1 1 1
# xxx io4 # xxx NT1 1 26 1 1 1
# xxx io4 # xxx NT1 1 27 1 1 1
# xxx io4 # xxx NT1 1 28 1 1 1
# xxx io4 # xxx NT1 1 29 1 0.001 1
# xxx io4 # xxx NT1 1 30 1 0.001 1
# xxx io4 # xxx NT1 1 31 1 0.001 1
# xxx io4 # xxx NT1 1 32 1 0.001 1

# xxx io4 # xxx TW0 1 13 1 0.001 1
# xxx io4 # xxx TW0 1 14 1 0.001 1
# xxx io4 # xxx TW0 1 15 1 0.001 1
# xxx io4 # xxx TW0 1 16 1 0.001 1
# xxx io4 # xxx TW0 1 17 1 1 1
# xxx io4 # xxx TW0 1 18 1 1 1
# xxx io4 # xxx TW0 1 19 1 1 1
# xxx io4 # xxx TW0 1 20 1 1 1
# xxx io4 # xxx TW0 1 21 1 0.001 1
# xxx io4 # xxx TW0 1 22 1 0.001 1
# xxx io4 # xxx TW0 1 23 1 0.001 1
# xxx io4 # xxx TW0 1 24 1 0.001 1
# xxx io4 # xxx TW0 1 25 1 0.001 1
# xxx io4 # xxx TW0 1 26 1 0.001 1
# xxx io4 # xxx TW0 1 27 1 0.001 1
# xxx io4 # xxx TW0 1 28 1 0.001 1
# xxx io4 # xxx TW0 1 29 1 0.001 1
# xxx io4 # xxx TW0 1 30 1 0.001 1
# xxx io4 # xxx TW0 1 31 1 0.001 1
# xxx io4 # xxx TW0 1 32 1 0.001 1

# xxx io4 # xxx TW1 1 13 1 0.001 1
# xxx io4 # xxx TW1 1 14 1 0.001 1
# xxx io4 # xxx TW1 1 15 1 0.001 1
# xxx io4 # xxx TW1 1 16 1 0.001 1
# xxx io4 # xxx TW1 1 17 1 1 1
# xxx io4 # xxx TW1 1 18 1 1 1
# xxx io4 # xxx TW1 1 19 1 1 1
# xxx io4 # xxx TW1 1 20 1 1 1
# xxx io4 # xxx TW1 1 21 1 0.001 1
# xxx io4 # xxx TW1 1 22 1 0.001 1
# xxx io4 # xxx TW1 1 23 1 0.001 1
# xxx io4 # xxx TW1 1 24 1 0.001 1
# xxx io4 # xxx TW1 1 25 1 0.001 1
# xxx io4 # xxx TW1 1 26 1 0.001 1
# xxx io4 # xxx TW1 1 27 1 0.001 1
# xxx io4 # xxx TW1 1 28 1 0.001 1
# xxx io4 # xxx TW1 1 29 1 1 1

# xxx io4 # xxx TW1 1 30 1 1 1
# xxx io4 # xxx TW1 1 31 1 1 1
# xxx io4 # xxx TW1 1 32 1 1 1


# xxx io4 # xxx NTP 1 13 1 1 1
# xxx io4 # xxx NTP 1 14 1 1 1
# xxx io4 # xxx NTP 1 15 1 1 1
# xxx io4 # xxx NTP 1 16 1 1 1
# xxx io4 # xxx NTP 1 17 1 0.001 1
# xxx io4 # xxx NTP 1 18 1 0.001 1
# xxx io4 # xxx NTP 1 19 1 0.001 1
# xxx io4 # xxx NTP 1 20 1 0.001 1
# xxx io4 # xxx NTP 1 21 1 1 1
# xxx io4 # xxx NTP 1 22 1 0.001 1
# xxx io4 # xxx NTP 1 23 1 0.001 1
# xxx io4 # xxx NTP 1 24 1 0.001 1
# xxx io4 # xxx NTP 1 25 1 0.001 1
# xxx io4 # xxx NTP 1 26 1 0.001 1
# xxx io4 # xxx NTP 1 27 1 0.001 1
# xxx io4 # xxx NTP 1 28 1 0.001 1
# xxx io4 # xxx NTP 1 29 1 0.001 1
# xxx io4 # xxx NTP 1 30 1 0.001 1
# xxx io4 # xxx NTP 1 31 1 0.001 1
# xxx io4 # xxx NTP 1 32 1 0.001 1


# xxx io4 # xxx TWP 1 13 1 0.001 1
# xxx io4 # xxx TWP 1 14 1 0.001 1
# xxx io4 # xxx TWP 1 15 1 0.001 1
# xxx io4 # xxx TWP 1 16 1 0.001 1
# xxx io4 # xxx TWP 1 17 1 1 1
# xxx io4 # xxx TWP 1 18 1 1 1
# xxx io4 # xxx TWP 1 19 1 1 1
# xxx io4 # xxx TWP 1 20 1 1 1
# xxx io4 # xxx TWP 1 21 1 1 1
# xxx io4 # xxx TWP 1 22 1 0.001 1
# xxx io4 # xxx TWP 1 23 1 0.001 1
# xxx io4 # xxx TWP 1 24 1 0.001 1
# xxx io4 # xxx TWP 1 25 1 0.001 1
# xxx io4 # xxx TWP 1 26 1 0.001 1
# xxx io4 # xxx TWP 1 27 1 0.001 1
# xxx io4 # xxx TWP 1 28 1 0.001 1
# xxx io4 # xxx TWP 1 29 1 0.001 1
# xxx io4 # xxx TWP 1 30 1 0.001 1
# xxx io4 # xxx TWP 1 31 1 0.001 1
# xxx io4 # xxx TWP 1 32 1 0.001 1


# xxx io4 # xxx A1 1 13 1 1 1
# xxx io4 # xxx A1 1 14 1 1 1
# xxx io4 # xxx A1 1 15 1 1 1
# xxx io4 # xxx A1 1 16 1 1 1
# xxx io4 # xxx A1 1 17 1 0.25 1
# xxx io4 # xxx A1 1 18 1 0.25 1

# xxx io4 # xxx A1 1 19 1 0.25 1
# xxx io4 # xxx A1 1 20 1 0.25 1
# xxx io4 # xxx A1 1 21 1 1 1
# xxx io4 # xxx A1 1 22 1 1 1
# xxx io4 # xxx A1 1 23 1 1 1
# xxx io4 # xxx A1 1 24 1 0.001 1
# xxx io4 # xxx A1 1 25 1 0.001 1
# xxx io4 # xxx A1 1 26 1 0.001 1
# xxx io4 # xxx A1 1 27 1 0.001 1
# xxx io4 # xxx A1 1 28 1 0.001 1
# xxx io4 # xxx A1 1 29 1 0.001 1
# xxx io4 # xxx A1 1 30 1 0.001 1
# xxx io4 # xxx A1 1 31 1 0.001 1
# xxx io4 # xxx A1 1 32 1 0.001 1


# xxx io4 4 1 1 1 1
# xxx io4 4 2 1 1 1
# xxx io4 4 3 1 1 1
# xxx io4 4 4 1 1 1
# xxx io4 4 5 1 1 1
# xxx io4 4 6 1 1 1
# xxx io4 4 7 1 1 1
# xxx io4 4 8 1 1 1
# xxx io4 4 9 1 1 1
# xxx io4 4 10 1 1 1
# xxx io4 4 11 1 1 1
# xxx io4 4 12 1 1 1

#
0 # (0/1) read specs for more stddev reporting
 # 0 1 -1 5 1 5 1 -1 5 # placeholder for selex type  len/age  year  N selex bins  Growth pattern  N growth ages  NatAge_area(-1 for all)  NatAge_yr  N Natages
 # placeholder for vector of selex bins to be reported
 # placeholder for vector of growth ages to be reported
 # placeholder for vector of NatAges ages to be reported
999